

Chapter 4. Beamline Engineering

4.1 Vacuum Components of Front End

4.1.1 The Design Overview of Beamline Vacuum Components

The installation of a beamline vacuum system is the most basic matter in beamline construction, and best systems of vacuum system will be an important matter for operation and maintenance of beamline. Therefore, it is necessary to check the roles and functions of the ion-pumps, gauges, and pumping stations that are absolutely necessary for maintaining the installed vacuum system, and also important considering the appropriate quantity. The 4GSR beamline can be largely divided into three parts: The Front-end, the optical hutch (OH), and the experimental hutch (EH), and each part has different vacuum systems. In particular, since the Front-end section is connected to the storage ring chamber, appropriate vacuum conditions must be set. And an interlock system must be installed in preparation for vacuum accidents.

This report is divided into three major sections: The Front-end, the optical hutch, and the experimental hutch. In general, the photon beamline can be functionally divided into four sections. The first section means the radiation source, which is the insertion device or the bending magnet. The second section is the Front-end, which is the area inside the shielding wall. This area serves as a bridge between the storage ring and the beamline, and the size of the photon beam is controlled and monitored in this area. The third section is the optical hutch, which is the experimental area outside the shielding wall and has the function of making monochromatic photon beams. The last fourth section is the experimental hutch, which is where the experiments are conducted.

4.1.2 The Design Criteria of Front End

A. Basic Requirements for Front-end Design

The Front-End of the beamline must be designed, manufactured, and installed to sufficiently satisfy five basic requirements.

1. The vacuum level of the Front-end must be equal to or better than that of the storage ring, and a device capable of quickly isolating the vacuum of the storage ring and beamline must be installed to protect against vacuum accidents in the storage ring or beamline. An interlock system must be installed for rapid isolation. The vacuum level of the Front-end is recommended to be 5×10^{-9} Torr during storage ring operation and 5×10^{-10} Torr when the storage ring is not in operation. To satisfy this vacuum level, ion pumps of sufficient capacity must be installed appropriately in the Front-end.
2. Generally, the rupture pressure wave that occurs due to a vacuum accident is classified as a shock wave, and the speed of the shock wave for air is known to be about 1,000 m/s and for helium about 2,000 m/s. The Front-End must detect this shock wave pressure and delay it using the FCS (Fast Closing Shutter) before it reaches the storage ring. At the same time, the gate valve between the storage ring and the beamline must be closed to protect the vacuum in the storage ring from shock waves.
3. The Front-End must minimize the range of bremsstrahlung radiation emitted from the storage ring during beamline experiments. In addition, when the safety shutter is activated, bremsstrahlung radiation must be completely shielded within the shielding wall, thereby protecting beamline users from bremsstrahlung radiation and providing a biologically safe experimental environment.
4. The vacuum components directly exposed to synchrotron radiation must be cooled using LCW (Low Conductivity Water) to prevent vacuum deterioration and damage. In addition, the glancing angle should be used to reduce the heat load intensity while supplying sufficient low-conductivity water for cooling. LCW usually has a purity (resistivity) of 1 M Ω cm or more and has high temperature precision, so it is used as a coolant in devices exposed to synchrotron radiation.
5. The operating status of the Front-end should be configured so that it can be detected by various types of sensors. Several conditions, such as ultra-high vacuum condition, shock wave detection, air pressure monitoring, LCW flow condition, and the positions of various switching devices, should be closely monitored.

B. General Design Criteria for Front-end Vacuum Components

It must be designed and manufactured to satisfy the basic requirements and vacuum component performance, and also to facilitate maintenance work. Some important points are as follows.

1. The minimum diameter of the Front-end vacuum tube should be greater than the vertical and horizontal beam sizes plus a certain amount of clearance. The minimum clearance is generally ± 10 mm. If the inner diameter of the vacuum tube is larger than the minimum clearance, the conductance of the vacuum tube can be improved, so it is desirable to enlarge the inner diameter of the vacuum tube if possible.
2. If possible, the vacuum spool should be installed with a rotating flange on the upstream side and a fixed flange on the downstream side for easy installation.
3. Formed bellows are easy to handle, economical in price, and have a small internal surface area, making them advantageous for vacuum, but their elongation is smaller than that of welded bellows. The displacement of the bellows can be calculated by (Equation 4.1.2.1) during the bake out process at 150°C .

$$\Delta l(m) = (t_2 - t_1) \times (17.3 - 18.7) \times 10^{-6} \times l_0(m) \quad (\text{Eq. 4.1.2.1})$$

Bellows must be installed in a fixed vacuum vessel that must remain in place during bake out. It is recommended that bellows be inserted at least 1.5 m apart for convenience of vacuum component installation and maintenance.

4. Since the Bremsstrahlung radiation value is very high inside the storage ring, it causes hardening of materials such as rubber and plastic. Therefore, seals or hoses made of elastomer or Buna-N must not be used, and metal seals and metal cooling pipes must be used.
5. It is recommended that the size of the cooling pipe be standardized into two types, 1/4 and 3/8 inches in outer diameter, to avoid confusion during production and installation. The cooling path should be configured so that the pressure drop is less than 0.5 atm, and the main cooling pipe should use a low-pressure, low-conductivity water cooling line. The material of the pneumatic pipe should be STS (Stainless Steel), and the diameter size should be standardized to 3/8 and 5/8 inches.
6. All vacuum components of the Front-end are for ultra-high vacuum. Therefore, electro-polishing and vacuum chemical cleaning must be performed, and the metal joining

method must be limited to TIG welding, vacuum brazing, electron beam welding, etc. In particular, when connecting the cooling water line in a vacuum, the connection part must be designed so that it is not directly exposed to the vacuum when the cooling water leaks.

C. Design Criteria for Cooling System

The fixed masks, beam stoppers, and photon shutters that are directly exposed to radiation require sufficient cooling by LCW, and materials with excellent heat transfer properties are required to be used in order to maintain ultra-high vacuum conditions and minimize structural deformation in components due to temperature rise. The main considerations in designing cooling devices for each component used in the beamline can be summarized as follows.

1. The vacuum components must be designed with sufficient safety factors in mind so that they can be operated stably from thermal loads even when the entire incident radiation is completely blocked.
2. When the FCS (Fast Closing Shutter) closes due to a vacuum accident, etc., and then the photon shutter closes, the radiation can heat the blade of the FCS for several seconds. Considering this case, the material of the shutter blade must be carefully selected.
3. The surface temperature of vacuum devices such as the fixed mask, beam stopper, and photon shutter, which are directly exposed to the radiation, must not exceed the softening temperature.
4. The wall temperature of the cooling pipe must not exceed 100°C.
5. The temperature difference between the inlet and outlet of the cooling water should not exceed 10°C, and the supply temperature of the cooling water should be in the range of 25 to 30°C.
6. The vacuum components should be designed with a structure to minimize the heat load density as much as possible.
7. The outer diameter of the cooling pipe should be standardized to maintain the compatibility of the components.
8. LCW should be used as a coolant to prevent corrosion of the vacuum device pipes and

to prevent electromagnetism of the cooling water.

D. Requirements and Guidelines for Radiation Shielding

The Front-end has a safety shutter (or Bremsstrahlung shutter) and a lead collimator as devices to protect against radiation. The safety shutter and lead collimator used to prevent radiation leakage must take into consideration the following:

1. In the injection mode, the shielding calculation must reflect radiation generated by the loss of electrons at multiple injected points within the storage ring tunnel, radiation generated by the loss of the entire electron beam at one point, gas Bremsstrahlung, and scattered radiation from secondary sources.
2. In the stored mode, radiation generated by the complete loss of the electron beam at any point, Gas Bremsstrahlung, and radiation generated by the gradual loss of electrons in orbit must be considered.

The requirements for safety shutter and shield to protect against the above-mentioned radiation and the guidelines for their design can be summarized as follows:

1) Safety shutter must be closed during the injection time and when the beamline is not in use. 2) Lead collimator and collimating spool must be constructed in a way that can minimize radiation penetration. 3) In order to have enough space for the beamline equipment, the structure must be as compact as possible.

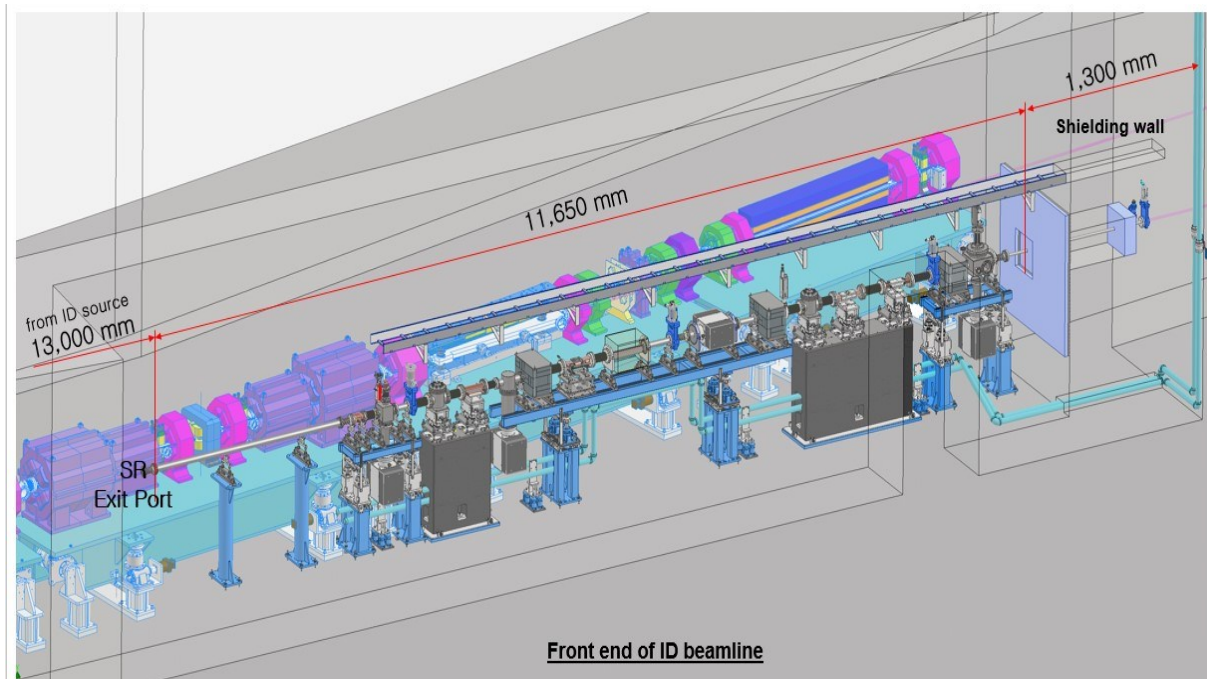
The Guidelines for shielding design include: 1) A shielding thickness equivalent to 200 mm lead should be maintained in any direction within the storage ring tunnel; 2) Safety shutter should be manufactured to a size that can block the photon beam and should be made of 200 mm thick tungsten; and 3) Safety shutter should be installed as close to the shielding wall as possible to minimize the size of the leakage angle.

E. Engineering Design Criteria

The 4GSR beamline applies three principles of standardization, modularization, and centralization to the design, manufacturing, and installation processes.

First, by standardizing the device, it is possible to reduce the budget, design efforts, shorten the manufacturing process, and facilitate quality control and quality assurance. As a result, the operation and maintenance of the device become easier and reliability can be improved. The second principle is modularization, which is very necessary for beamline operation. Due to the characteristics of beamline operation, maintenance work can only be performed during the inspection period in summer and winter, so it is necessary to modularize each section to effectively complete the work within a short period of time. The third principle is centralization, which is required in the basic configuration of the beamline. Usually, a beamline is approximately 55 to 60 m long and many control devices are distributed over a wide area. In order to operate this effectively, it is necessary to centralize the distributed control devices by gathering them in one place and intensively controlling and monitoring them.

4.1.3 Vacuum Components



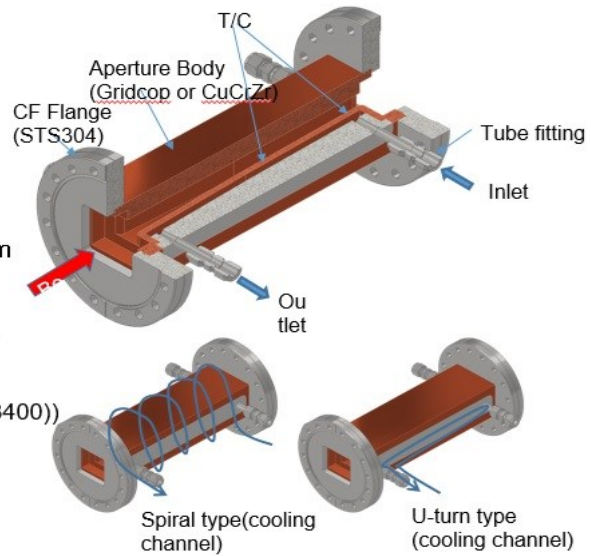
<Figure 4.1.3.1> Front-End layout of IVU beamline.

<Figure 4.1.3.1> shows the layout of IVU beamline Front-End. The main components are Fixed Mask, Beam Stopper, Photon Shutter, Movable Mask, Screen Monitor, etc. installed in the Front-end, and optical devices (DCM, Mirror), slit, diagnostic devices, etc. are installed in the optical hutch (OH). The description of the main vacuum components is as follows.

○ **Fixed mask:** The Fixed mask is the component that is first exposed to radiation from the Front-end, and is made of GlidCop. Its role is to block unnecessary radiation and prevent damage to major components located downstream of the beam. A cooling water pipe with an outer diameter of 1/4 inch was applied, and a glancing angle was applied to reduce the heat load per unit area, and a K-type thermocouple was installed near the opening to detect whether the mask is overheated. <Figure 4.1.3.2> shows the assembly drawing and internal shape of the fixed mask.

Specification

From the source EPU98:	17355 mm
IVU24:	17355 mm
Incidence Angle EPU98:	2.6 °
IVU24:	2.6 °
Exit Aperture EPU98:	10.41(H) × 10.41(V) mm
IVU24:	5.21(H) × 5.21(V) mm
Cooling Pipe & Number:	1/4"(ID 4.6 mm), 2 sets
	U-turn Type
Flange Size [inch] & Length:	6", 000 mm
Base Material:	GlidCop(or CuCrZr(C18400))
Thermocouple:	K-type, 2ea

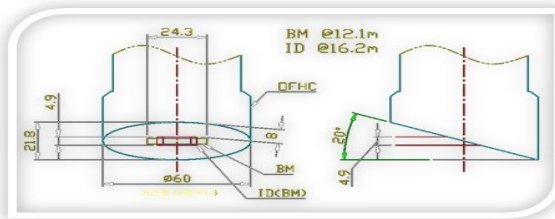


<Figure 4.1.3.2> Fixed mask assembly.

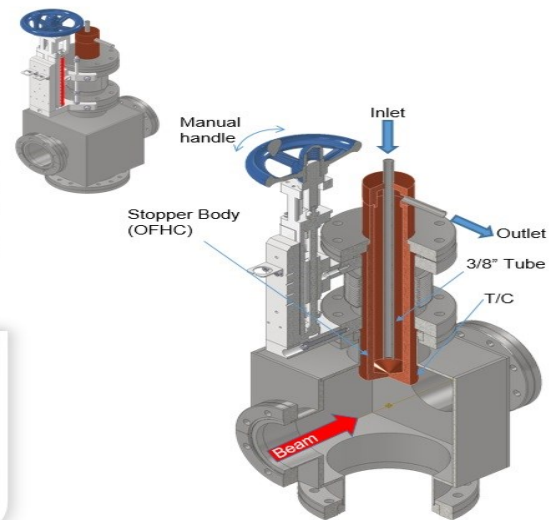
○ **Beam stopper:** The beam stopper is installed at the Front-end of the photon shutter and blocks the BM beam in conjunction with the ID. OFHC is used as the material and the incident angle is 20° to reduce the heat load. <Figure 4.1.3.3> shows the internal shape and assembly layout of the beam stopper.

Specification

From the source BM:	12135 mm
EPU98:	16195 mm
IVU24:	16195 mm
Incidence Angle:	20 °
Beam Size BM(2.0×0.3mrad):	24.27(H)×3.64(V) mm
EPU98(2.0×0.3mrad):	16.20(H)×4.86(V) mm
IVU24(2.0×0.3mrad):	11.34(H)×4.86(V) mm
Cooling Pipe & Number:	3/8"(ID 7.0 mm), 1 set
Flange Size [inch] & Length:	4.5", 000 mm
Base Material:	OFHC
Thermocouple:	K-type, 1ea



Front & Side view



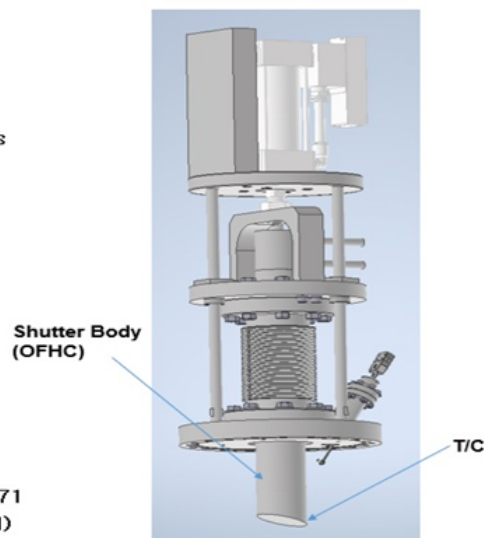
<Figure 4.1.3.3> Beam stopper assembly.

○ **Photon shutter:** The photon shutter is a key component installed in the Front-end, and operates at high speed to completely block the photon beam to protect downstream components during vacuum accidents and in the maintenance periods. The blade is made of GlidCop (or CuCrZr) material, and the incident angle is designed to be as small as possible to lower the power density of the beam and minimize the heat load.

• Photon Shutter(BM)

Specification

From the source:	14612 mm
Beam Size(2.0x0.3mrad):	29.22(H)x4.38(V) mm
Incidence Angle:	20 °
Cooling Pipe & Number:	3/8"(ID7.0 mm), 2 sets
Flange Size[inch] & Length:	4.5", 000 mm
Base Material:	OFHC
Thermocouple:	K-type, 1ea
Stroke:	50 mm
Motion Repeatability:	0.5 mm
Actuator Flange :	CF160
Pneumatic Pressure:	5 atm
Pneumatic Damping:	in each end position
Maximum Closing Time:	50 ~ 600 mm/sec
Solenoid:	24V DC
Vacuum:	UHV Compatible
Limit Switches:	in each end position
Welded Bellows:	MLAKK101731 (KSM)
Pneumatic Cylinder:	DDV-50 X 50-DC24V-71 -ZC130A-3 (KOGANEI)

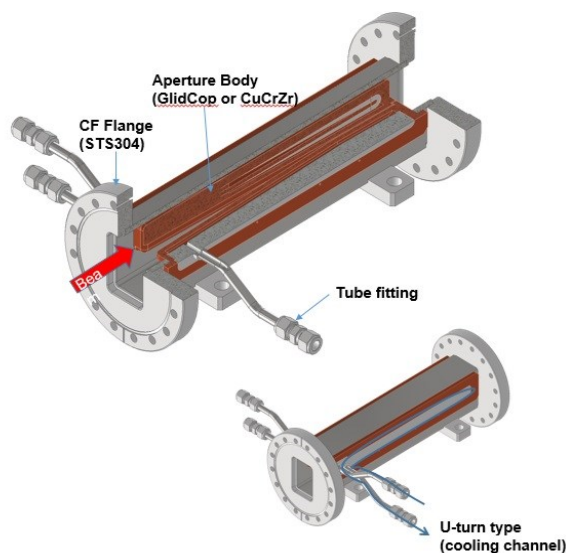


<Figure 4.1.3.4> BM photon shutter assembly.

• Photon Shutter(EPU98, IVU24)

Specification

From the source EPU98:	18800 mm
IVU24:	18800 mm
Beam Size EPU98:	11.28(H)x11.28(V) mm
IVU24:	5.64(H)x5.64(V) mm
Entrance Aperture EPU98:	21.29(H) x 22(V) mm
IVU24:	13.87(H) x 22 (V) mm
Incidence Angle EPU98:	3.6 °
IVU24:	1.6 °
Cooling Pipe & Number:	1/4"(ID4.6 mm), 2 sets
	U-turn Type
Flange Size[inch] & Length:	6", 000 mm
Base Material:	GLIDCOP/CuCrZr(C18400)
Thermocouple:	K-type, 4ea
Stroke:	24 mm
Motion Repeatability:	0.5 mm
Actuator Flange :	CF160
Pneumatic Pressure:	5 atm
Pneumatic Damping:	in each end position
Maximum Closing Time:	50 ~ 600 mm/sec
Solenoid:	24V DC
Vacuum:	UHV Compatible
Limit Switches:	in each end position
Welded Bellows:	MLAKK101731 (KSM)
Pneumatic Cylinder:	DDV-50 X 50-DC24V-71 -ZC130A-3 (KOGANEI)



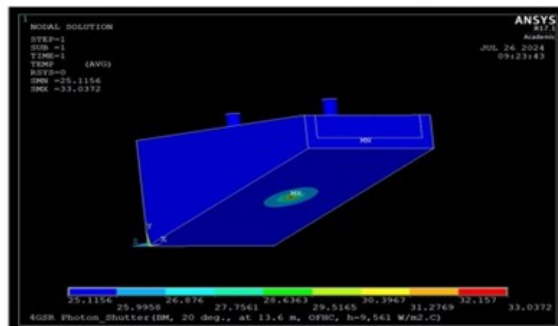
<Figure 4.1.3.5> IVU (EPU) photon shutter assembly.

As mentioned above, the photon shutter completely blocks the beam to protect the lower vacuum components and optical devices. Therefore, it is very important to review the safety of the blade that comes into direct contact with the photon beam. <Figure 4.1.3.4 to 5> show the assembly layout of the BM and IVU (EPU) photon shutter. Cooling conditions applied to the 4GSR beamline vacuum components are as follows.

○ Criteria of cooling conditions

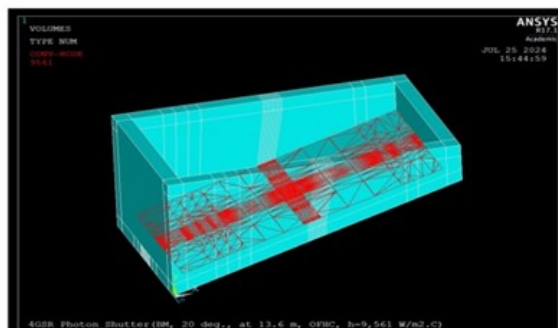
- Maximum von mises stress is smaller than the yield strength.
 - OFHC: von-mises stress < 295 MPa
 - GlidCop: von-mises stress < 400 MPa
- Maximum temperature should be less than the softening temperature of the material.
- Maximum temperature of the cooling channel wall should be less than the boiling temperature.

* HEM(BM) Photon shutter(20 degree) *

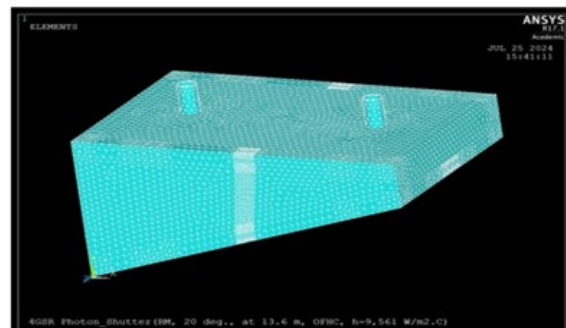


(20 deg. : Max Temp. 33 °C(blade surface),
h=9,561 W/m²°C)

- **Parameters**
 - Thickness : 5 mm
 - Incidence angle : 20 degree
- **Material**
 - OFHC(Softening temperature 150 °C)
- **Convection Heat Transfer**
 - Film coefficient(W/m² °C) : 9,561
(inner diameter: 7 mm, flow rate: 5 l/min, flow velocity : 2.16 m/s)
- **Distance**
 - 13.6 m from source point



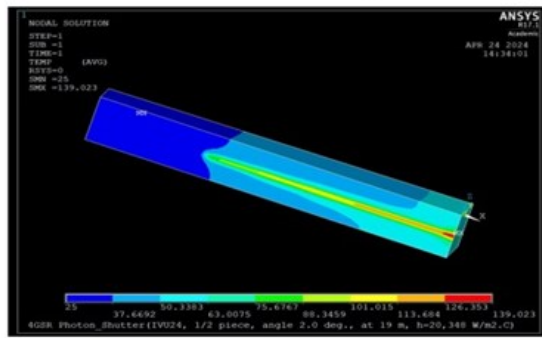
(Cooling channel)



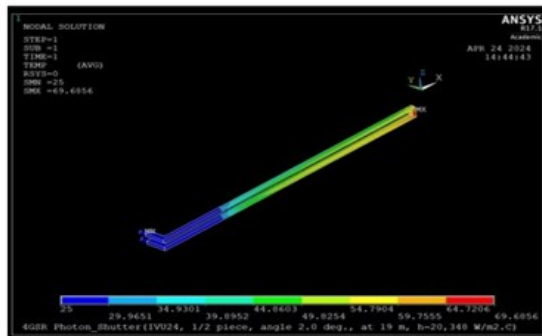
(PS modeling)

<Figure 4.1.3.6> Thermal analysis results of BM photon shutter.

* IVU24 Photon shutter(2.0 degree) *

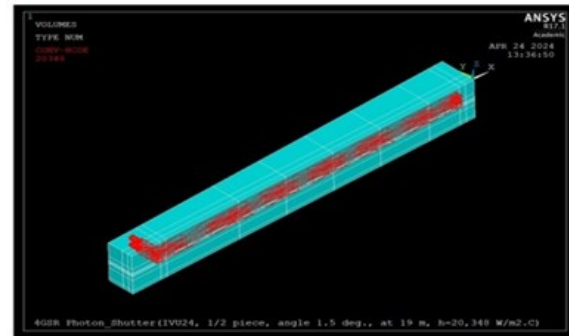


(2.0 deg. : Max Temp. 139.0 °C(blade surface),
h=20,348 W/m²°C)



(Cooling channel, Max. temp 69.7 °C)

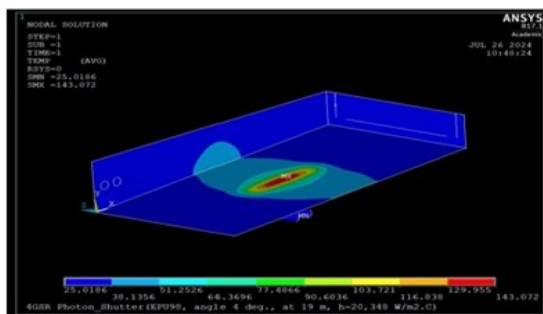
- **Parameters**
 - Thickness : 5 mm
 - Incidence angle : 2.0 degree
- **Material**
 - GlidCop(Softening temperature 300 °C)
- **Convection Heat Transfer**
 - Film coefficient(W/m²°C) : 20,348
(inner diameter: 4.6 mm, flow rate: 5 l/min, flow velocity : 5.01 m/s)
- **Distance**
 - 19 m from source point



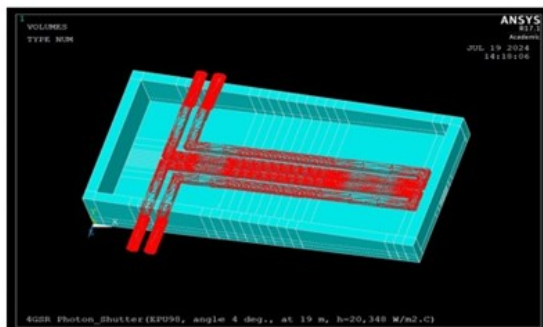
(Cooling channel)

<Figure 4.1.3.7> Thermal analysis results of EPU98 photon shutter.

* EPU98 Photon shutter(4.0 degree) *

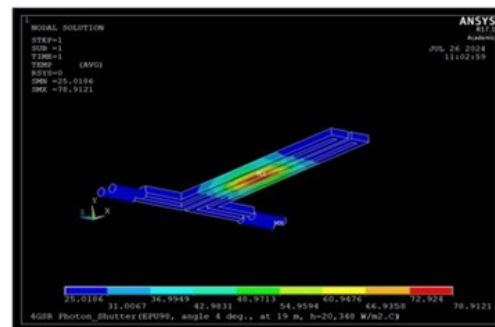


(4.0 deg. : Max Temp. 143 °C(blade surface),
h=20,348 W/m²°C)



(Cooling channel)

- **Parameters**
 - Thickness : 5 mm
 - Incidence angle : 4.0 degree
- **Material**
 - GlidCop(Softening temperature 300 °C)
- **Convection Heat Transfer**
 - Film coefficient(W/m²°C) : 20,348
(inner diameter: 4.6 mm, flow rate: 5 l/min, flow velocity : 5.01 m/s)
- **Distance**
 - 19 m from source point



(Cooling channel, Max. temp 78.9 °C)

<Figure 4.1.3.8> Thermal analysis results of EPU98 photon shutter.

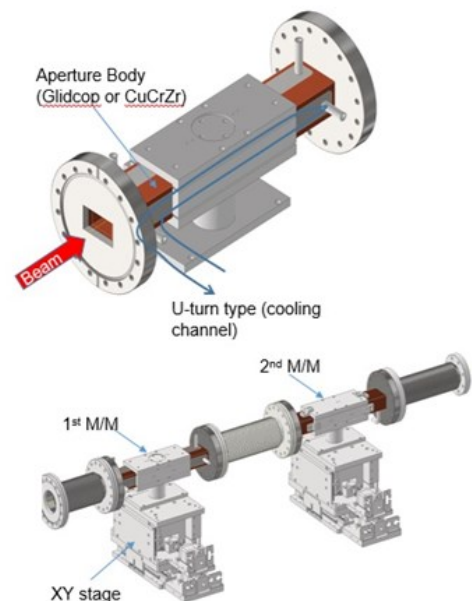
<Figure 4.1.3.6 to 8> show the temperature distribution of the BM, EPU98, and IVU24 photon shutter blade that blocks the synchrotron beam. Since the IVU24 undulator beamline has a very large heat load, it is necessary to make the incident angle as small as possible and to install it as far away from the source point as possible.

○ **Movable mask:** The movable mask has the function of a slit to remove unnecessary beams before they are applied to the optical device. It is also designed to completely block the beam when necessary. It was designed so that the material of the blade in contact with the beam can be changed depending on the type and purpose of the experiment, and the precision was improved by using an LM actuator and a stepping motor, and remote control was enabled for convenience of use. <Figure 4.1.3.9> shows the internal shape and assembly layout of the movable mask.

- **Movable Mask(EPU98, IVU24)**

Specification

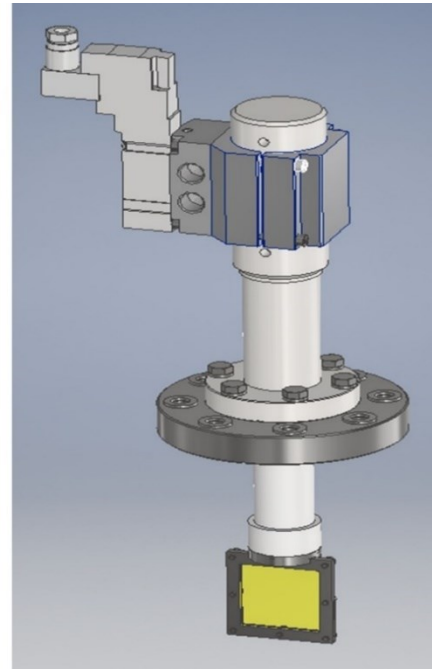
From the source EPU98:	22927 mm
IVU24:	22927 mm
Beam Size EPU98:	13.76(H)x13.76(V) mm
IVU24:	6.88(H)x6.88(V) mm
Incidence Angle EPU98:	3 °
IVU24:	3 °
Cooling Pipe & Number:	1/4"(ID 4.6 mm), 2 sets
	U-turn Type
Flange Size[inch] & Length:	6", 000 mm
Base Material:	GLIDCOP/CuCrZr(C18400)
Blade Material:	Tungsten with polished knife edges
Slits parallelism:	< ± 0.1 degree
Blade surface roughness :	< 1um
Vacuum:	UHV Compatible
Welded Bellows:	MLAKK101731 (KSM) 3 ea
Cooling:	LCW Convection(Fitting:1/4 PT)
Thermocouple:	"K" type
XY Stage(EPU98, IVU24):	2 sets



<Figure 4.1.3.9> Movable mask assembly.

○ **Screen monitor (Imager & Pop-in):** Various diagnostic devices are installed in the beamline, and a screen monitor is installed to check the shape and position of the beam. The basic shape of the Imager and Pop-in is similar, and the Imager has improved camera performance to check more precise information, and therefore the Pop-in is installed in various places where beam information needs to be checked. <Figure 4.1.3.10> shows the shape and assembly layout of the screen monitor.

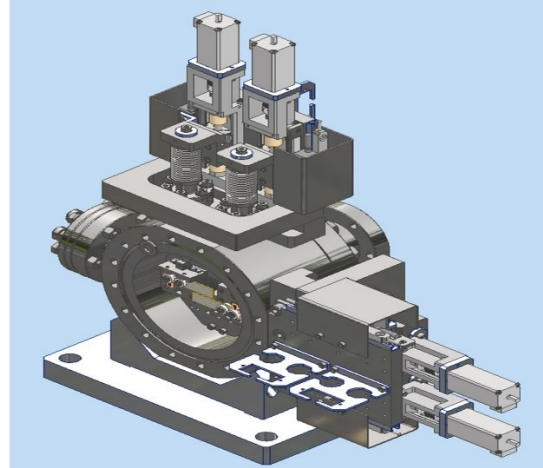
Beam Size:	00(H)x00(V) mm
Incidence Angle:	90 °
Screen Material:	YAG
Screen Size:	40(W) mm X 40(H) mm
Signal Pick-up:	via BNC Connector
Insulating Material:	BeO
Stroke:	50 mm
Motion Repeatability:	0.5 mm
Actuator Flange:	CF100
Pneumatic Pressure:	5 atm
Pneumatic Damping:	in each end position
Solenoid:	24V DC
Vacuum:	UHV Compatible
Limit Switches:	in each end position
Pneumatic Cylinder:	DDV-50 X 50-DC24V-71 -ZC130A-3 (KOGANEI)



<Figure 4.1.3.10> Screen monitor assembly.

○ **Slit:** Slit plays a role in precisely controlling the beam size applied to the optical device. Therefore, it must be designed, assembled, and installed with great precision. In particular, the blade that comes into contact with the beam must be precisely machined to reduce radiation scattering. Slit is installed in front of the optical device (DCM, Mirror) installed in the optical hutch, and is also installed inside the experimental hutch where the experimental device is located. <Figure 4.1.3.11> shows the internal shape and assembly layout of the Slit.

Specification	
Blade material:	Tungsten with polished knife edges
Slits parallelism:	$< \pm 0.1$ degree
Blade surface roughness:	$< 1 \mu\text{m}$
Aperture:	10 x 10 mm (overlapping blades)
Step resolution:	0.1 μm (driver control)
Encoder resolution:	0.05 μm
Repeatability:	$< 0.2 \mu\text{m}$



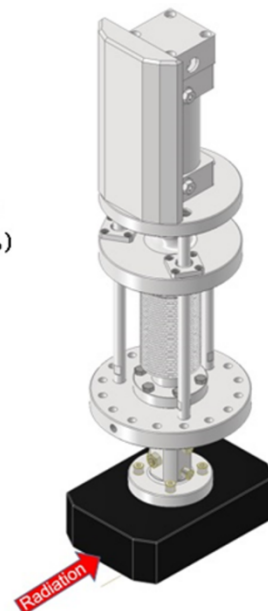
<Figure 4.1.3.11> Slit assembly.

○ **Safety shutter:** The safety shutter has the function of completely shielding the bremsstrahlung radiation inside the concrete barrier when the beamline is not in operation even during normal operation of the storage ring, or when the FCS (Fast Closing Shutter) is suddenly closed due to a vacuum accident in the beamline. Since the safety shutter does not have a cooling system, it must be interlocked with the photon shutter. <Figure 4.1.3.12> shows the assembly layout of safety shutter.

- **Safety Shutter(BM,EPU98, IVU24)**

Specification

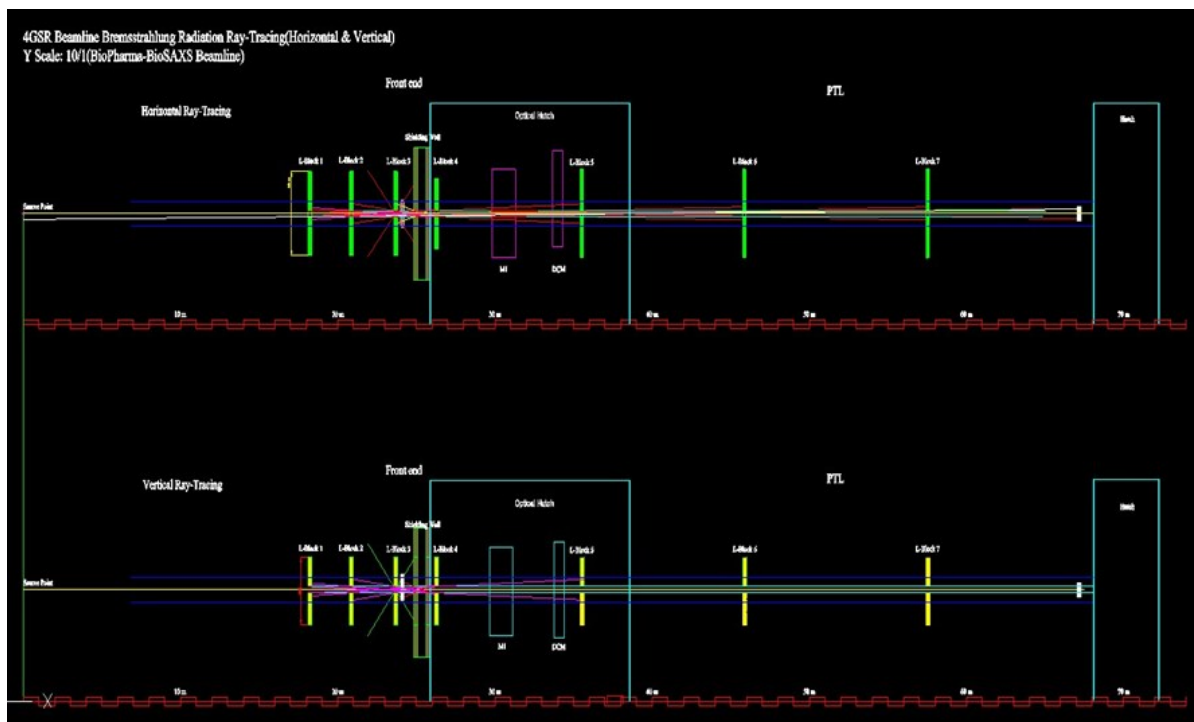
From the source BM:	11400 mm
ID:	15840 mm
Flange Size[inch] & Length:	4.5", 000 mm
Shutter Size:	120(W) mm X 50(H) mm X 180(L) mm
Shutter Material:	W-alloy (W 90.2%, Ni 6.86%, Fe 2.94%)
Stroke:	50 mm
Motion Repeatability:	0.5 mm
Total Axial Load:	20.8 kg
Vacuum Load:	28 kg
Actuator Flange :	CF160
Pneumatic Pressure:	5 atm
Pneumatic Damping:	in each end position
Maximum Closing Time:	50 ~ 600 mm/sec
Solenoid:	24V DC
Vacuum:	UHV Compatible
Limit Switches:	in each end position
Welded Bellows:	MLAKK101731, Cycle Life 100,000 cycles (KSM)
Pneumatic Cylinder:	DDV-50 X 50-DC24V-71-ZC130A-3 (KOGANEI)



<Figure 4.1.3.12> Safety shutter assembly.

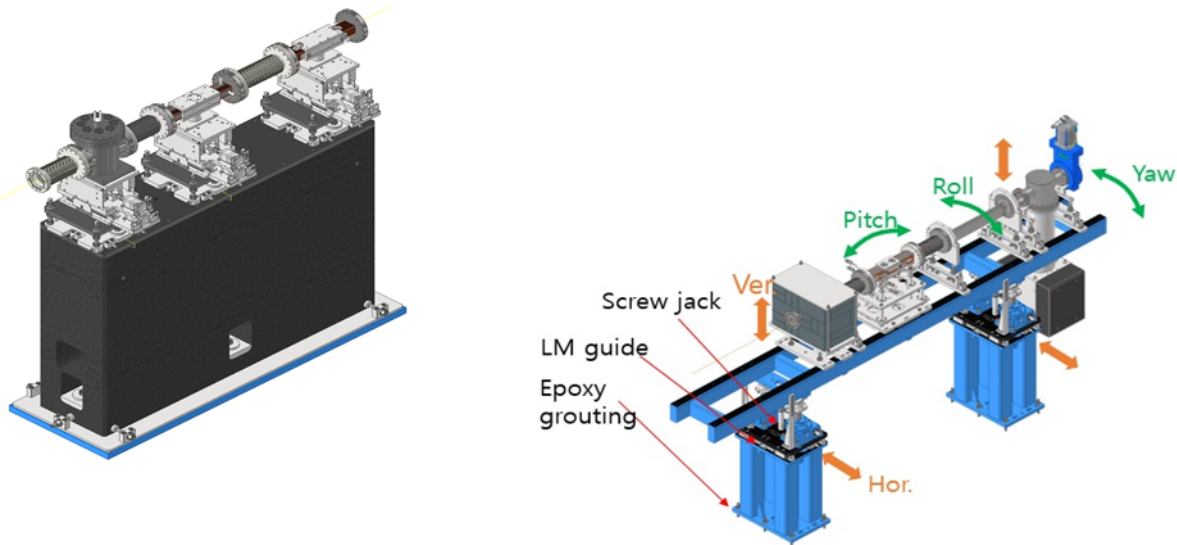
Safety shutter is usually installed at the Front-end, i.e., in front of the shielding wall. This

is to maximize the shielding of the bremsstrahlung radiation, and in order to block the bremsstrahlung radiation generated from the storage ring into the vacuum spool, appropriate lead blocks should be installed in the Front-end and the optical hutch. At the same time, the aperture size of the collimating spool should be minimized to ensure the safety of users in the experimental hall. The aperture size of collimating spool should be determined by sufficiently considering the effect of ground motion, and the bremsstrahlung ray tracing (horizontal, vertical) in <Figure 4.1.3.13> shows the quantity and location of lead blocks installed in the IVU beamline.



<Figure 4.1.3.13> Bremsstrahlung ray tracing of IVU beamline.

○ **Girder & Support System:** This is a structure that supports the vacuum device of the beamline. It must be manufactured to meet the design requirements such as precision adjustment device, vibration absorption, and thermal expansion absorption. The girder system uses a screw-jack at the bottom for rough adjustment, and detailed adjustments are made at the top. In particular, since the Front-end has limited space, it is useful to apply an integral girder for efficient alignment. <Figure 4.1.3.14> shows the integral girder system applied to the beamline. The support structure is designed to have the rigidity to withstand vacuum and seismic loads. The inside of the girder system is filled with dry sand to pursue a vibration-proof effect, and the surface is applied with powder coating that is economical, corrosion-resistant, and durable.



<Figure 4.1.3.14> Integral girder systems.

○ **LCW:** The LCW system applied to the beamline must be installed firmly to minimize the vibration impact on the floor or girder system. Basically, it would be best to remove the vibration source, but it would also be a good idea to increase the stiffness of each system to minimize the vibration displacement and prevent transmission to the peripheral devices. <Figure 4.1.3.15> shows the vibration displacements measured at PLS-II beamline 1C. The basic vibration displacement criterion in PLS-II is $0.1 \mu\text{m}$ or less. It is necessary to manage the vibration displacement below that criterion, and the vibration displacement in the Front-end and hutch meets the criterion and shows very good results. This LCW system will also be applied to 4GSR.



(1C LCW at Front end : with support)

- Supply : 26.4 nm(rms)
- Return : 43.5 nm(rms)



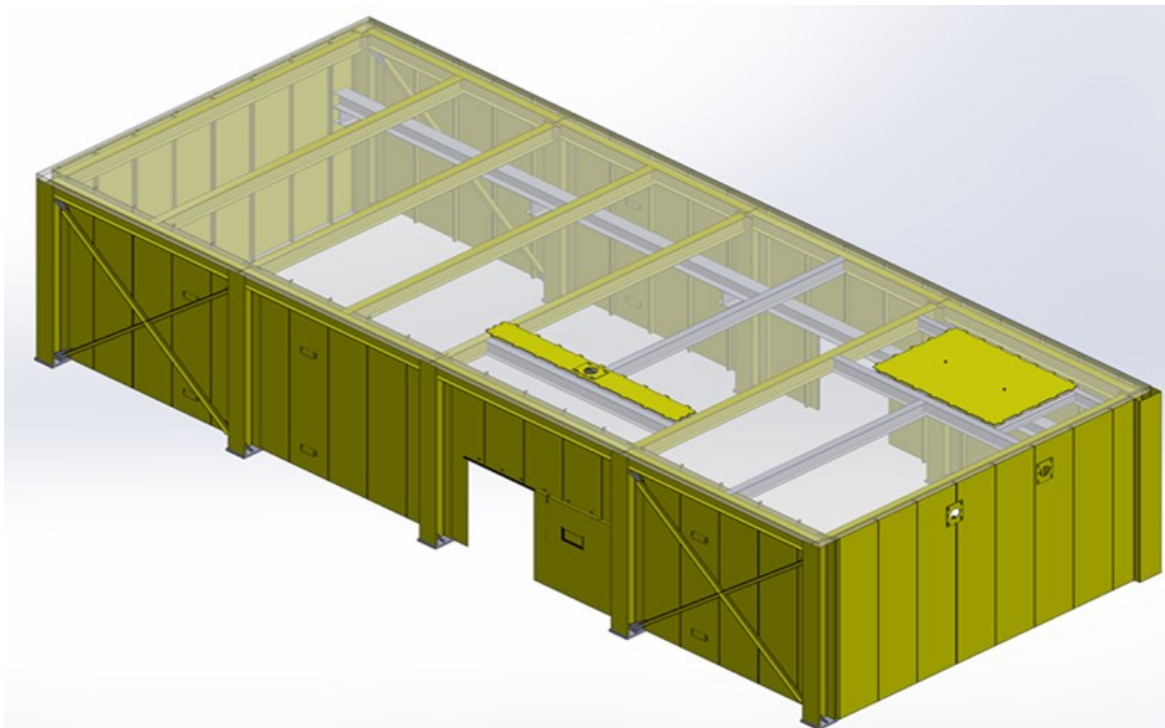
(1C LCW at Optical hutch)

- Supply : 12.0 nm(rms)
- Return : 10.6 nm(rms)

<Figure 4.1.3.15> Vibration displacements of LCW in beamline.

○ **Hutch:** The hutch is a space where experimental devices are installed to allow experiments to be performed according to the characteristics of each beamline, and radiation shielding is a very important element. The hutch is divided into an optical hutch and an experimental hutch. Various optical devices and diagnostic devices are installed in the optical hutch, and experimental devices related to experiments are installed in the experimental hutch.

Each hutch is installed according to the characteristics of the beamline, and since the shielding specifications are basically applied in common, standardization is also an important part. Depending on the radiation characteristics, it can be made of concrete or steel plate (including lead), and the door can be selected from a manual sliding door or a swing type, and if possible, a large door should be installed on the ceiling of the hutch to facilitate the installation of large equipment. Windows, interlocks, power panels, gas cylinders, hoods, and lead blocks for radiation shielding are installed in appropriate locations on the hutch walls. <Figure 4.1.3.16> shows a conceptual design of the hutch, and the size and shape can be changed according to the characteristics of the beamline.

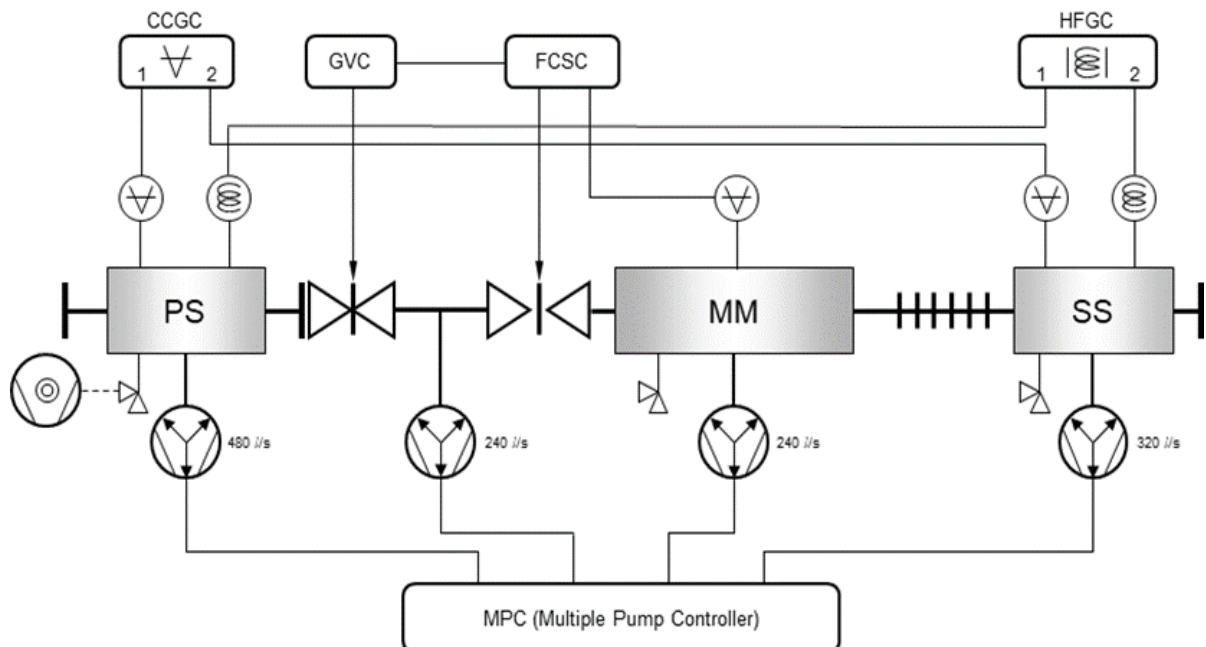


<Figure 4.1.3.16> Hutch layout.

4.1.4 Vacuum System of Front End

The Front-end acts as a bridge between the storage ring and the beamline, so the vacuum condition of one side directly affects the other side. Therefore, in order to operate the storage ring stably, the vacuum condition of the Front-end must always be better than that of the storage ring. The vacuum condition of the Front-end is designed to be 2×10^{-10} Torr or less when the storage ring is not operated, but actually it should be maintained at 5×10^{-10} Torr or less when the storage ring is not operated, and 5×10^{-9} Torr or less when the beamline is operated.

In order to satisfy the above conditions, all vacuum components must meet the conditions, and materials that can be heat treated up to 200°C must be selected to obtain the desired vacuum level. In addition, rubber seals that are easily hardened by radiation must not be used within the storage ring. The vacuum system is divided into a vacuum measuring system, vacuum vessel and valve, and exhaust system as shown in <Figure 4.1.4.1>. (PS: Photon Shutter, MM: Movable Mask, SS: Safety Shutter, CCGC: Cold Cathode Gauge Controller, HFGC: Hot Filament Gauge Controller, FCSC: Fast Closing Shutter Controller, GVC: Gate Valve Controller)



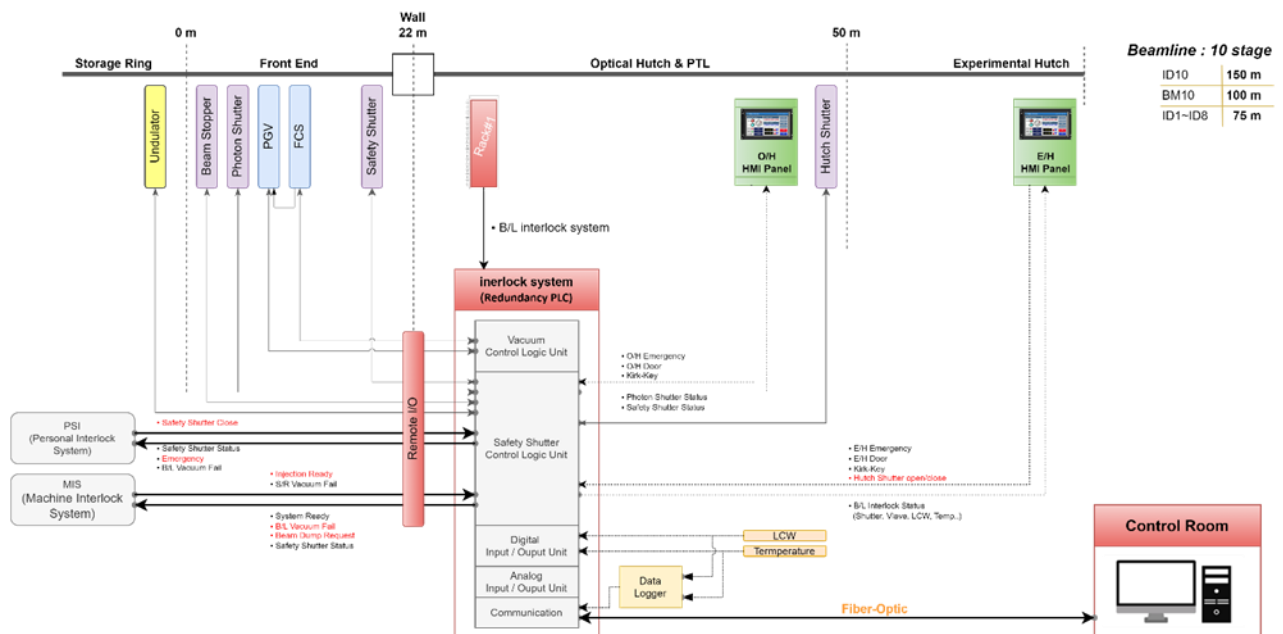
<Figure 4.1.4.1> Diagram of Front-end vacuum system.

4.1.5 Interlock System

The interlock system consists of a Personal Safety Interlock system (PSI) and a Machine Interlock System (MIS). The interlock system shares the interlock conditions occurring in the storage ring and beamline with the PSI and MIS, and protects various devices and users. The operating conditions include various valves and shutters of the vacuum system, the flow conditions and temperature of the cooling water, and the operating status of the storage ring. If there is a problem with the interlock system, it can cause a great danger, so it must satisfy the requirements of reliability, fail safe, redundancy, cable protection, etc.

The beamline interlock system can be divided into the Front-end and the hutch. <Figure 4.1.5.1> shows the beamline interlock system concept diagram.

The controller of the beamline interlock system consists of a PLC (Programmable Logic Controller), and is used in various fields of industry and experimental physics. Since various guidelines are presented for securing reliability and responding to failures of the PLC system, it is easier to configure the system than other types of controllers.

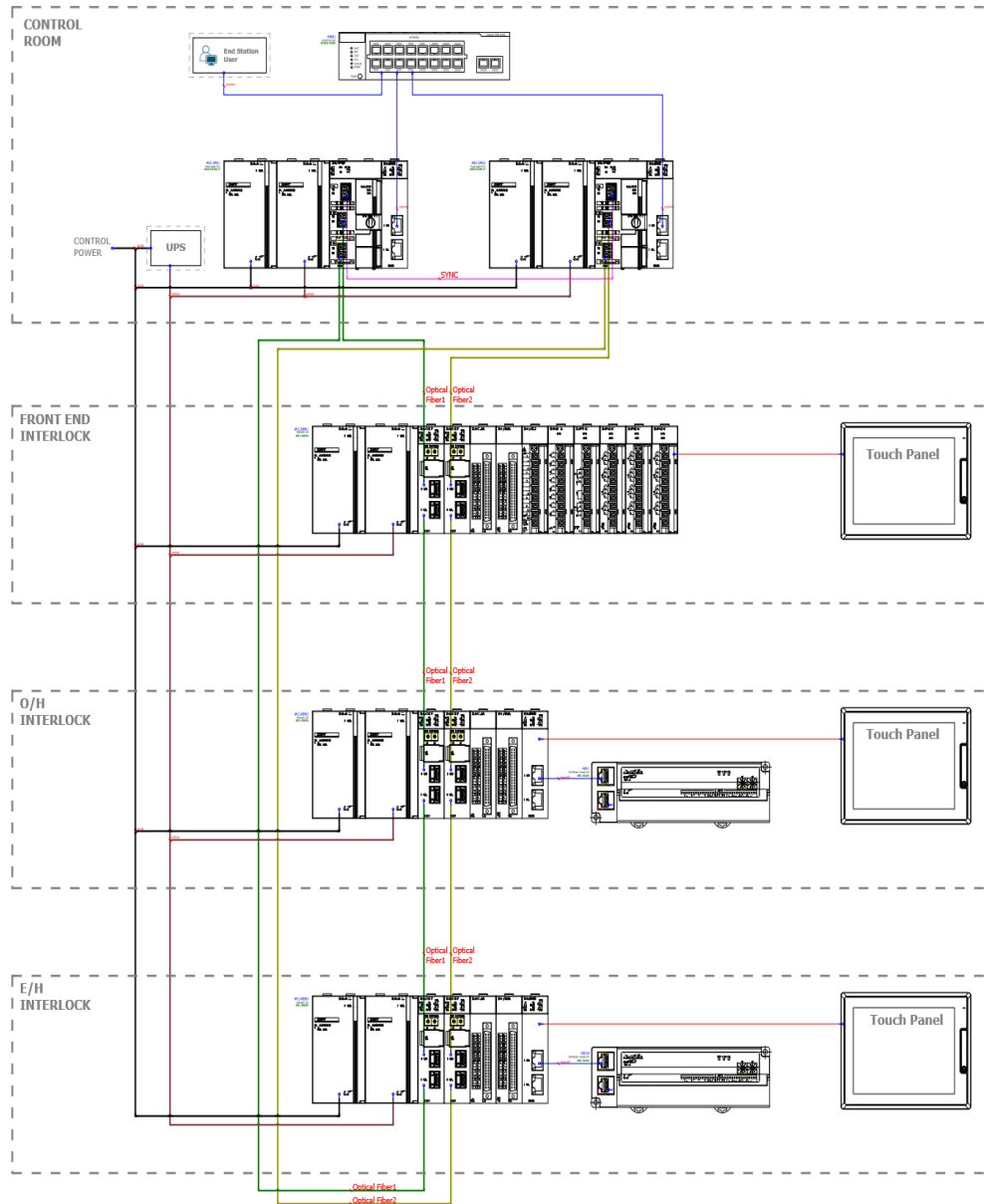


<Figure 4.1.5.1> Concept diagram of beamline interlock system.

A. Beamline Interlock System

The controller of the beamline interlock system consists of a PLC (Programmable Logic Controller), and is used in various fields of industry and experimental physics. Since various guidelines are presented for securing reliability and responding to failures of the PLC system, it is easier to configure the system than other types of controllers. The beamline interlock should be configured to protect users from beamline radiation and ensure high availability by considering device failure situations (PLC failure, vacuum accidents, component overheating, etc.).

In addition, designing for High Reliability that considers the safety and reliability of data is essential. The connection between the Local PLC and the Control Room uses the industrial Ethernet protocol (Profinet) to communicate. It also features the ability to provide services for users by linking with EPICS IOC. <Figure 4.1.5.2> shows the configuration of the local PLC CPU duplication and remote I/O local devices of the beamline interlock system.



<Figure 4.1.5.2> Interlock CPU Redundancy and Remote I/O Configuration of beamline.

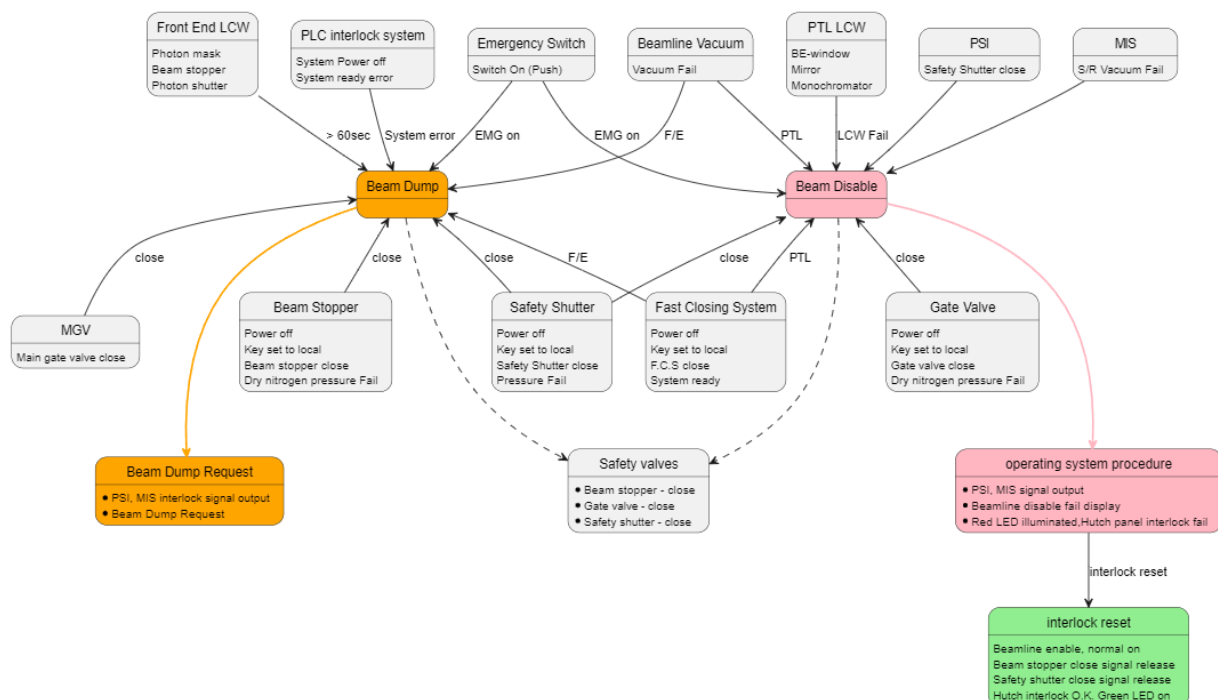
The Local PLC is redundant with two PLCs. The two PLCs are programmed with the same content to perform the same function. The purpose of redundant control systems is to ensure that the beamline interlock operates normally through the other system even if a problem occurs in one system. In the event that both systems are inoperable, the Photon Shutter and Safety Shutter are designed to close for the safety of the user and equipment.

B. The Front End System

(1) Interlock Logic

The electron beam is incident on the photon shutter and safety shutter while they are open, and the safety shutter and photon shutter must be closed when the beam is disabled or in the beam dump state. When the vacuum level of the Front-end is 10^{-6} or higher, the Front-end fail occurs and the fast closing shutter (FCS), gate valve, photon shutter, and safety shutter must be closed simultaneously with the beam dump.

According to the three operating modes of the storage ring, the user cannot open the photon shutter and safety shutter in the entrance mode, and in the store mode, the photon shutter and safety shutter can be opened when the entrance mode is finished. In the top-up mode, the user can always open/close the photon shutter and safety shutter as needed. If there is a problem with the photon shutter, safety shutter, vacuum, cooling water, hutch, and power status, take corresponding measures. In addition, the photon shutter, safety shutter, and gate valve are opened sequentially in the specified order to protect the users and equipment. <Figure 4.1.5.3> shows the configuration of the main interlocks that occur in the beamline interlock.

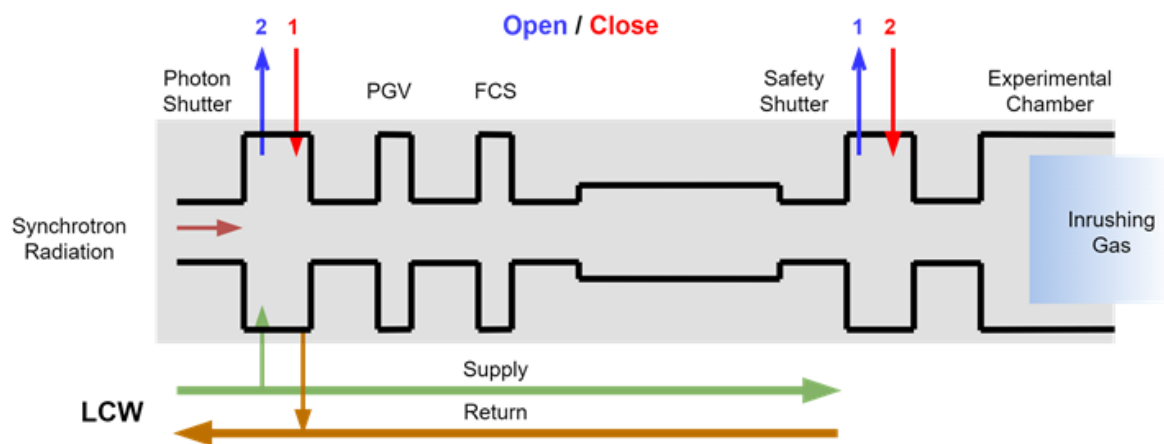


<Figure 4.1.5.3> Configuration of beamline interlock logic.

(2) Opening and Closing of Photon Shutter and Safety Shutter

The photon shutter and safety shutter block the radiation to protect the users. Unlike the photon shutter, the safety shutter is vulnerable to temperature rise due to the photon beam, so it should not be directly exposed to the radiation. Therefore, when using the radiation, the safety shutter should be opened first and then the photon shutter should be opened, and when finished using, the photon shutter should be closed first and then the safety shutter should be closed.

Therefore, the photon shutter and the safety shutter should be operated in conjunction with each other. If a problem occurs in this system, a signal is sent so that it can be recognized. <Figure 4.1.5.4> shows the relationship between the photon shutter and the safety shutter.



<Figure 4.1.5.4> Sequence of photon shutter and safety shutter opening/closing.

(3) LCW/Temperature

The interlock system monitors the LCW and temperature to minimize damage caused by temperature rise of the equipment due to electron beam and radiation. A flow meter is used for LCW monitoring, and a thermocouple is used for temperature check. In the case of LCW and temperature, a signal can be sent when a problem occurs instantly. Generally, if a problem occurs at the downstream of the photon shutter, the photon shutter is closed to block the radiation, and if a problem occurs at the front part, the electron beam of the storage ring is dumped to minimize damage. <Figure 4.1.5.5> shows the flow meter and thermocouple components used in the beamline.

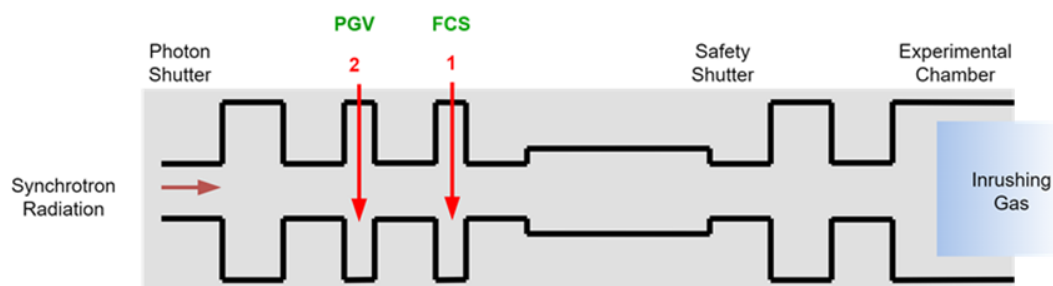


<Figure 4.1.5.5> Flowmeter & Thermocouple.

(4) Vacuum

The valves used in the Front-end can be divided into MGV (Manual Gate Valve) and PGV (Pneumatic Gate Valve). The MGV is manually operated to separate the vacuum, and the PGV is automatically opened and closed according to the set value. The interlock system constantly monitors the vacuum level, and when the Front-end vacuum level is higher than the set value (when the vacuum level is not good), it dumps the electron beam, and when the vacuum level in the PTL (Photon Transfer Line) is higher than the set value, it disables only the relevant beamline.

The beamline is also equipped with a fast-close shutter controller. Since the vacuum system of the beamline is interconnected with the storage ring, when a vacuum accident occurs in the beamline, it affects the vacuum level of the storage ring as well as the beamline. The fast closing shutter controller is linked to the vacuum valve of the Front-end, and when the vacuum suddenly fails, it closes quickly regardless of the state of the safety shutter, minimizing the impact of the vacuum accident. At this time, the electron beam dump must also be performed to prevent subsequent accidents. <Figure 4.1.5.6> shows the relationship between PGV and FCS.

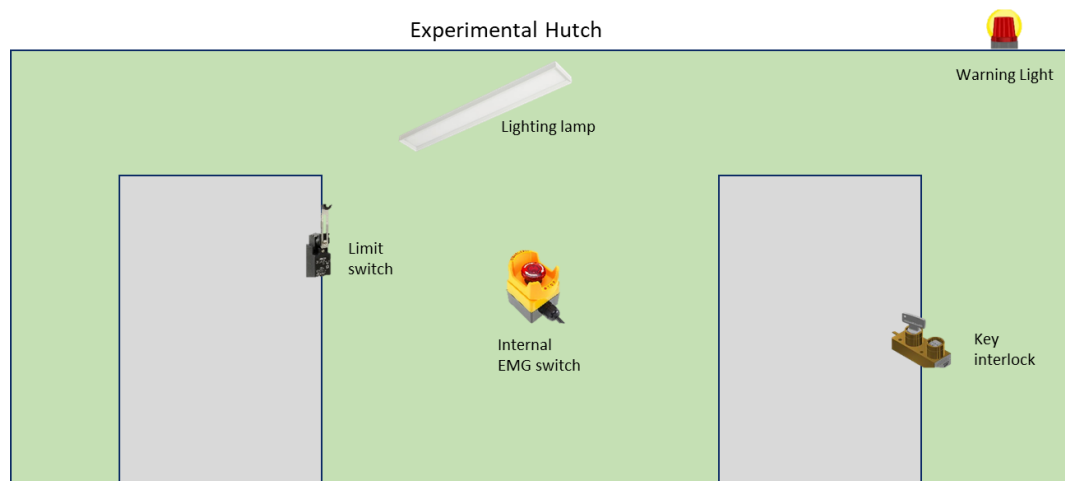


<Figure 4.1.5.6> Sequence of PGV & FCS.

C. Hutch Interlock System

The purpose of the interlock system of the experimental hutch is to protect users from radiation. Since the experimental hutch is always entered and exited when the user conducts an experiment, the user protection using the interlock system is necessary. When conducting an experiment in the experimental hutch, it is important to check the presence of the user and to ensure that the radiation generated during the experiment is shielded. Therefore, the Kirk-key should be used when entering and exiting the hutch so that the safety shutter cannot be opened if the user does not close the door properly.

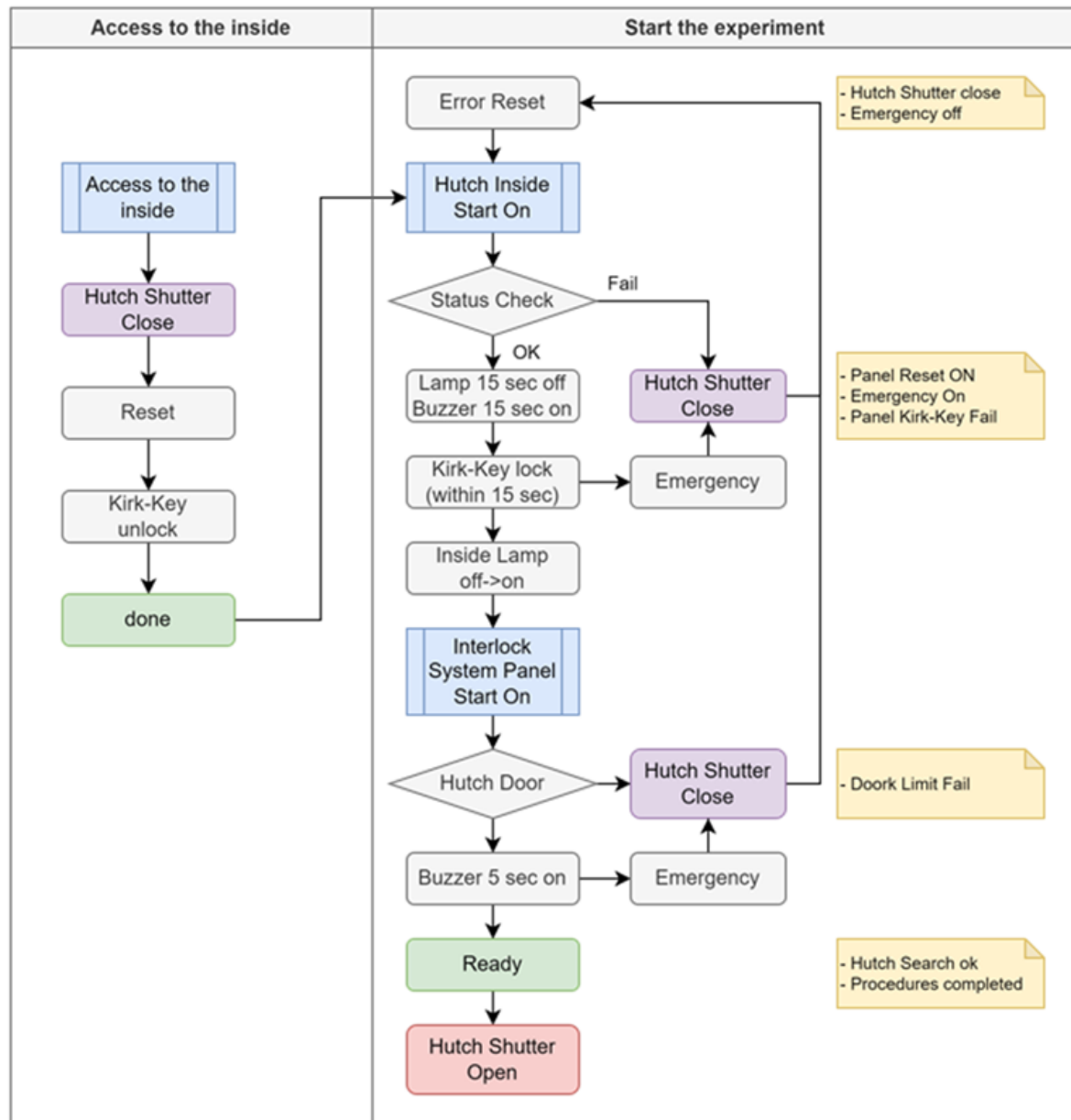
In addition, a warning system and an emergency switch should be used to stop personnel inside from opening the safety shutter. In addition, in the case of a hutch with multiple doors, limit switches should be installed on all doors, and the safety shutters should be operated only after confirming whether the door is open or closed. A status panel should be installed on the outside of the experimental hutch so that users can easily understand the status of the experimental hutch. <Figure 4.1.5.7> shows the interlock system applied to the hutch.



<Figure 4.1.5.7> Configuration of hutch interlock system.

When using the hutch, the hutch shutter is designed to be opened only when the hutch door is locked. If the user wants to operate the hutch shutter, users must check if there is anyone left inside the hutch. When the start switch inside the hutch is pressed, the light turns off, the warning light comes on, and a warning sound sounds for a certain period of time. If there is someone inside the hutch, the next process of opening the hutch shutter can be stopped at any time by pressing the emergency switch inside or outside the hutch within the specified period of time that the warning sound sounds.

The hutch interlocking system does not allow a person inside the hutch to release the emergency switch and re-operate the operating switch. It must be re-operated by opening and closing the hutch door. The hutch can only be opened through the prescribed procedure. <Figure 4.1.5.8> shows the procedure for entering and exiting the hutch.



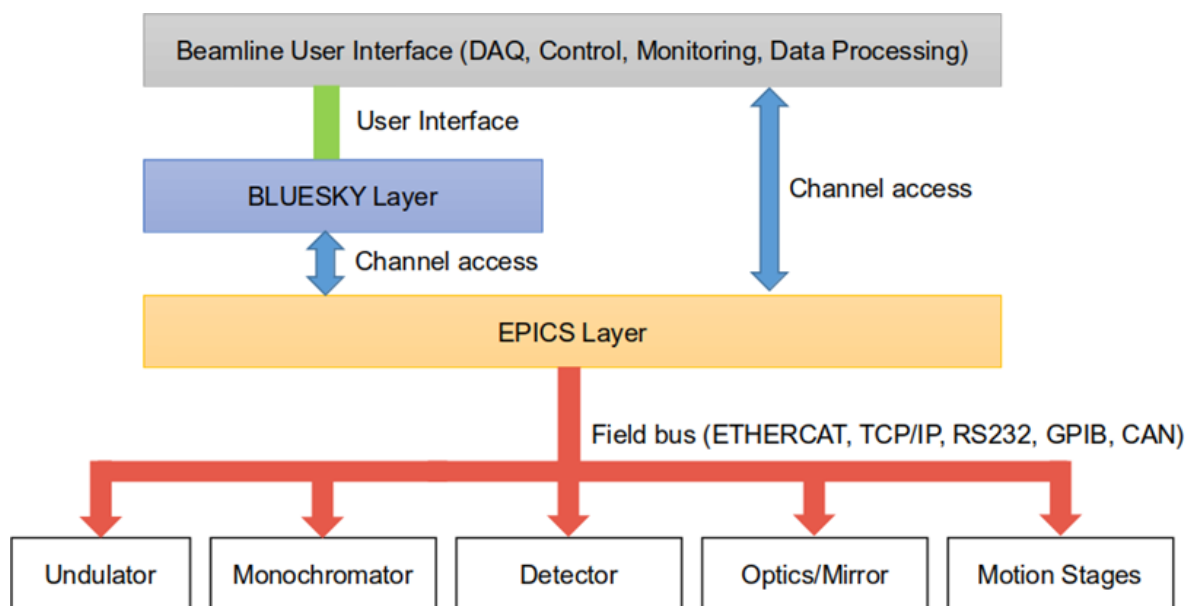
<Figure 4.1.5.8> Entry procedures of experimental hutch.

4.2 Beamline Control/DAQ

4.2.1 Concept

Beamline Control/DAQ includes the following tasks:

- Beamline network
- User interface of insertion device
- Optical device control and beamline components control and monitoring
- Synchronization of related devices for data acquisition
- Beamline diagnostic support and sample environment control
- Data acquisition and storage
- User interface and experiment control



<Figure 4.2.1.1> Configuration of beamline Control and DAQ.

The system configuration is as shown in <Figure 4.2.1.1>. All devices, including optical devices, detectors, diagnostic devices, and driving devices, use the EPICS (Experimental Physics and Industrial Control System), and there is a device server (EPICS Layer in <Figure 4.2.1.1>) implemented with multiple IOC (Input Output Controller) for each device. It is accessed and controlled from clients (Monitoring, DAQ, Archive, etc.) using the CA (Channel Access) / PVA (Processor Variable Access) protocol. The control and measurement devices of the beamline configure their own Virtual LAN for the beamline,

considering their functions and network occupancy.

Server virtualization is applied to minimize the number of servers for easy maintenance, and the virtualization infrastructure is advanced through the configuration of HCI (Hyper Converged Infrastructure) and XCP-NG, an open source that patches XEN, is applied. Through this, various X86-based Guest OS support (Windows and Linux, etc.) required for beamline control and DAQ is possible, so Debian 11 Linux is standardized as the operating system, but there is no need to specifically define a single operating system.

A. Control

Control of beamline components is implemented with EPICS IOC. Related modules utilize synApps for stability, performance enhancement, and documentation, except when not supported or absent.

- EPICS Base: Version 7.x

- synApps: http://epics-synapps.github.io/support/synApps_docs_all.html

EPICS V7 is the latest development thread in the toolkit and allows for more complex data structure communication over TCP/IP, called Process Variable Access (PVA). PVA works with Channel Access (CA) to allow generic process variables (PVs) to exist on the same network as PVA data. PVA is a significant development for maintaining metadata along with data, making it immediately applicable to image capture or processing applications performed at beamline detectors. The user interface for device management will use the Phoebus application that does not use the Eclipse/RCP framework of CS-Studio.

The principle is to use EPICS Base version-7, which supports data compression of 2D detectors that supply images with large data volumes and can expand the range of supported data types beyond scalar and array types. The beamline components, except the detector, are implemented as Soft IOC. Position-synchronized data acquisition, which will be completed in 2024, is under development with an FPGA-based IOC. This data is also required for data counters and on-the-fly tests. The counter and position-synchronized signal generator receive incremental encoder signals as position-synchronized signals and divide them to generate measurement and synchronization signals.

The field bus used for real-time control communication of EPICS IOC and beamline devices uses EtherCAT for devices with a control speed of less than 1,000 Hz. EtherCAT is

an Ethernet-based field bus system whose protocol is standardized. The following are considerations for EtherCAT applications:

(1) Network Topology

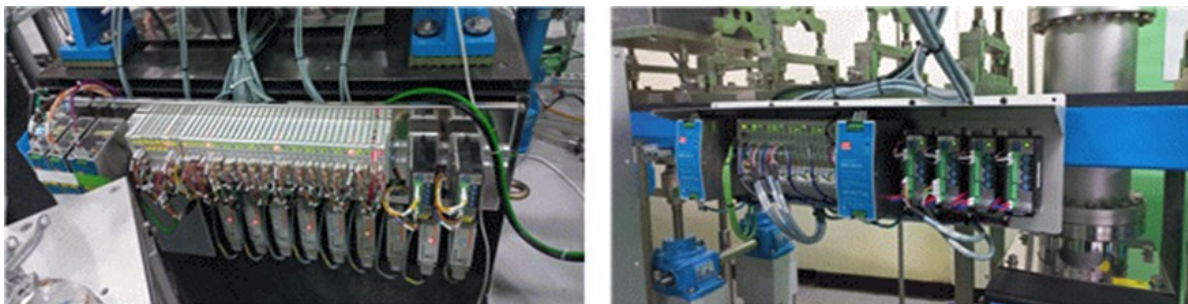
EtherCAT provides a flexible networking topology, but since experimental conditions change due to the characteristics of the beamline, frequent changes in equipment are required. A STAR topology is applied that can flexibly adapt to such changes and minimize control system reboots due to hardware changes.

(2) EtherCAT Realtime Master

As a real-time control system, jitter in the network master causes jitter in the entire control system. TwinCAT3 from Beckhoff, the developer of EtherCAT, is applied.

(3) Controller Program Language

Devices that do not require real-time control of the beamline use a PLC (Programmable Logic Controller). TwinCAT XA will be used as PLC. <Figure 4.2.1.2> shows the appearance of devices that use EtherCAT.



<Figure 4.2.1.2> Optics and slit control system with EtherCAT.

The optical system, detector alignment device, spectrometer, slit, and other adjustment devices are driven by motors. Motors are in the category of non-real-time and account for approximately 90% of beamline control. The Front-end controller is installed in a 19-inch rack for maintenance. In addition, PTL and some experimental devices install the control module on the support to minimize noise generation through cable simplification, and as a result, the number of 19-inch racks is significantly reduced. The PLC uses TwinCAT3, a PC-based PLC. The PLC task can be separated by important devices (Optics, Sample Load, Slit, etc.), and it is designed to have the same function as changing one motor controller by considering changes such as moving, changing, and adding devices.

Each task of the PLC is implemented 1:1 with the Soft IOC, and the number of IOCs in the control IOC computer is the same as the number of PLC tasks. Recently, there is a requirement for motion synchronization between the DCM and the insertion device gap control. The insertion device controller will be manufactured with an EtherCAT/TwinCAT3-PLC combination, and the DCM controller will also be configured with an EtherCAT/TwinCAT3-PLC combination, so that operation of each device can be performed first, and then, without hardware changes, it is possible to develop a program for synchronization. The control units, PLCs and instrumentation equipment standardize their drawings using EPLAN.

B. Data Acquisition

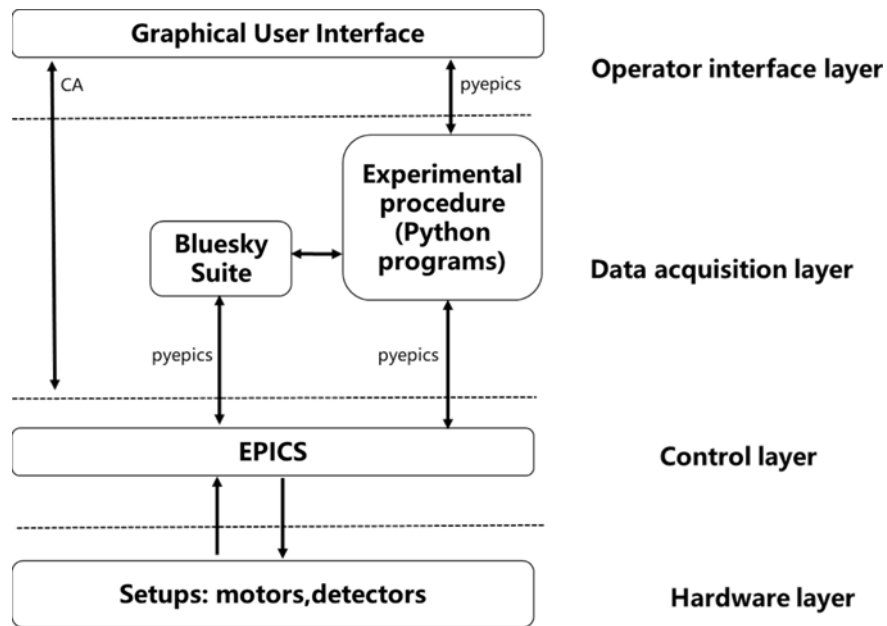
(1) Data Acquisition Concept

Data acquisition is driven by the following concepts:

- Use and expandability of commercial/proven hardware
- Flexibility in using new systems
- Logic for ensuring stable storage and transmission/reception
- Segmentation of physical networks
- Processing of large data bandwidth generated by detectors
- Storage of experimental data using databases
- Storage and processing of local data using ASCII and HDF5 formats

(2) Data Acquisition Layer

- The composition of the data acquisition software is based on Bluesky released by NSLS-II
- The data acquisition layer uses Python-based Bluesky
- The GUI of the operation interface layer is composed based on Qt5, and visualization uses pyqtgraph



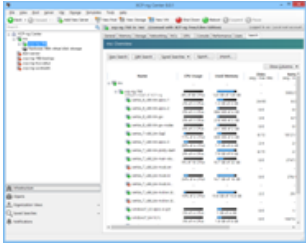
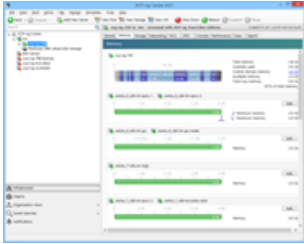
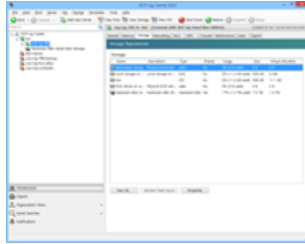
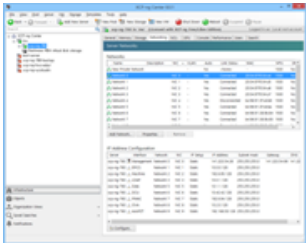
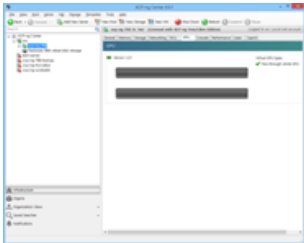
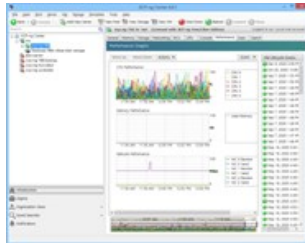
<Figure 4.2.1.3> Control (EPICS) & DAQ (Bluesky) Standard Framework Relationship Diagram.

(3) Data Acquisition System

- System unification and centralized management through xcp-ng virtualization application
- Consistency of operating system for interoperability between systems
- Bandwidth expansion of network devices (≥ 100 Gbps)
- Utilization of InfiniBand (Infinite) to ensure short latency

(4) Establishment and Management of Data Acquisition System

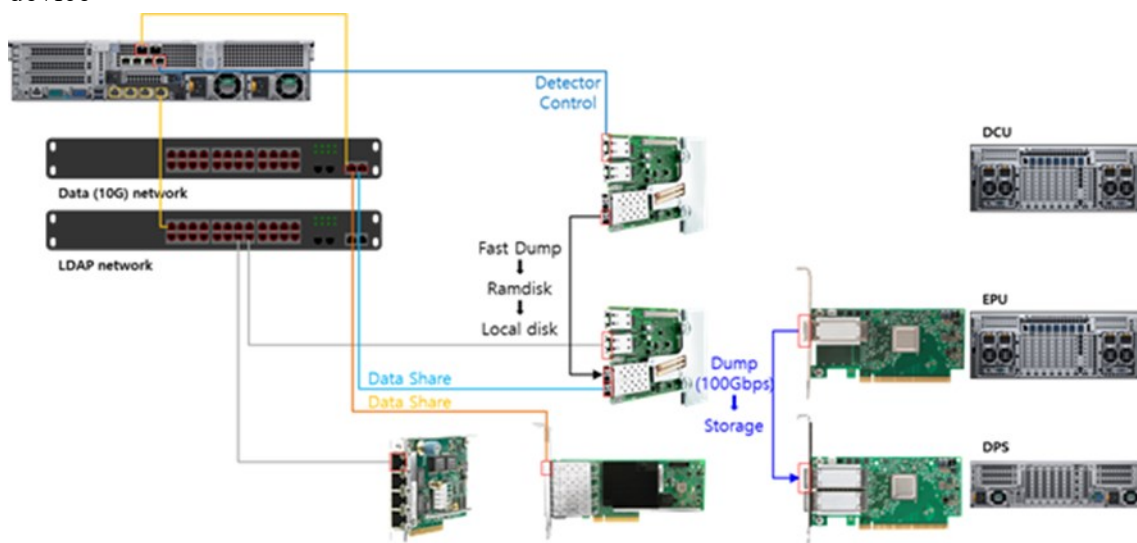
- System management through xcp-ng center tool

Virtual machine management	Memory management	Hard-disk management
		
Network management	Setting and usage of GPU	Status of system usage (Graph)
		

<Figure 4.2.1.4> Method of managing beamline computer system resources for DAQ.

(5) Data Acquisition and Processing

- Detector control and data measurement through EPICS IOC installed in DCU
- Instantaneous data storage in RAM disk area prepared in EPU
- Instantaneous data transmission and processing to DPS through Ethernet or InfiniBand device



<Figure 4.2.1.5> Configuration of network and computer system for DAQ.

C. Data Acquisition Software

(1) Concept

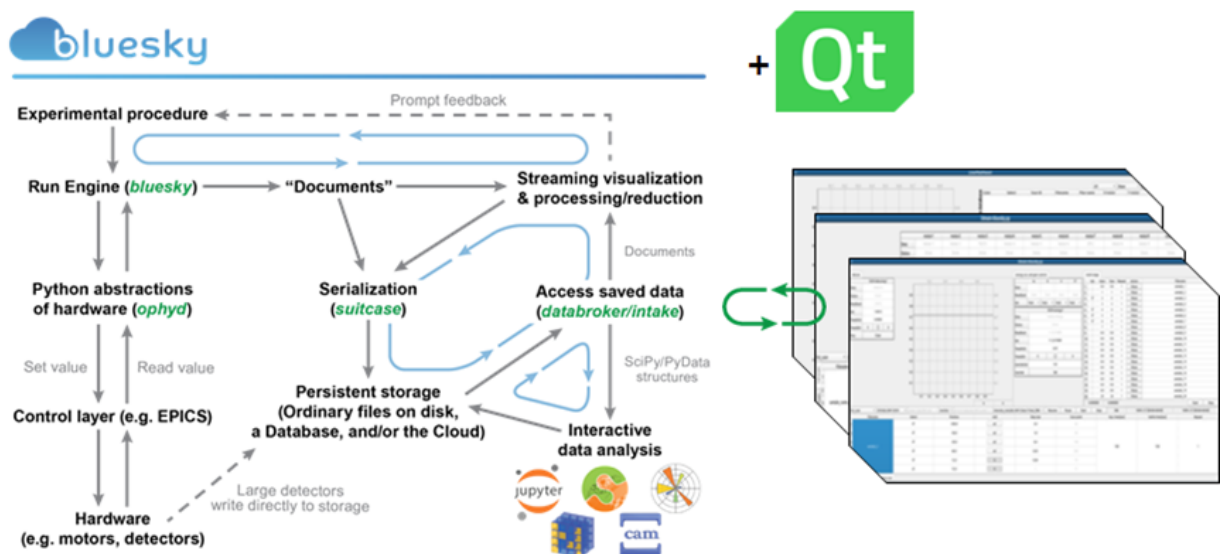
- Bluesky-based data collection, processing and analysis for standardization (MxDC data acquisition software of crystallography beamline is excluded from Bluesky)
- Data collection is provided based on CLI (Command Line Interface)
- Develop and provide GUI (Graphics User Interface) for static/repetitive data collection

(2) Tools

- Software development and operation environment uses Python ($\geq 3.10.0$)
- GUI for user convenience uses Qt5 ($\geq 5.14.2$)
- Pyqtgraph (opengl) graphic library is used for data visualization
- Data acquisition (excluding MxDC) uses bluesky, ophyd, and databroker Python packages
- Data management uses MongoDB system

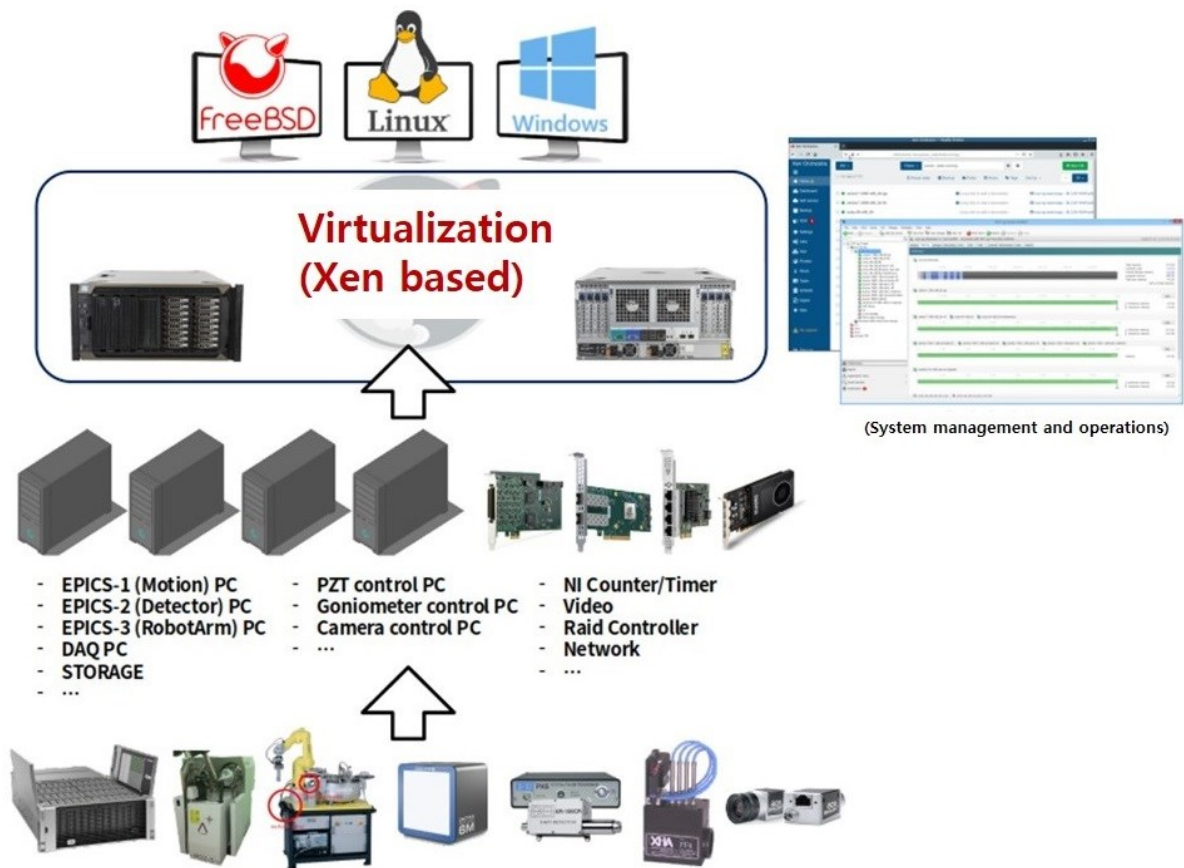
(3) Hierarchy and Flow

- Ophyd: Abstraction of hardware devices (motors, counters/timers, detectors, measuring instruments, etc.)
- Bluesky: Acquire data (procedure) according to the experimental plan using abstracted hardware
- Suitcase & Databroker: Store and manage data acquired through Bluesky



<Figure 4.2.1.6> Example of DAQ processing and document system.

D. Beamline computer system



<Figure 4.2.1.7> Virtualization application of beamline computer system.

A beamline consisting of control/detector/DAQ/special devices uses various computers for various purposes. <Figure 4.2.1.7> shows the application of beamline computer system virtualization. Depending on the supplier, the operating system used varies, and the number of operating systems used increases over time. As the number of devices increases, additional computers gradually increase. As the number of computers increases, experiments may be stopped due to sudden failures and management is difficult. Apply virtualization techniques that enable management and failure response, and rapid creation of new computers when necessary. The virtualization technique, which places a powerful computer and network in the center and allows creation of multiple soft computers internally, has the advantages of rapid response to failures, separate computer environments by function, and 100 GBit internal network speed between each computer.

Except for hardware-dependent devices (devices that do not support path-through), all computers use virtualization techniques to create virtual computers for specific purposes and

store images separately to enable rapid recovery in the event of a failure. It is not necessary to use only virtualized computing infrastructure, and the computing infrastructure should provide both local servers and central servers. The primary function of these servers is to provide a platform for running EPICS IOC. Containerized environments allow for the isolation of specific versions of the server OS from the OS required to run the IOC itself. This allows the server OS and IOC OS to evolve and be updated without interdependence. The local server is prepared to be instantiated close to the hardware controlled by the IOC. The central server provides the ability to run multiple IOCs and other monitoring systems on each beamline virtual computer. The computing infrastructure also provides operator workstations and the EPICS archiving tool.

The computer requirements for the virtualization server are as follows:

- CPU Core: 128 core
- Memory: 1,024 GByte
- Video card: 4 ea
- Storage device: NVME (1T), SSD (20T)
- LAN CARD: 100 G×4, 10 G×2, 1 G×2 ea

The VM to be run on the hardware configured as above will run 2 EPICS IOCs (Windows, Linux), 4 work stations (DAQ, beamline monitor×2, data processing terminal), and Archive Appliance.

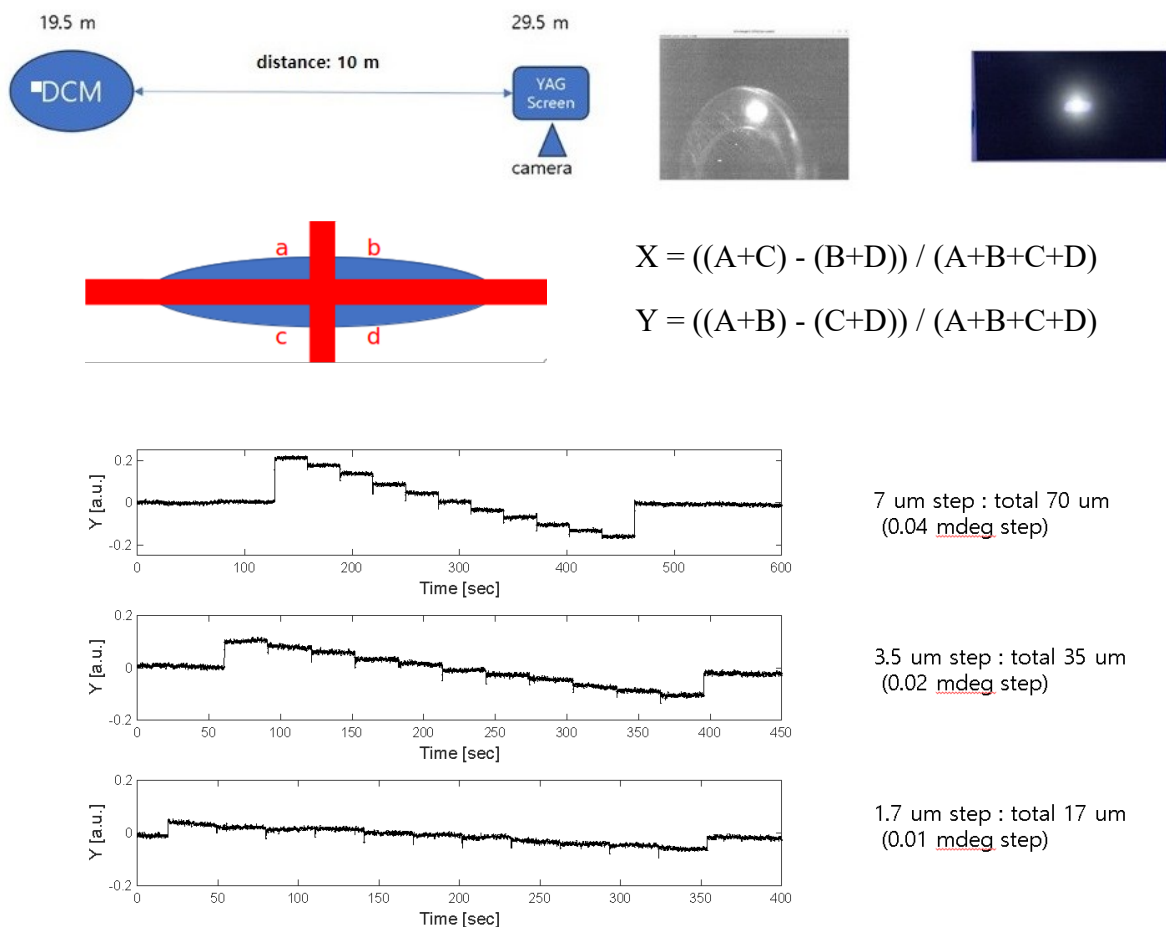
(1) Vision for Diagnosis (Camera System)

Among the diagnostic devices that identify the location of the photon beam from the light source to the experimental device, visual confirmation through a camera is required. If a camera supporting “GigE Vision/GenICam” is used, the image can be digitized by applying EPICS areaDetector. Using the image supplied from the AreaDetector, you can visually confirm the beam shape, measure the beam size at each location, and record the long-term drift of the beam position. The installed camera uses POE to reduce the number of power cables, configures a separate network for the camera, and requires an Ethernet switch of 1 Gbit or more that supports POE.

The position measurement calculates the position by applying the QBPM method to the image supplied from the IOC that applied the areaDetector. In order to obtain accurate position information, a GUI that designates and calculates four areas is required. All cameras that are essential for diamond filter for thermal load reduction, YAG for beam position

diagnosis, mirrors, DCM, etc. will be installed with EPICS areaDetector so that images will be digitized and location information, brightness information, etc. will be recorded in the archive.

The results obtained by implementing QBPM using the Vision system (camera) and EPICS areaDetector are as follows. If the pixel size of the camera and the type of lens are appropriately selected considering brightness, distance, size, etc., the resolution will be improved by more than twice the results obtained in the test.



<Figure 4.2.1.8> Utilization of diagnostic device with Vision system for YAG/Diamond filter.

The camera images converted to AreaDetector can be used to obtain profiles of specific areas using ROI and plugins, check sums and changes, and record and view through archives, which are used to track changes in the status of beamline. <Figure 4.2.1.8> shows an example of applying a vision system to a YAG/Diamond filter.

(2) Archive System for Beamline Status Monitoring

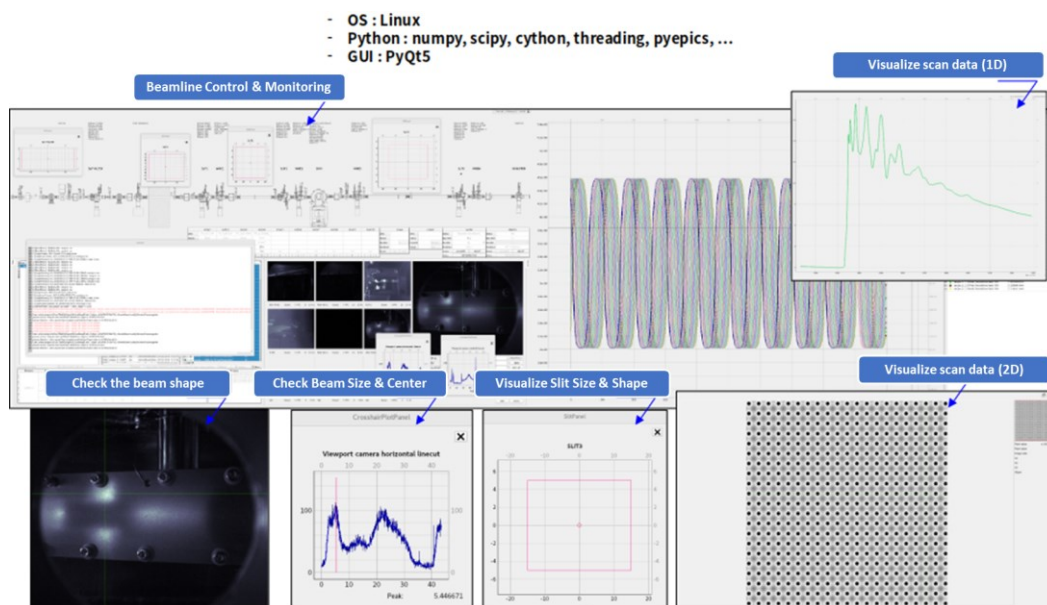
Recording the status of the beamline, such as vacuum level, temperature, motor status, and beam position, as time series data is used for beamline maintenance, management,

accident prevention, and cause tracking.

For this purpose, an EAA (EPICS Archive Appliance) is built in each beamline to store, manage, and retrieve a large amount of data supplied from the EPICS control system. The repository uses the local storage of the beamline integrated computer system. EAA can set the life cycle of data, so that older data can be automatically removed. EAA can change the cycle of PV to be stored according to the settings. Static data is targeted to be stored at 1-second intervals, and one beamline is expected to not exceed 10,000 PVs, so less than 1 TB of data will be accumulated per year. The stored data can be searched and visualized by the beamline manager with CSS and web browser, and supports raw data export and provides a Python interface.

(3) Alignment and Operation Program

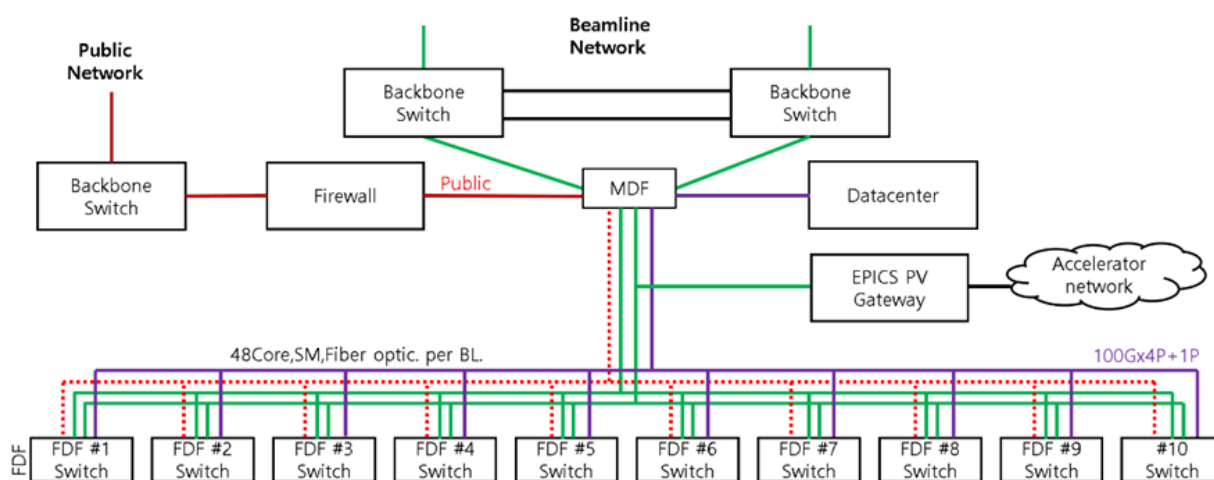
An operation program is needed to diagnose and check the status of each part installed in the beamline, and this is a client program with IOC as a server. For the purpose of setting up and diagnosing the device, MEDM/EDM/CS-Studio will be used, and a management program using Python + Qt will be implemented for the purpose of user interface for beamline alignment and beamline status monitoring.



<Figure 4.2.1.9> Program of beamline metenance and alignment.

(4) Beamline Network

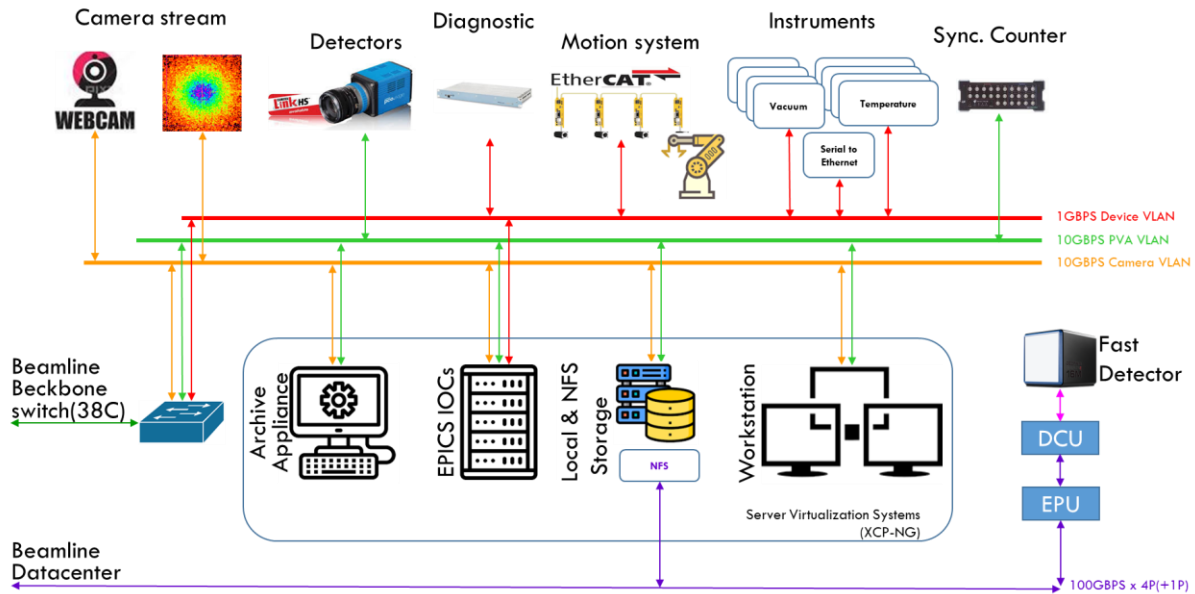
Beamlines do not need to exchange real-time information with adjacent beamline devices. Networks are classified into control networks, camera networks, and DAQ networks that constitute beamline hardware, and a network that can support remote experiments may be required. The control network is used to set up and control beamline devices, monitor them, and record the status of the devices that constitute the beamline (vacuum, temperature, beam position, etc.). <Figure 4.2.1.10> shows the overall beamline control network configuration diagram.



<Figure 4.2.1.10> Configuration of the entire beamline control network.

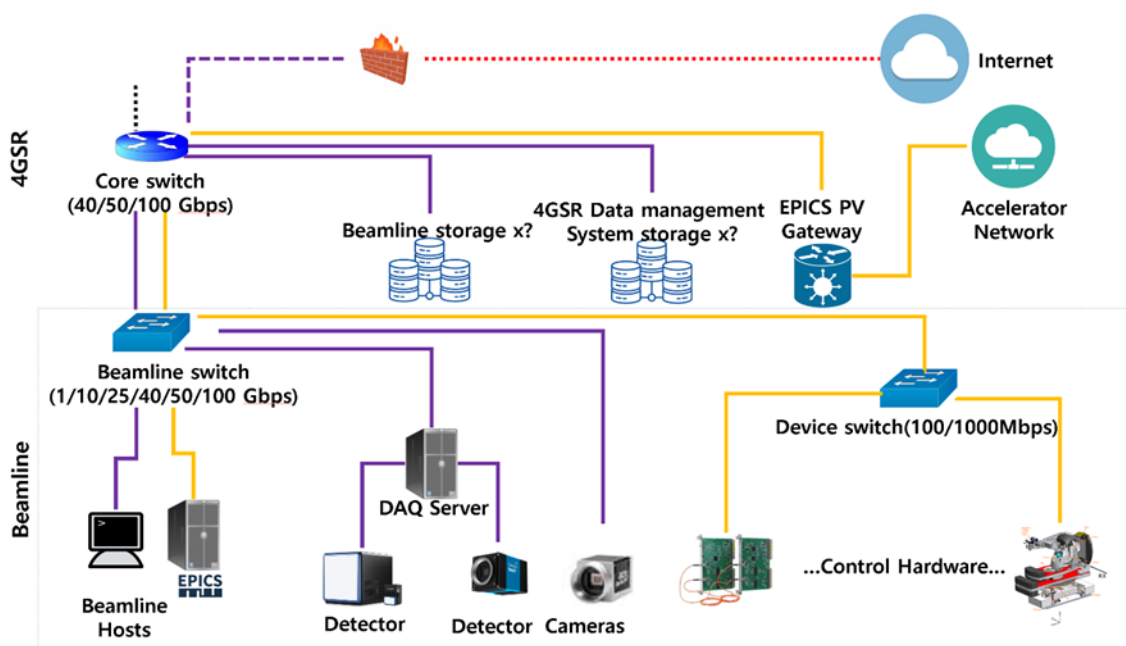
All data exchange with the accelerator control system is done through the EPICS PV gateway. The DAQ network is a high-speed data network that stores large 2D/3D experimental data including detectors and is used for feedback after analyzing experimental data from the data center. The Core Switch is located in the beamline data center, and 48 core optical cables are laid to each beamline. The connection speed is 10 G considering the image beamline, which has a relatively large amount of data. Four 100 G lines are prepared so that beamline experimental data can be stored directly in a remote data center via NFS.

One extra line is added considering the case where it is fed back to the beamline from the data center in the future. <Figure 4.2.1.11> shows the network configuration of each beamline.



<Figure 4.2.1.11> Configuration of each beamline network.

Each beamline constructs a VLAN according to the device configuration as shown in the figure. It is implemented with a camera (10 G), Ethernet devices such as motion and vacuum (1 G), detectors, and EPICS networks (10 G). Networks separated by VLANs enable stable data transmission because traffic generated from devices is not transmitted to separate devices. Open Virtual Switch (vSwitch) operates as software on the virtualization server, so that each virtualization device can secure 100 GBPS without traffic being transmitted externally. Stable data transmission between EPICS IOCs and workstations is achieved using vSwitch.



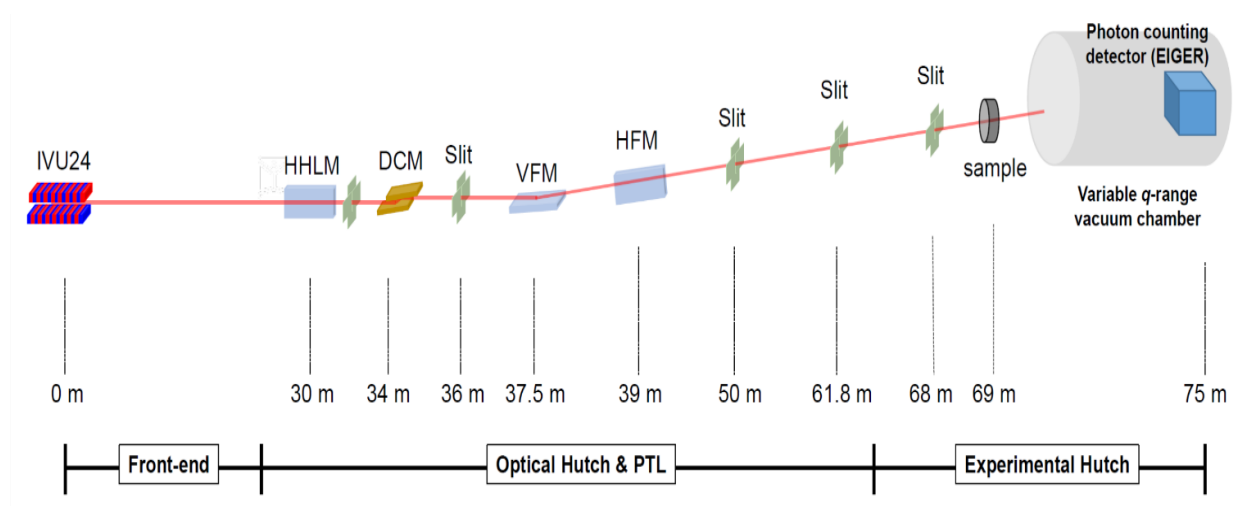
<Figure 4.2.1.12> Configuration of experimental and control data network.

<Figure 4.2.1.12> shows the configuration of experimental and control data network. For beamline that do not use high-speed 2D detectors, there is no need to build a dedicated network to a data center.

4.3 Beamline Optics

4.3.1 The Design Overview of Beamline Optics

As the initial 10 beamline construction project of 4GSR is underway, optical design is in progress, and securing the manufacturing technology for the DCM and mirror devices, which are core beamline components, and localization are recognized as important tasks. To this end, it is necessary to develop optical devices optimized for the beamline characteristics of the 4GSR synchrotron radiation accelerator domestically, manufacture spectrometers and mirror devices so that the beam can be operated stably in the initial 10 beamlines, and secure the technology to improve performance through continuous research and development. <Figure 4.3.1.1> is an example showing the optical device layout of the IVU beamline, and <Table 4.3.1.1> is a summary of the demand for optical devices by 4GSR beamline.



<Figure 4.3.1.1> Beamline layout of 4GSR BioPharma-BioSAXS.

<Table 4.3.1.1> Status of 4GSR 10 beamline optical devices

Beamline	Beam Energy	Resolution	Light Source	Experimental techniques	Applications	Mirror System	Monochromator
1. Bio Pharma-Bio SAXS Beamline (Industry Priority Support Beamline)	5 to 20 keV	8 to 4000 Å (SAXS) $\Delta E/E < 2 \times 10^{-4}$	IVU24	Solution SAXS	Bio	3 EA	1 EA
2. Material Structure Analysis Beamline (IndustryPrioritySupportBeamline)	5 to 40 keV	$\Delta E/E < 2 \times 10^{-4}$	IVU24	Powder XRD, XAFS	Materials, Energy	2 EA	1 EA
3. Soft X-ray Nano- probe Beamline (Industry Priority Support Beamline)	0.1 to 5 keV	sub-micro beam $\Delta E/E < 1.5 \times 10^{-4}$ @400 eV, 4 keV	EPU78 IVU24	XPS, XAS	Semiconductor, Materials	4 EA	2 EA
4. Nanoscale Angle-resolved Photoemission Spectroscopy Beamline	0.1 to 2 keV	Under 100 nm $\Delta E/E < 10^{-4}$	EPU98	ARPES	Semiconductor, Materials	4 EA	1 EA
5. Coherent X-ray Diffraction Beamline	3 to 30 keV	sub-micro beam	IVU22	XRD, CDI	Semiconductor, Geology, Materials, Chemistry	2 EA	1 EA
6. Coherent Small -angle X-ray Scattering Beamline	4 to 40 keV	nm to μm $\Delta E/E < 1 \times 10^{-4}$	IVU20	SAXS/WAXS (including GI, XPCS)	Materials, Chemistry	4 EA	1 EA
7. Real-time X-ray Absorption Fine Structure Beamline	5 to 40 keV	under 100 μm $\Delta E/E < 2 \times 10^{-4}$	IVU24	XAFS	Energy, Environment, Materials, Geology	3 EA	2 EA
8. Bio Nano crystallography Beamline	5 to 20 keV	0.7 to 3.5 Å	IVU20	MX	Bio	3 EA	1 EA
9. High Energy Microscopy Beamline	5 to 100 keV	0.3 to 0.5 μm	Centerbend	Projection imaging	Materials, Energy, Bio	-	1 EA
10. Nano-probe Beamline	5 to 25 keV	below 50 nm @10 keV	IVU24	Ptychography/ XRF	Semiconductor, Materials, Energy, Environment, Chemistry	3 EA	1 EA
Total						28 EA	12 EA

4.3.2 The Design Goals of Beamline Optics

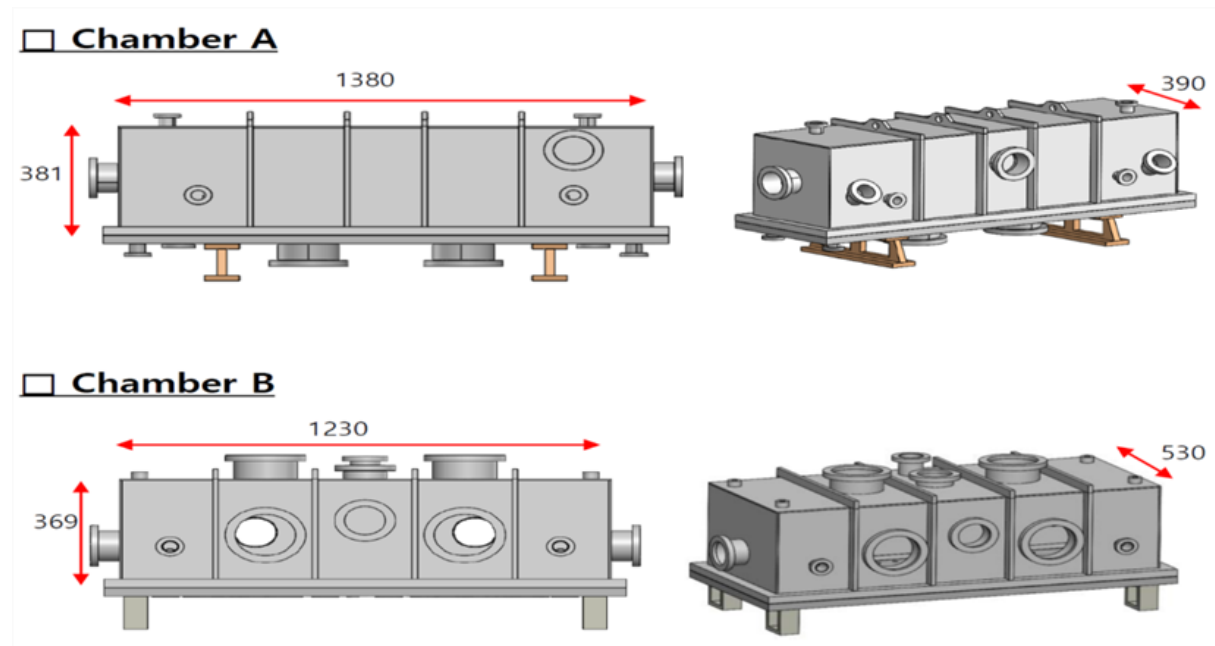
Since the emittance of the 4GSR beam is reduced to less than 1/100th of that of the 3rd generation synchrotron accelerator, the instability of the beam increases. In order to obtain excellent experimental results from the beamline, stable beam provision is essential. Since the performance of optical devices greatly affects the provision of stable beams, it is important to identify the factors affecting the performance of optical devices and design more stable and improved optical devices. The factors that determine the performance of optical devices are largely precision, vibration, temperature, and vacuum. When the beam is focused on the optical device, very precise reflection angle adjustment is required, so precise driving performance with resolution of tens of nm position and tens of nrad angle is required. In addition, components used in optical devices should be manufactured as parts that can be used in UHV (5×10^{-10} Torr or less) environments to reduce surface contamination of the crystal or mirror, which are key components of optical devices, by the beam.

Therefore, materials that can be baked out at 120°C and have a low outgassing rate should be selected and machining techniques that are suitable for use in UHV environments should be considered. And the optical device should be designed to minimize vibrations generated or transmitted from inside and outside, and for this purpose, the girder and chamber design should be designed to increase structural rigidity. Finally, in order to reduce the slope error, which is the deformation of the crystal and mirror reflection surfaces due to the high heat load of the photon beam, an optimized design of the LN2 cooling device structure and cooling channels is required. To this end, an efficient cooling device design is required through thermal and structural analyses, including the shape of the mirror.

4.3.3 The Design Criteria of Beamline Optics

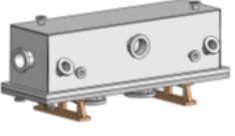
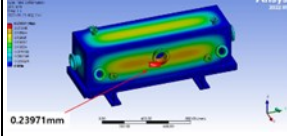
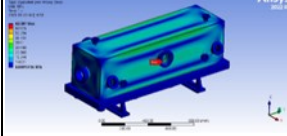
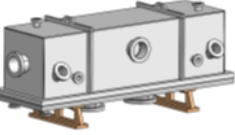
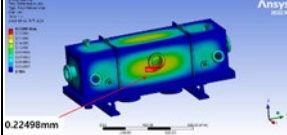
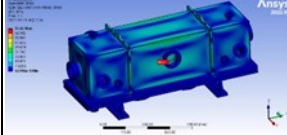
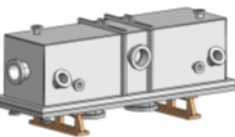
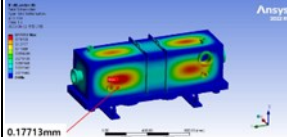
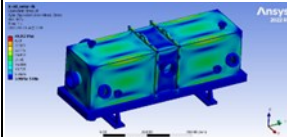
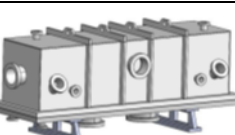
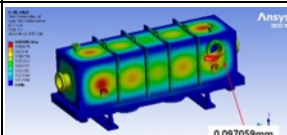
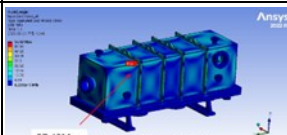
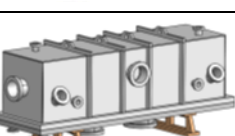
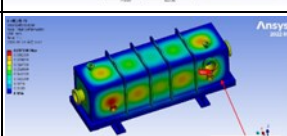
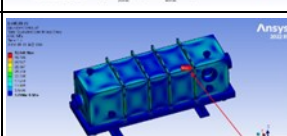
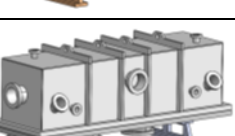
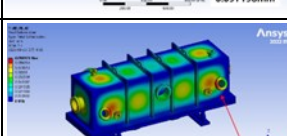
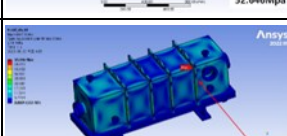
A. Vacuum chamber

The main devices of the 4GSR optical device (spectrometer, mirror device) operate in a UHV environment ($\leq 5 \times 10^{-10}$ torr). Therefore, it is essential to manufacture a vacuum chamber considering the deformation due to vacuum force, and it is also important to develop a device with improved and enhanced performance by comparing and analyzing the optical devices operating in PLS-II and overseas accelerators. In order to consider the deformation of the chamber due to vacuum force in the production of the vacuum chamber, six types were set as analysis models by changing the position and height of the vacuum chamber reinforcement application based on the mirror device of two models as shown in <Figure 4.3.3.1>.



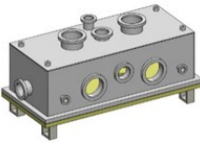
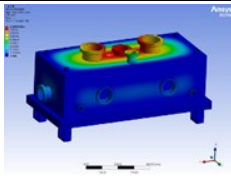
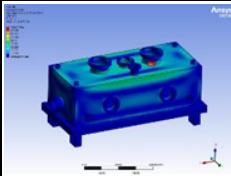
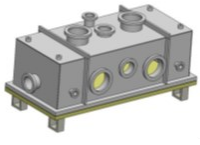
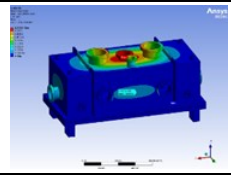
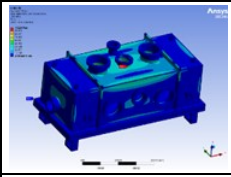
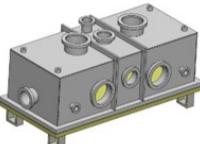
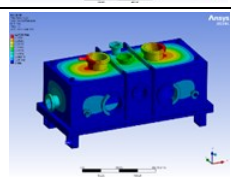
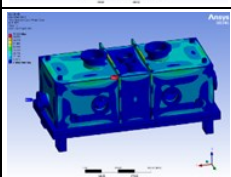
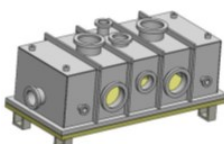
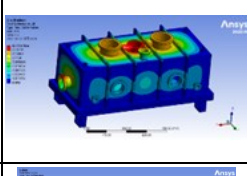

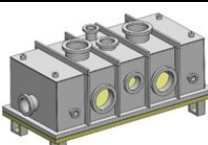
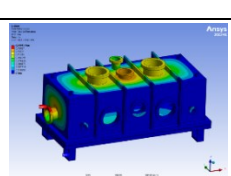
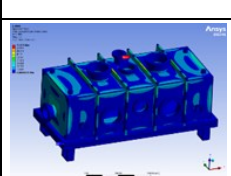
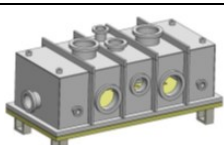
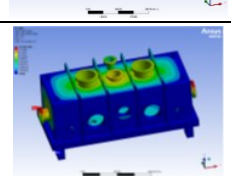
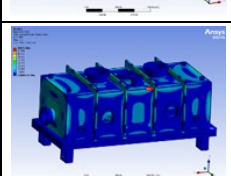
<Figure 4.3.3.1> 3D modeling of type-A and type-B in mirror vacuum chamber.

<Table 4.3.3.1> Deformation results of type-A

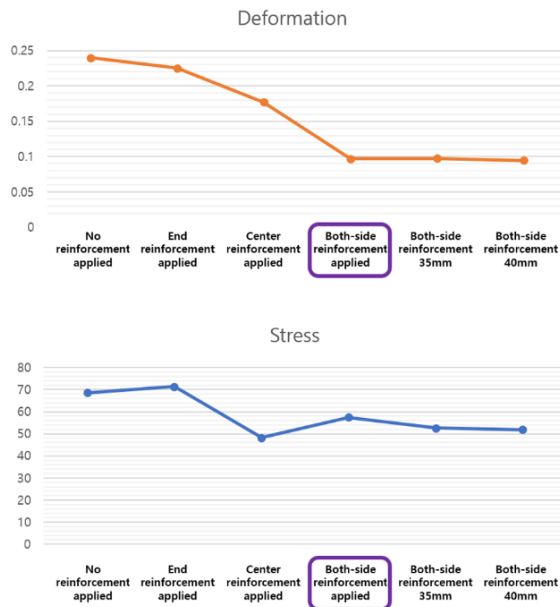
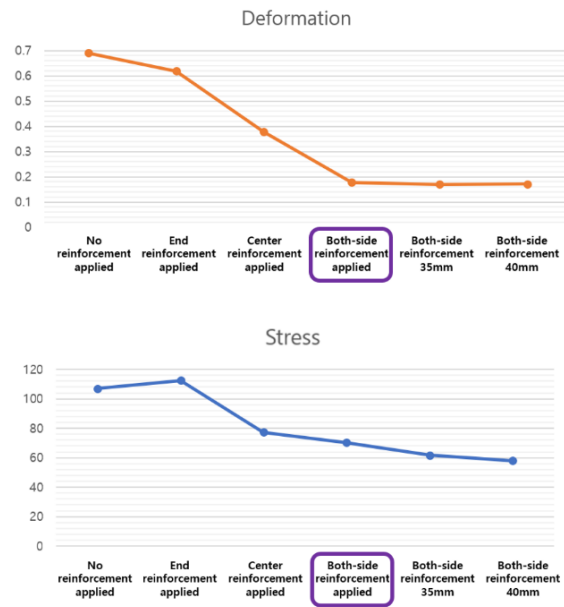
(Chamber A) (390 W×381h×1380 L)	Name	Deformation shape	Total Deformation	Equivalent Stress shape	Equivalent Stress
	Chamber A Noreinforcementapplied		0.23971 mm		68.597 MPa
	Chamber A End reinforcementapplied		0.22498 mm		71.42 MPa
	Chamber A Center reinforcementapplied		0.17713 mm		48.262 MPa
	Chamber A Both-side reinforcement applied (Present)		0.097059 mm		57.42 MPa
	Chamber A both-side reinforcement applied 35mm		0.097198 mm		52.646 MPa
	Chamber A both-side reinforcement applied 40mm		0.094515 mm		51.946 MPa

The model currently being designed is one that applies reinforcement bars to both the center and the end of chamber A, and this has a chamber displacement value of up to about 97 μm . <Table 4.3.3.1> shows six cases deformation of type-A. Compared to the model without reinforcement having a deformation amount of 200 μm , it can be confirmed that the model with reinforcement applied to both the center and end of the chamber has a deformation amount of about half. When compared based on the height of the reinforcement bar, they all have similar values of around 90 μm .

<Table 4.3.3.2> Deformation results of type-B

(Chamber B) (530 W×369h×1230 L)	Name	Deformation shape	Total Deformation	Equivalent Stress Shape	Equivalent Stress	Safety Factor
	Chamber B Noreinforcementapplied		0.69009 mm		106.97 MPa	2.3566
	Chamber B End reinforcementapplied		0.61887 mm		112.39 MPa	2.243
	Chamber B Center reinforcementapplied		0.37789 mm		77.234 MPa	3.2641
	Chamber B Both-side reinforcement applied (Present)		0.17760 mm		70.32 MPa	3.585
	Chamber B both-side reinforcement applied 40mm		0.16973 mm		61.815 MPa	4.0783
	Chamber B both-side reinforcement applied 45mm		0.17167 mm		58.044 MPa	4.3433

The model currently being designed is one that applies reinforcement bars to both the center and the end of chamber B, and this has a chamber displacement value of up to about 178 μm . <Table 4.3.3.2> shows six cases deformation of type-B. Compared to the model without the reinforcement, which has a deformation of 690 μm , it can be confirmed that the current model has a deformation level of about 25%. When compared based on the height of the reinforcement, they all have similar values of about 170 μm .

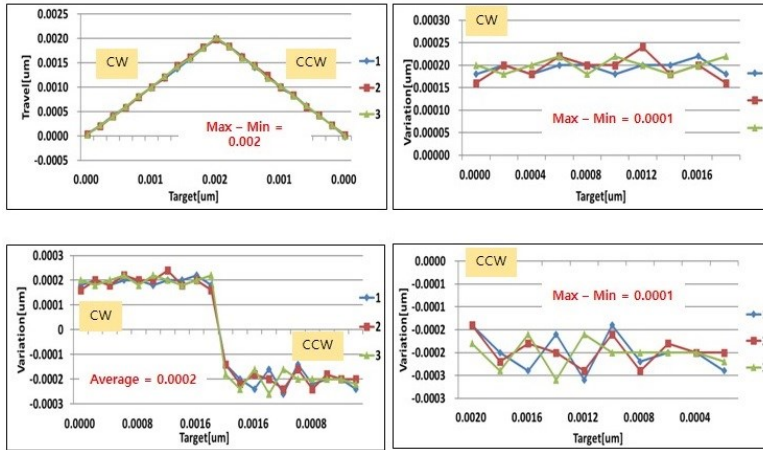
Chamber A (390w x 381h x 1380L)**Chamber B (530w x 396h x 1230L)****<Figure 4.3.3.2> Deformation results of type-A and type-B in mirror vacuum chamber.**

B. Actuator of UHV

As part of the localization technology development project for core devices to secure a high level of precision, Pohang Accelerator Laboratory developed a UHV actuator that has sub-micron precision and can align and adjust optical devices very precisely in a vacuum environment. In order to measure the precision of the actuator and confirm its applicability to optical devices, the precision of the actuator was measured and analyzed when it was moved to the precision levels of $0.2\ \mu\text{m}$, $1.0\ \mu\text{m}$, and $10.0\ \mu\text{m}$ by 10 round trips and 3 repetitions using a 20 nm precision encoder.

The measurement results are shown in <Figure 4.3.3.3>, <Figure 4.3.3.4>, and <Figure 4.3.3.5> below. The precision of an actuator is an indicator of how accurately the actuator can reach the target position, and if the precision level is below micrometers (0.001 mm), it can be classified as a precision-grade level. Therefore, the device with sub-micron level precision can be defined as a precision-grade actuator, and it is expected that it will be applied to the optical devices of the 4GSR beamline as well as the driving units of various UHV devices, contributing to improving the precision of the devices.

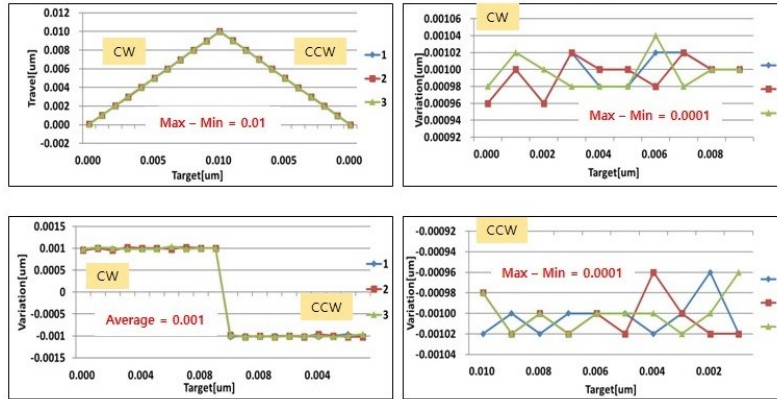
UHV Actuator Precision Measurement Results (0.2um step)



Position Index	Encoder reading (3 times)			PV Error
0.0000	0.00004	0.00004	0.00002	0.00002
0.0002	0.00022	0.00020	0.00022	0.00002
0.0004	0.00042	0.00040	0.00040	0.00002
0.0006	0.00060	0.00058	0.00060	0.00002
0.0008	0.00080	0.00080	0.00082	0.00002
0.0010	0.00100	0.00100	0.00100	0.00000
0.0012	0.00118	0.00120	0.00122	0.00004
0.0014	0.00138	0.00144	0.00142	0.00006
0.0016	0.00158	0.00162	0.00160	0.00004
0.0018	0.00180	0.00182	0.00180	0.00002
0.0020	0.00198	0.00198	0.00202	0.00004
0.0018	0.00184	0.00184	0.00184	0.00000
0.0016	0.00164	0.00162	0.00160	0.00004
0.0014	0.00140	0.00144	0.00144	0.00004
0.0012	0.00124	0.00124	0.00118	0.00006
0.0010	0.00098	0.00100	0.00102	0.00004
0.0008	0.00084	0.00084	0.00082	0.00002
0.0006	0.00062	0.00060	0.00062	0.00002
0.0004	0.00042	0.00042	0.00042	0.00000
0.0002	0.00022	0.00022	0.00022	0.00000
0.0000	-0.00002	0.00002	0.00000	0.00004
Average				0.00003
max-min				0.00006

<Figure 4.3.3.3> Accuracy measurement (0.2 μ m step) of UHV actuator

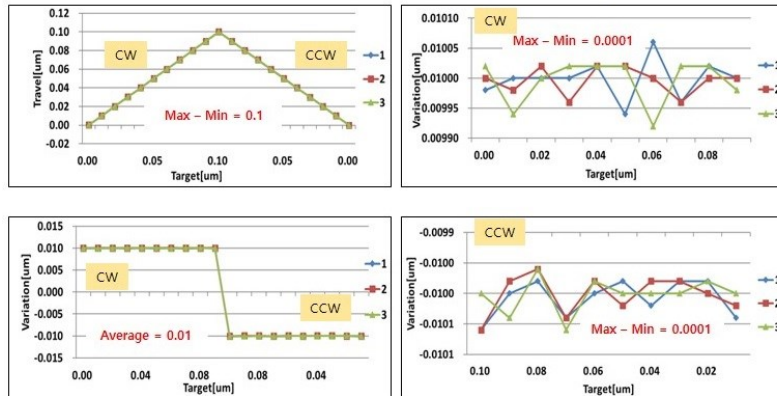
UHV Actuator Precision Measurement Results (1.0um step)



Position Index	Encoder reading (3 times)			PV Error
0.0000	0.00008	0.00006	0.00004	0.00004
0.0010	0.00104	0.00102	0.00102	0.00002
0.0020	0.00204	0.00202	0.00204	0.00002
0.0030	0.00300	0.00298	0.00304	0.00006
0.0040	0.00402	0.00400	0.00402	0.00002
0.0050	0.00500	0.00500	0.00500	0.00000
0.0060	0.00598	0.00600	0.00598	0.00002
0.0070	0.00700	0.00698	0.00702	0.00004
0.0080	0.00802	0.00800	0.00800	0.00002
0.0090	0.00902	0.00900	0.00900	0.00002
0.0100	0.01002	0.01000	0.01000	0.00002
0.0090	0.00900	0.00902	0.00902	0.00002
0.0080	0.00800	0.00800	0.00800	0.00000
0.0070	0.00698	0.00700	0.00700	0.00002
0.0060	0.00598	0.00598	0.00598	0.00000
0.0050	0.00498	0.00498	0.00498	0.00000
0.0040	0.00398	0.00396	0.00398	0.00002
0.0030	0.00296	0.00300	0.00298	0.00004
0.0020	0.00196	0.00200	0.00196	0.00004
0.0010	0.00100	0.00098	0.00096	0.00004
0.0000	-0.00002	-0.00004	0.00000	0.00004
Average				0.00002
max-min				0.00006

<Figure 4.3.3.4> Accuracy measurement (1 μ m step) of UHV actuator

UHV Actuator Precision Measurement Results (10.0um step)



Position Index	Encoder reading (3 times)			PV Error
0.0000	0.00004	0.00004	0.00004	0.00000
0.0100	0.01002	0.01004	0.01006	0.00004
0.0200	0.02002	0.02002	0.02000	0.00002
0.0300	0.03002	0.03004	0.03000	0.00004
0.0400	0.04002	0.04000	0.04002	0.00002
0.0500	0.05004	0.05002	0.05004	0.00002
0.0600	0.05998	0.06004	0.06006	0.00008
0.0700	0.07004	0.07004	0.06998	0.00006
0.0800	0.08000	0.08000	0.08000	0.00000
0.0900	0.09002	0.09000	0.09002	0.00002
0.1000	0.10002	0.10000	0.10000	0.00002
0.0900	0.08996	0.08994	0.09000	0.00006
0.0800	0.07996	0.07996	0.07996	0.00000
0.0700	0.06998	0.07000	0.07000	0.00002
0.0600	0.05994	0.05996	0.05994	0.00002
0.0500	0.04994	0.04998	0.04996	0.00004
0.0400	0.03996	0.03996	0.03996	0.00000
0.0300	0.02994	0.02998	0.02996	0.00004
0.0200	0.01996	0.02000	0.01996	0.00004
0.0100	0.00998	0.01000	0.00998	0.00002
0.0000	-0.00006	-0.00002	-0.00002	0.00004
Average				0.00003
max-min				0.00008

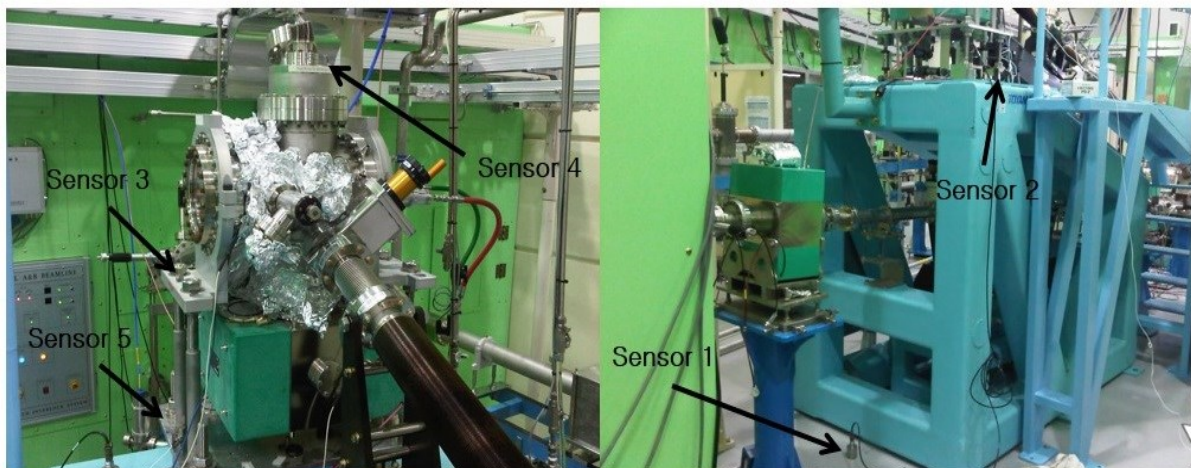
<Figure 4.3.3.5> Accuracy measurement (10 μ m step) of UHV actuator.

C. Vibration

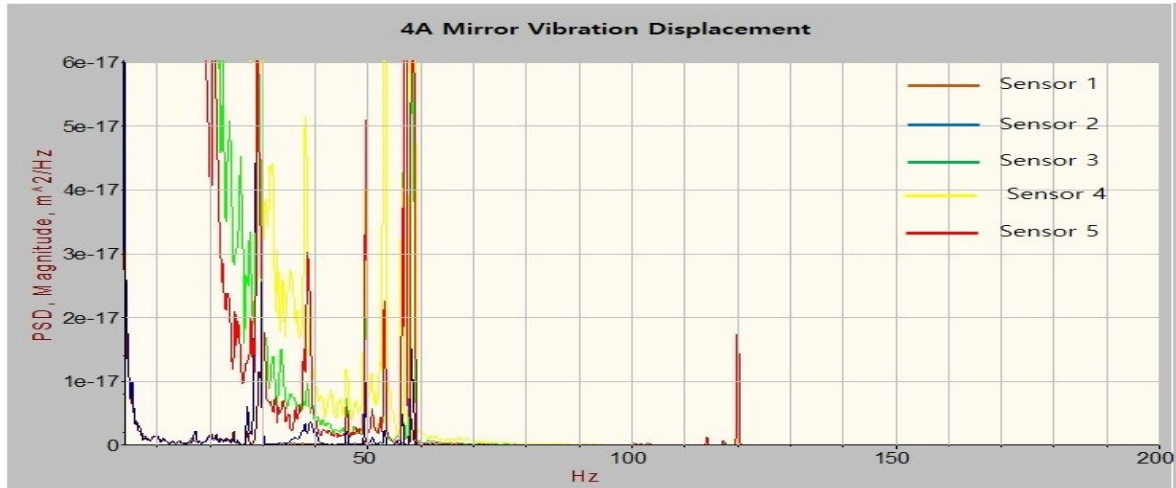
In order to design and manufacture precise and stable optical devices, it is important to check the stability of the device due to the heat load of the photon beam and to examine the structural deformation, but it is also very important to attenuate vibrations from vibration sources such as cooling devices. Therefore, the support structure of the optical device needs to have increased rigidity to reduce vibration displacement, and the design of an adjustment device for efficient alignment of the optical device is also essential.

(1) Vibration Measurement

In order to design the support structure of the 4GSR mirror system, the vibration situation of the mirror system installed in PLS-II was checked. As shown in <Figure 4.3.3.6>, a vibration sensor was attached to the mirror device installed in the PLS-II beamline experimental hall to measure vibration displacement at each location, and the measurement results are as shown in <Table 4.3.3.3>.



<Figure 4.3.3.6> Vibration sensors on mirror system.



<Figure 4.3.3.7> Vibration displacements (PSD) of mirror system.

<Table 4.3.3.3> Vibration displacements at position

Position	RMS	PkPk
1-sensor	7.74 nm	21.5 nm
2-sensor	13.0 nm	36.2 nm
3-sensor	490.5 nm	1.38 μm
4-sensor	651.8 nm	1.81 μm
5-sensor	603.6 nm	1.68 μm

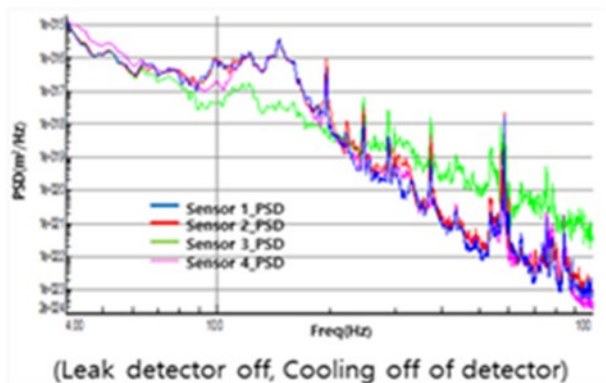
The vibration of the floor, frame, and vacuum chamber where the mirror is installed was measured, and although the vibration displacement at each location does not show a relatively large value, it is necessary to further increase the stiffness in order to obtain the effect of vibration reduction through the damping of the structure. In addition, it is necessary to increase the weight of the structure itself to reduce the vibration displacement, which will be reflected in the design of the 4GSR mirror system. In general, floor vibration is related to repetitive forces generated by human activities such as walking or machines, and walking is particularly more complex than other factors, and the location of the force changes step by step. The applied force is expressed as a combination of sinusoidal forces, and the frequency due to the sinusoidal load is a multiple or harmonic frequency of the fundamental frequency due to the repetitive force, such as the step frequency for human activity. The repetitive force that is time-dependent is expressed by the Fourier series as (Equation 4.3.3.1).

$$F = P[1 + \sum \alpha_i \cos(2\pi i f_{step} t + \Phi_i)] \quad (\text{Eq. 4.3.3.1})$$

Here, P is the weight, α_i is the dynamic coefficient for the harmonic force, i is the harmonic multiple (1, 2, 3, ...), f_{step} is the excitation frequency due to the activity, t is time, and Φ_i is the phase angle for the harmonic frequency. Since the natural frequencies of almost all concrete slabs and steel structures supported on the floor are equal to or very close to the harmonic forcing frequency caused by human activity, resonance amplification is related to most vibration problems in steel buildings.

Therefore, the support structure of the optics needs to be manufactured taking these effects into account. On the floor where the optical device is installed, it is greatly affected not only by human footsteps but also by the air conditioning system. To evaluate these effects, vibration was measured using the KB-mirror system installed in PAL-XFEL. In general, in order to minimize the influence of air conditioners on precision devices, it is necessary to construct a system that indirectly contacts the wind direction, and as shown in <Figure 4.3.3.8> and <Figure 4.3.3.9> below, the vibration influence due to air conditioners cannot be ignored. <Figure 4.3.3.8> shows the vibration displacement results measured while the air conditioner is in operation, and <Figure 4.3.3.9> shows the results measured while the air conditioner is not in operation.

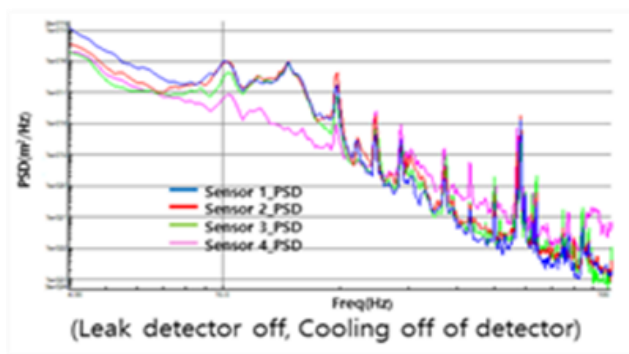
The influence of vibration displacement cannot be ignored, and accordingly, it is necessary to consider and reflect such results in the design of 4GSR optical devices and building air conditioning.



	RMS	PkPk
Sensor 1	36.8 nm	104 nm
Sensor 2	37.0 nm	105 nm
Sensor 3	25.9 nm	73.3 nm
Sensor 4	40.7 nm	115 nm

- Sensor 1 : Upstream of KB Mirror Stage
- Sensor 2 : Downstream of KB Mirror Stage
- Sensor 3 : Floor of EH2
- Sensor 4 : Top plate of KB Mirror

<Figure 4.3.3.8> Vibration displacements in the AHU operating.



	RMS	PkPk
Sensor 1	25.6 nm	71.2 nm
Sensor 2	25.9 nm	73.4 nm
Sensor 3	20.1 nm	56.8 nm
Sensor 4	14.9 nm	42.3 nm

- Sensor 1 : Upstream of KB Mirror Stage
- Sensor 2 : Downstream of KB Mirror Stage
- Sensor 3 : Top plate of KB Mirror
- Sensor 4 : Floor of EH2

<Figure 4.3.3.9> Vibration displacements in the AHU not operating.

In general, the magnitude of the dynamic coefficient decreases with increasing harmonic frequency. The dynamic coefficients associated with the first four harmonic frequencies of walking are 0.05, 0.1, 0.2, and 0.5, respectively. People and machines give a sinusoidal vertical force on their masses.

(2) Vibration Analysis of Girder Systems

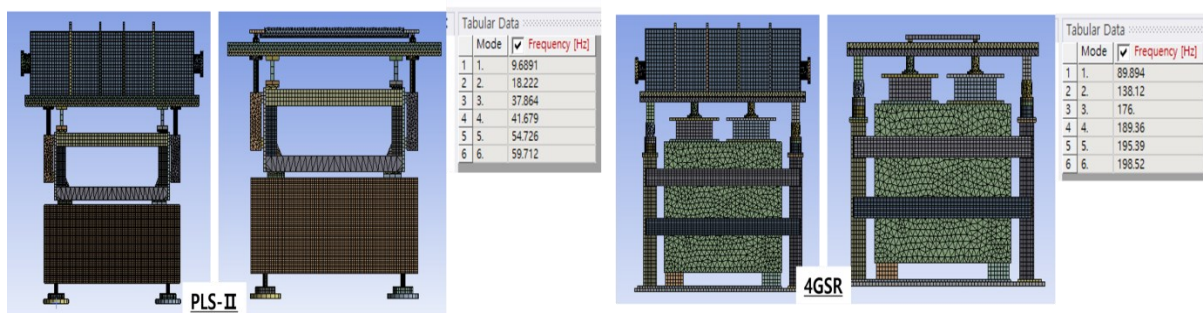
The support structure of PLS-II mirror system has a granite stone plate, and an adjustment device is installed underneath it, which can be aligned in six axes. In addition, a steel frame assembled on the stone plate supports the mirror device. On the other hand, the case of 4GSR girder is epoxy molded on the ground and a double-layer steel base plate device is installed on top of the epoxy molding to align the horizontal direction (x, z) and the high-load wedge mount assembled on the bottom of the granite stone plate enables fine alignment in the height direction (y, roll, pitch) of the device. Most of the major components of the optical device are installed inside the vacuum chamber, and the vacuum chamber creates a vacuum environment for the crystal, mirror, and precision actuators.

However, since external force and vibration caused by the vacuum chamber can be transmitted to the internal device, the internal precision device is designed to have a separate support, so that it has a structure that is more stable against vibration than the existing PLS-II girder structure. The 4GSR girder system is designed to have a stable structure from the vibration of the ground floor by molding epoxy on the floor for vibration prevention and leveling. The natural frequency is the natural frequency or resonant frequency of an object, and damping is the property of reducing vibration by dissipating energy in a vibrating system. The

equation for natural frequency can be expressed as (Equation 4.3.3.2). Here, m = mass, k = stiffness.

$$f_n = \frac{1}{T} = \frac{1}{2\pi} \sqrt{\frac{k}{m}} \quad (\text{Eq. 4.3.3.2})$$

When designing the support structure of an optical device, the stiffness and mass should be changed to avoid resonance occurrence and to have a relatively high natural frequency. Therefore, the natural frequencies were compared through modal analysis of the PLS-II and 4GSR mirror device girders, as shown in <Figure 4.3.3.10>.



<Figure 4.3.3.10> Comparison of natural frequency of PLS-II and 4GSR girder system.

It can be confirmed that the first natural frequency of the PLS-II mirror girder is 9.689 Hz, and that of the 4GSR mirror girder is 89.894 Hz, which is approximately 9.3 times higher than that of the PLS-II mirror girder.

D. Cooling systems

The mirror reflects a beam with high thermal energy, and surface deformation occurs due to heat, and the slope error may increase proportionally depending on the size of the deformation. Therefore, in 4GSR, the cooling system of the PLS-II optical device is analyzed and the results are reflected in building an efficient cooling system.

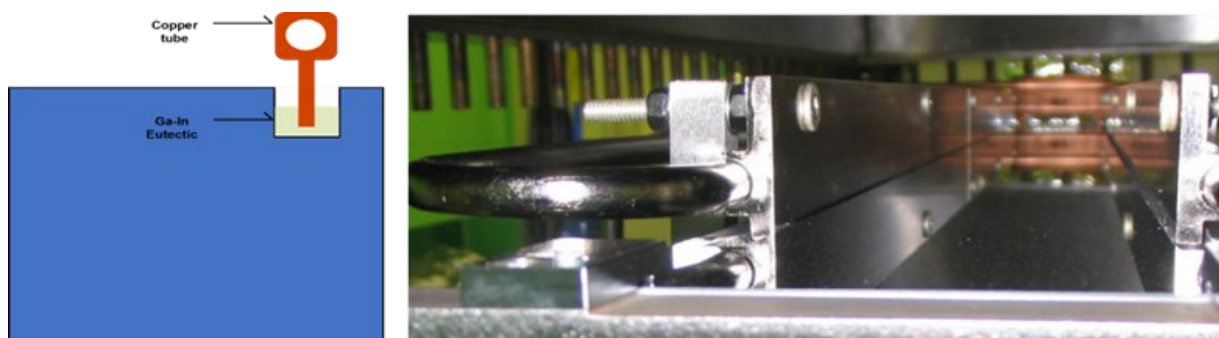
(1) Cooling

There are three types of cooling system for mirrors: Galinstan Bath Cooling, Side Contact Cooling, and direct cooling, which creates cooling channels inside the mirror reflective surface.

○ Galinstan Bath Cooling

This method processes a groove (bath) on the mirror surface or side, injects Galinstan (Ga-In eutectic mixture), and then fixes a copper pad and a copper tube by brazing. It is a method of indirectly cooling the mirror surface by flowing LCW inside the tube. <Figure 4.3.3.11> shows the Ga-In cooling method. This method has been adopted and is being used in many overseas accelerators. Since the mirror and cooling pad do not physically contact each other, they are separated from the vibration generated in the cooling line, and since no physical external force is applied to the cooling pad to contact the mirror cooling surface, the slope error of the mirror can be reduced.

In addition, the cooling pad can be installed only in the footprint section where the photon beam is reflected on the mirror, thereby reducing the temperature difference on the mirror surface and reducing the overall slope error. This method requires caution when assembling or operating the device, as accidents may occur in which the liquid Galinstan may fly and contaminate the mirror surface due to excessive tilting during movement or operation of the mirror device or due to minor carelessness during vacuum operation.

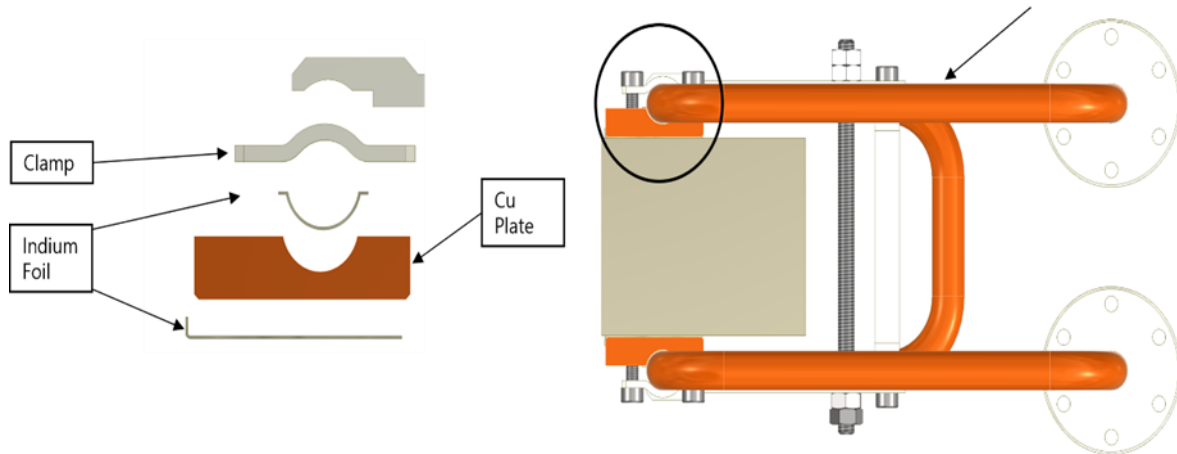


<Figure 4.3.3.11> Mirror Ga-In Bath Cooling.

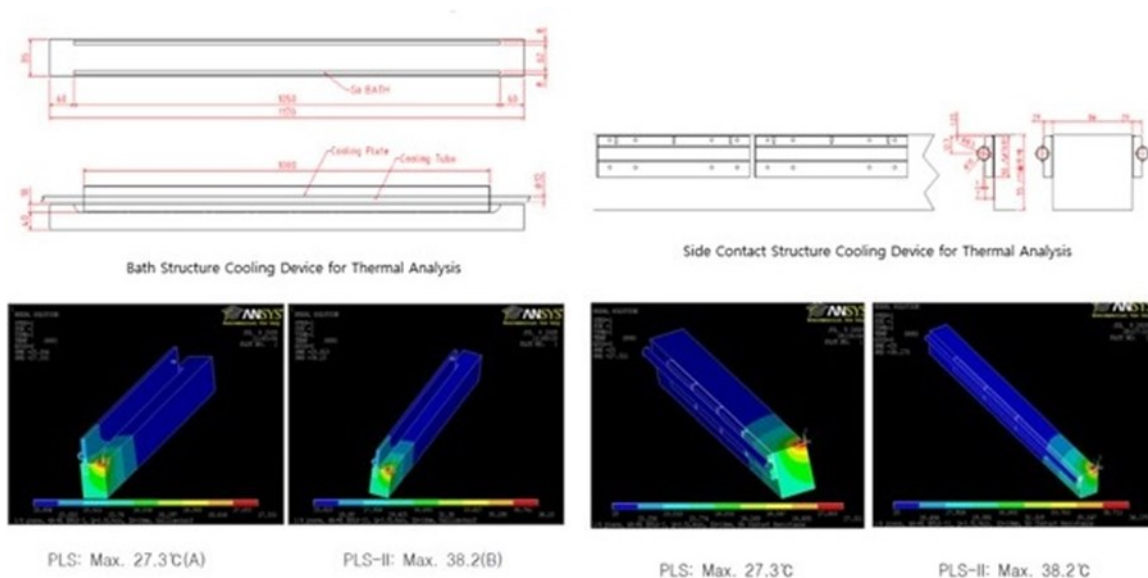
○ Side Contact Cooling

This method is to attach a cooling copper pad to the mirror side and attach the contact surface of the copper pad and the copper pipe with indium foil, and then flow LCW into the copper pipe to cool the mirror. The side contact cooling method is commonly applied to the mirror devices of many overseas accelerators, but since the cooling pad must be pressed against the side of the mirror to increase the cooling efficiency, the slope error of the precisely machined mirror reflection surface can increase due to the physical external force applied to the mirror, so high technology is required during design and assembly.

The better the flatness of the surface where the mirror side and the cooling plate contact each other, the higher the heat conduction efficiency when the two objects come into contact, and thus the higher the cooling efficiency. Therefore, as shown in <Figure 4.3.3.12>, multiple cooling plates assembled in the order of Indium foil + Cu Pad + Indium foil + Water Cooled Cu pipe are attached to both sides of the mirror using a bolt-type clamp method to increase the contact efficiency.



<Figure 4.3.3.12> Assembly of side contact cooling in mirror.



<Figure 4.3.3.13> Ga-In Bath Cooling vs Side Contact Cooling.

In PAL, there is a case where thermal analysis of the Ga-In bath method and the side contact

cooling method was performed using a mirror model, and the analysis conditions are as follows.

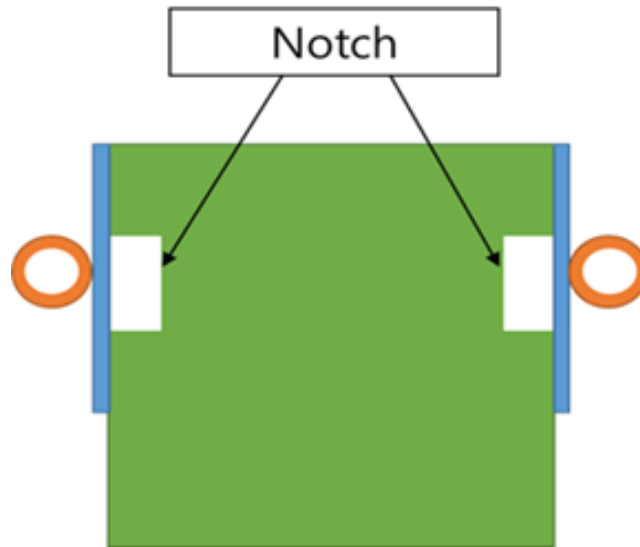
- Incident angle: 4.2 mrad
- Heat Power PLS: 0.0676 kW/mrad²
- Heat Power PLS-II: 0.221 kW/mrad²
- Water Temp: 25 °C

Comparing the analysis results of the two methods, we can see that the temperature difference is not large, and <Figure 4.3.3.13> shows this result. Therefore, 4GSR adopted the side contact cooling method for the mirror device that requires cooling installed in front of the spectrometer, and applied a design to secure the stability of device management and maintenance, increase the adhesion between the cooling device and the mirror side, and reduce slope error.

○ Notch

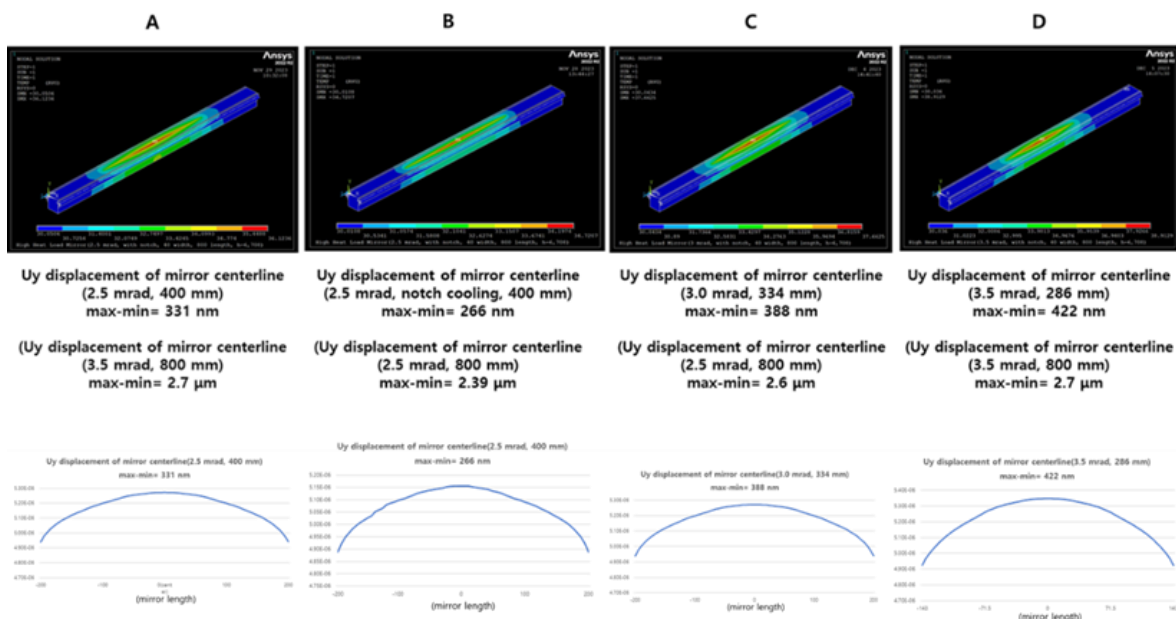
As the emittance of 4GSR is reduced to 1/100 of the PLS-II level, the size of the beam incident on the mirror device is also greatly reduced. As a result, the peak power density acting on the mirror reflection surface is greatly increased, and design technology is required to maximize the efficiency of the cooling device and minimize the slope error. Therefore, efforts were made to reduce the slope error of the reflective surface due to the heat load of the beam by considering various design factors such as the shape and size of the mirror as well as the cooling system. Thermal analysis was performed on side contact cooling using a notch shape. A groove was dug lengthwise on the side of the mirror, and the mirror side and the cooling pad were assembled in the order of Mirror + Indium foil + Cu pad + Indium foil + Copper pipe to increase contact efficiency. <Figure 4.3.3.14> shows the side contact cooling method with a notch shape. The thermal analysis conditions are as follows.

- Distance from source: 30 m
- Mirror length: 800 mm
- Incident angle: 2.5 mrad, 3.0 mrad, 3.5 mrad



<Figure 4.3.3.14> Side contact cooling (with notch).

<Figure 4.3.3.15> shows that the maximum displacement difference value is 331 nm when the beam incident angle on the mirror is 2.5 mrad, 388 nm when the beam incident angle is 3.0 mrad, and 422 nm when the beam incident angle is 3.5 mrad. In particular, it was confirmed that the B type model, which incident the beam at 2.5 mrad and cooled all the notch faces, had a relatively low slope error value. Therefore, in order to improve the slope error of the mirror reflection surface due to the heat load of the beam, it was confirmed that the notch shape on the side of the mirror should be considered, and the arrangement of the cooling structure and the position of the structure assembled with the mirror are also necessary factors.



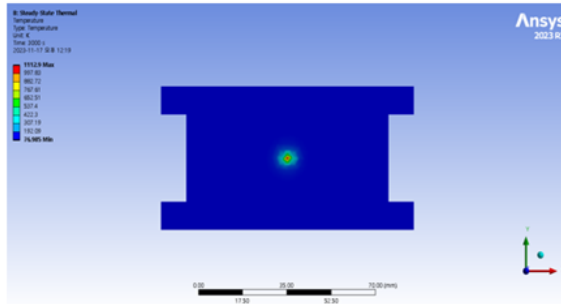
<Figure 4.3.3.15> Thermal analysis results according to incident angle.

○ DCM crystal

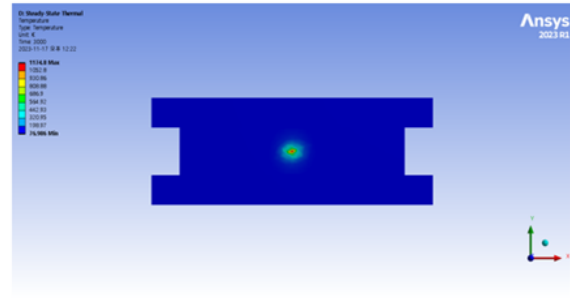
Due to the high heat load of the photon beam, a design technology is needed to minimize the temperature difference between the part of the crystal surface directly irradiated with the beam and the part not irradiated with the beam. The larger the temperature difference on the crystal surface, the larger the slope error, which makes the beam unstable in the experiment. Therefore, it is important to cool the heat of the crystal surface where the beam is irradiated as quickly as possible. In order to cool the crystal quickly, it is important to select the optimal cooling channel structure and crystal size through simulation of the LN2 cooling channel structure and the cooling efficiency of the crystal surface according to the change in crystal width or thickness. The crystal of the 4GSR DCM cooled with LN2, and both types of Si (111) or Si (111) & Si (311) are installed depending on the beamline characteristics.

The DCM cooling system attaches cooling pads (GlidCop) to both sides of the crystal, and Galinstan, a liquid metal alloy, is applied between the crystal and the cooling pad to increase the contact efficiency and heat transfer rate. The DCM that installs two types of crystals also has a cooling system installed in the same way, and the design structure is as shown in <Figure 4.3.3.16> and <Figure 4.3.3.17>. Thermal analysis was performed to examine the cooling efficiency by changing the shape of the cooling channel and the thickness of the crystal, which are important design factors for cooling efficiency, and structural analysis was also performed to minimize crystal surface deformation. The analysis conditions and results are as follows.

- Initial T: 295 K
- LN2 temperature & convection coefficient: 77 K (2,500 W/mm² K)
- Heat flux: 100 W/mm²
- Aging time: 77 K (0 to 25 second)
- Beam irradiation: 25 to 50 second



- Absorbed Power: 100W/mm²K
- Cooling condition: Cu block 77K
(film coefficient: 2500 W/mm²K)
- Beam position Temp: 1178K



- Absorbed Power: 100W/mm²K
- Cooling condition: Cu block 77K
(film coefficient: 2500 W/mm²K)
- Beam position Temp: 1174K

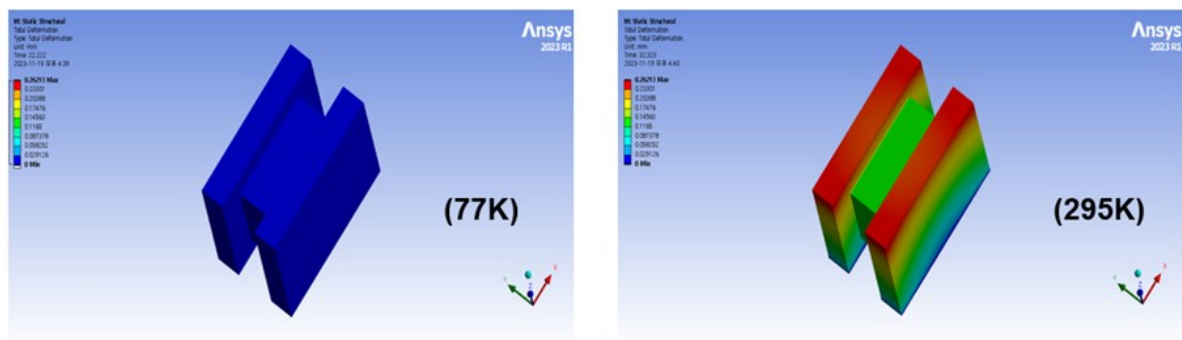
<Figure 4.3.3.16> Thermal analysis results according to crystal shape.

<Table 4.3.3.4> Temperature analysis results of crystal thickness-dependent

Crystal Size	Maximum Temp.
30 mm × 80mm × 40 mm	939
15 mm × 80 mm × 40 mm	918
30 mm × 60 mm × 40 mm	934
15 mm × 60 mm × 40 mm	878
30 mm × 40 mm × 40 mm	968
15 mm × 40 mm × 40 mm	911

As shown in <Table 4.3.3.4>, the lowest temperature result was obtained under the condition of crystal size of 15 mm × 60 mm × 40 mm, and structural analysis was performed under the conditions below to additionally confirm the amount of deformation due to thermal stress. The results are as shown in <Figure 4.3.3.17>.

- Initial T: 295 K
- LN2 temperature & convection coefficient: 77 K (2,500 W/mm² K)
- Heat flux: 100 W/mm²
- Aging time: 295 (0 to 24 second)
- Cooling time: 77 K (25 to 100 second)
- Beam irradiation: 50 to 100 second



<Figure 4.3.3.17> Structural deformation of crystal.

4.3.4 Spectrometers

The spectrometer is the main optical device of the beamline installed in the PTL section of the beamline to separate and extract the monochromatic beam required for the experiment from the white beam extracted from the storage ring. Spectrometers are largely divided into DCM (Double Crystal Monochromator) and DMM (Double Multilayer Monochromator) used in hard X-ray beamline, and SGM (Single Grating Monochromator) used in soft X-ray beamlines. Depending on the experimental purpose of each beamline, an appropriate spectrometer is selected by considering the characteristics such as wavelength range, energy resolution, thermal load conditions, and operating precision.

The DCM scheduled to be installed in the 4GSR beamline is currently under development in four types: Vertical in Vacuum Type and Horizontal in Vacuum Type for the hard X-ray beamline, DMM for the hard X-ray center bender beamline, and SGM for the soft X-ray beamline. The design of the spectrometer for the 4GSR beamline aimed to improve key factors affecting spectrometer performance, such as mechanical precision, vibration stability, and reduction of temperature drift.

A. DCM (Double Crystal Monochromator)

DCM (Double Crystal Monochromator) is installed in the hard X-ray beamline, and uses two crystals to separate and extract specific monochromatic beam required for experimental purposes from white beam. DCM crystal is installed as a 1st & 2nd combination, and 1 pair Si (111) or 2 pairs Si (111) + Si (311) can be installed depending on the energy range required for the beamline experiment. The DCM is composed of silicon crystal (1st Crystal & 2nd Crystal), a precision motion stage that drives the crystal, an optical encoder and various sensors, a control device for controlling and monitoring the entire unit, a cooling device to reduce thermal deformation of the crystal, a granite structure support to attenuate vibrations and enhance the stability of the device, and a vacuum chamber that maintains a vacuum.

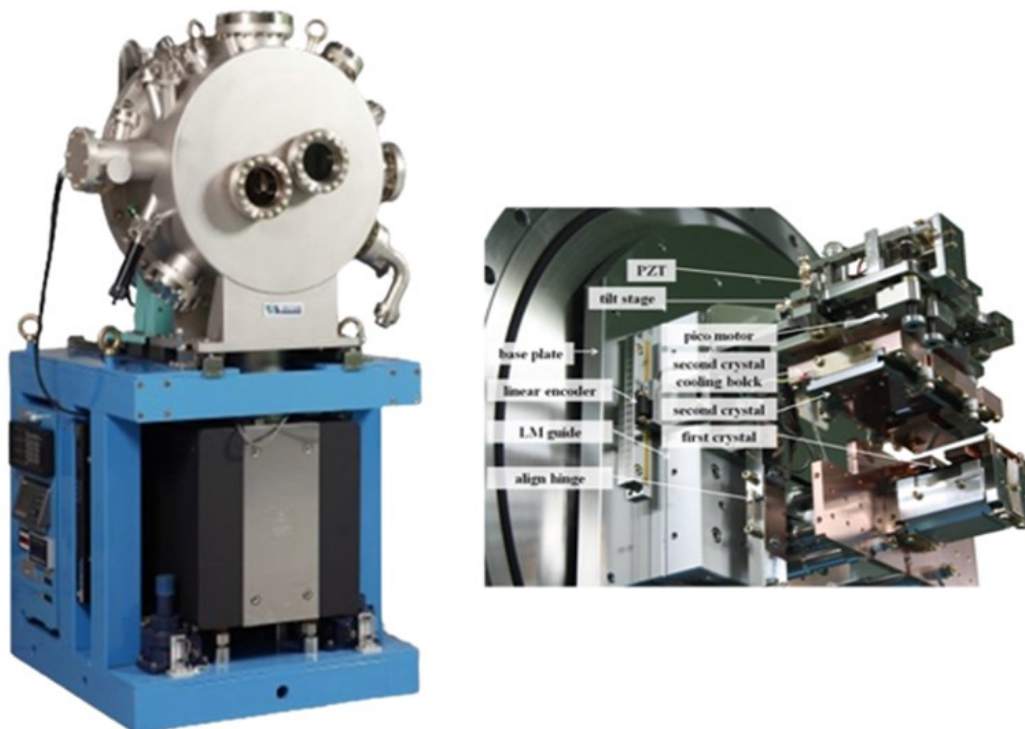
The 1st crystal receives a lot of heat load from the photon beam, so if sufficient cooling is not achieved, it becomes difficult to provide an optimized beam due to thermal deformation, which has a significant impact on the performance of the entire beamline. Therefore, theoretical verification through simulations such as thermal and structural analysis is necessary, and a

prototype reflecting the analysis results was manufactured and tested before manufacturing this product. The 2nd crystal has a much lower thermal load than the 1st Crystal, so it will be applied by combining direct and indirect cooling methods according to the beamline characteristics.

The factors that have a significant impact on the performance of DCM are as follows:

- (1) Cooling device for reducing crystal temperature deviation
- (2) Vibration due to cooling device or structural characteristics
- (3) High-angle resolution goniometer for increasing energy resolution
- (4) Precision driving device for precise alignment of crystal system and stable operation
- (5) Vacuum chamber for maintaining ultra-high vacuum for a long time
- (6) Stable support structure for efficient alignment of DCM

Considering the above factors, various technologies were applied to improve performance. <Figure 4.3.4.1> shows the internal and external shapes of the DCM device installed and operated in PLS-II, and <Table 4.3.4.1> shows the motion specifications of the DCM.



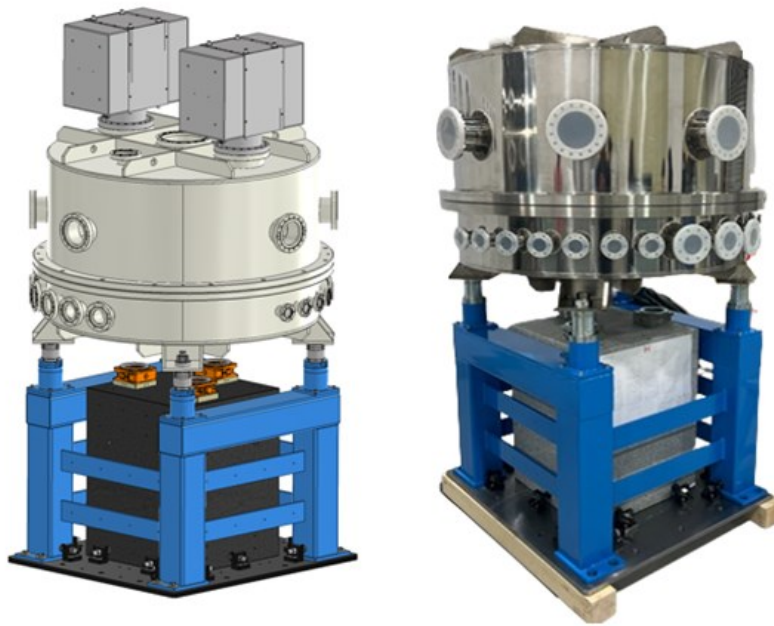
<Figure 4.3.4.1> Assembly of PLS-II DCM.

<Table 4.3.4.1> Motion specifications of PLS-II DCM

Part	Function	Actuator / Monitor (Encoder)	Range	Resolution	Remark
	Bragg angle	Huber 420 goniometer + Paker HV343 micro-stepping motor + Zeta6108 controller	360°	0.07" min	-
		RCN829 angle encoder + ND287 display (Heidenhain)	360°	0.0024"	-
		Electrical limit	0 to 35°	-	Typical
		Mechanical limit	<0°, >35°	-	Typical
2 nd Crystal	Pitch	8302-UHV pico-motor + 8753 driver (New-focus)	> ±1°	0.013"	
		HSA750-050 LVDT + DMC-A2-812 display (Macro Sensors)	> ±1°	-	Calibration necessary
	Fine Pitch	P-843K027 PZT + E-625.SR(PI)	150 μrad	0.3 nrad	-
	Roll	8302-UHV pico-motor + 8753 driver (New-focus)	> ±1°	0.018"	-
		HSA750-050 LVDT + DMC-A2-812 display (Macro Sensors)	> ±2°	-	Calibration necessary
	Y2	N-216K002 PZT actuator + E755.101 controller (PI)	10 to 35 mm	6 μm max 0.03 nm min	Typical
		RGS20-S scale + REF0400E01A Amp + RGH25F15M01C read head (Renishaw) + LY72 display	>30 mm	50 nm	-

(1) Vertical Motion DCM (In-Vacuum Type)

Two crystals move horizontally to select a wavelength, and the driving part for the Bragg angle is installed inside the vacuum chamber. This device has a beam offset value set to 25 mm, and a Vacuum Stage is applied to implement the Horizontal Motion Mechanism between crystals. The 1st crystal system is configured to control pitch and roll, and the 2nd crystal system is configured to control 3 axes: Pitch, Y, and Z. Equipped with PZT, it enables feedback and precise control of the precision pitch drive of the 2nd crystal, and UHV encoder, limit switch, and motor temperature sensor are applied to improve the mechanical position precision and reproducibility of the device. The drive system for controlling the device consists of actuators controlled by stepper motors that can be used in UHV environments ($\leq 5 \times 10^{-10}$ torr), and all signal lines are led out of the vacuum chamber through feedthroughs.



<Figure 4.3.4.2> 4GSR horizontal motion DCM.

<Table 4.3.4.2> Motion specifications of 4GSR DCM (Horizontal motion)

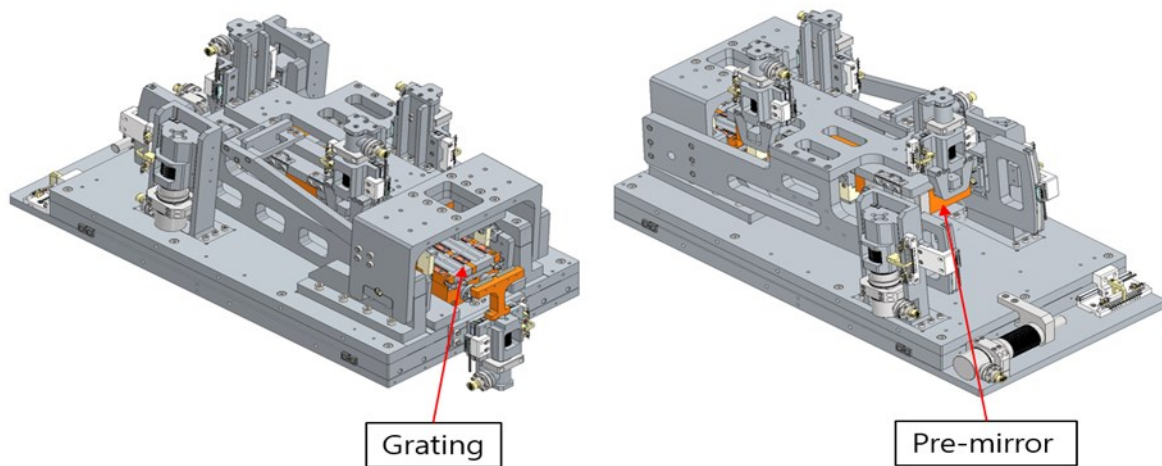
Part	Function	Actuator / Monitor (Encoder)	Range	Resolution	Remark
	Bragg angle	Huber 430 goniometer + Stepping motor + Harmonic gear type + Micro drive	360°	0.34 μ rad min.	-
		RCN829 angle encoder + ND287 display (Heidenhain)	360°	0.012 μ rad	-
		Electrical limit	0 to 65°	-	Typical
		Mechanical limit	$\leq 0^\circ$, $\geq 65^\circ$	-	Typical
1 st Crystal	Roll	VSS32.200.1,2 + GPL (PHYTRON) + Micro drive	$\geq \pm 1^\circ$	5 μ rad	-
		RGSZ20 scale + TI0400A10A + T1631-15M read head (Renishaw)	$\geq \pm 2^\circ$	0.065 μ rad	-
2 nd Crystal	Pitch	VSS32.200.1,2+GPL (PHYTRON) + Micro drive	$\geq \pm 1^\circ$	5 μ rad	-
		RGSZ20 scale + TI2000A10A + T1631-15M read head (Renishaw)	$\geq \pm 1^\circ$	0.013 μ rad	-
	Fine Pitch	P-843K027 PZT + E-625.SR (PI)	$\geq 150 \mu$ rad	0.3 nrad	-
		RGSZ20 scale + TI2000A10A + T1631-15M read head (Renishaw)	$\geq \pm 1^\circ$	0.013 μ rad	-
	Y2	VSS42.500.2,5+GPL (PHYTRON) + Micro drive	10 to 35 mm	0.05 μ m	Typical

B. SGM (Single Crystal Monochromator)

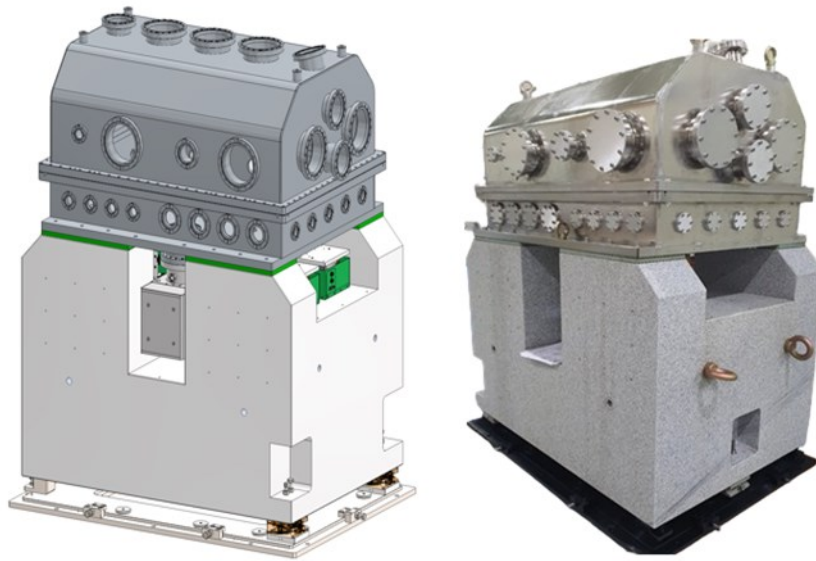
SGM (Single Grating Monochromator) is installed in a soft X-ray beamline, and is a device that separates and extracts a specific monochromatic beam required for the experimental purpose by adjusting the angle of the beam incident on the grating. In general, the pre-mirror and grating are installed together in a single vacuum chamber. The pre-mirror plays a role in allowing the reflected beam to be incident on a certain location on the grating, and as a result, a beam of stable energy can be extracted. SGM is utilized in soft X-ray beamlines that require a relatively wide wavelength selection.

(1) PGM (Plane Grating Monochromator)

PGM is a type of SGM, and this device is an In Vacuum Type with one Pre-mirror and two Grating Substrates installed, and all driving devices are installed and driven inside a vacuum chamber. The Sine Bar system was applied for energy scanning through grating and mirror, and a mechanism was implemented to obtain the desired wavelength by adjusting the grating angle. <Figure 4.3.4.3> and <Figure 4.3.4.4> show the internal device structure of the PGM and the external shape including the chamber and support structure.



<Figure 4.3.4.3> Grating and Pre-mirror of PGM.



<Figure 4.3.4.4> PGM assembly.

This device can control the Pitch, Roll, and Yaw using three actuators, and the Grating Substrate can control the Pitch, Roll, and Yaw using three actuators. The UHV encoder, limit switch, and motor temperature sensor are applied to improve the mechanical position precision and reproducibility of the device. The drive system for controlling the device consists of actuators controlled by stepper motors that can be used in UHV environments, and all signal lines are led out of the vacuum chamber through feedthroughs. To enable stable beam operation, the PGM Motion specifications were determined as shown in <Table 4.3.4.3> to <Table 4.3.4.5>.

<Table 4.3.4.3> Motion specifications of PGM Grating

Position	Motor resolution	Encoder resolution	Precision	Range
Scan motor	$\leq 0.02 \mu\text{rad}$	$\leq 0.03 \mu\text{rad}$	$\leq 0.25 \mu\text{rad}$	0.5 to 4.0 deg.
Pitch align motor	$\leq 0.5 \mu\text{rad}$	$\leq 0.25 \mu\text{rad}$	$\leq 2.5 \mu\text{rad}$	± 1.5 deg.
Roll align motor	$\leq 0.4 \mu\text{rad}$	$\leq 0.25 \mu\text{rad}$	$\leq 2.5 \mu\text{rad}$	± 1.5 deg.
Y align motor	$\leq 0.01 \mu\text{m}$	$\leq 0.1 \mu\text{m}$	$\leq 0.5 \mu\text{m}$	± 15.0 mm

<Table 4.3.4.4> Motion specifications of PGM Pre-mirror

Position	Motor resolution	Encoder resolution	Accuracy	Range
Scan motor	$\leq 0.02 \mu\text{rad}$	$\leq 0.03 \mu\text{rad}$	$\leq 0.25 \mu\text{rad}$	0.5 to 4.0 deg.
Pitch align motor	$\leq 0.5 \mu\text{rad}$	$\leq 0.25 \mu\text{rad}$	$\leq 2.5 \mu\text{rad}$	± 1.5 deg.
Roll align motor	$\leq 0.4 \mu\text{rad}$	$\leq 0.25 \mu\text{rad}$	$\leq 2.5 \mu\text{rad}$	± 1.5 deg.
Y align motor	$\leq 0.01 \mu\text{m}$	$\leq 0.1 \mu\text{m}$	$\leq 0.5 \mu\text{m}$	± 15.0 mm

<Table 4.3.4.5> X-axis specifications of PGM

Position	Motor resolution	Encoder resolution	Accuracy	Range
X align motor	$\leq 0.01 \mu\text{m}$	$\leq 0.1 \mu\text{m}$	$\leq 0.5 \mu\text{m}$	± 25.0 mm

C. DMM (Double Multilayer Monochromator)

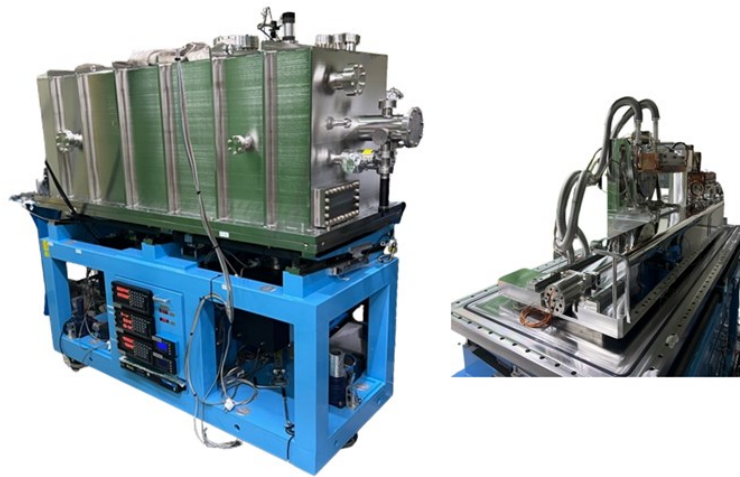
DMM (Double Multilayer Monochromator) is a device that extracts monochromatic beam from white beam using two multilayers. The multilayer of the DMM device consists of 1st & 2nd combinations, and uses Ruthenium/Carbon (Ru/C) and Tungsten/Boron carbide (W/B4C) on the Si crystal to create monochromatic light in the 10–22 keV and 22–60 keV regions, respectively, according to the required energy range. Since the two multilayers are coated at a distance of several millimeters, the position of the Si crystal substrate can be moved to select which multilayer to use. The main devices that make up the DMM are as follows:

- Driving device that controls the movement of the multilayer
- Vacuum chamber that provides an ultra-high vacuum environment
- Cooling device to protect the multilayer from thermal load
- Support structure that supports and aligns the device
- Vacuum pump, etc.

The 1st multilayer produces monochromatic beam through Bragg reflection, and the 2nd multilayer reflects the produced monochromatic beam parallel to the ground. At this time, it can be selected different coating parts by using the linear stage installed in each multilayer, and it can also be moved the multilayers in the Z and -Z directions to pass the beam as it is for white beam use. DMM has a similar driving mechanism to DCM, but the difference is that

DCM uses crystals for Bragg reflection, while DMM uses multilayers that stack two types of materials with large differences in density. In addition, DMM has the characteristic that the wavelength width of monochromatic beam is 1% and the brightness of the emitted light is about 100 times brighter than that of DCM, so it is mainly used in fields where the amount of light is more important than energy resolution, such as X-ray imaging or radiation therapy.

<Figure 4.3.4.5> shows the internal and external shapes of the DMM device, and <Table 4.3.4.6> shows the motion specifications of the DMM. By referring to the operating experience of the DMM installed in PLS-II and devices operating in overseas accelerators, we have improved the problems and enabled stable beam operation with improved performance while matching the characteristics of the 4GSR beamline.



<Figure 4.3.4.5> Internal and external shapes of DMM.

<Table 4.3.4.6> Motion specifications of DMM

Part	Function	Actuator / Monitor (Encoder)	Range	Resolution	Remark
1st Crystal	Pitch	Huber 411-X2W2 Goniometer + stepping motor + motor drive	360°	0.18"	-
		RESR20USA206 scale + REE0400A08A + RGH20F30M30C readhead (Renishaw)	360°	0.1"	-
2nd Crystal	Pitch	HUBER 411-X2W2 Goniometer + stepping motor + motor drive	360°	0.18"	-
		RESR20USA206 scale + REE0400A08A + RGH20F30M30C readhead (Renishaw)	360°	0.1"	-
	Roll	Pico-motor	±0.63°	0.00001"	-
	Z2	KOHZU MVXA16A-R1 Linear Stage	±25 mm	1 μm	-
		RGS20-S scale + REE0040E01A + RGH25F30M01C readhead (Renishaw)	±25 mm	0.5 μm	-
	Longitudinal	PHYRTON VSS80.200-7.5 Stepper Motor + Rack and Pinion	±500 mm	1 μm	-
		RGS20-S + REE0040E01A + RGH25F30M01C readhead (Renishaw)	±500 mm	0.5 μm	-
Chamber (including 1st & 2nd Crystal)	Lateral	Oriental PK596A-P24 Stepper Motor + SAMYANG SJ-32 (24:1) Screw Jack	±50 mm	33 nm	-
		MGSCALE GB-010ER Linear Encoder	±50 mm	0.5 μm	-
	Vertical	Oriental PK596A-P24 Stepper Motor + SAMYANG SJ-32 (24:1) Screw Jack	±6.537 mm	2.88 nm	-
		MGSCALE GB-015ER Linear Encoder	±75 mm	0.5 μm	-

The 1st & 2nd multilayers are installed on the goniometer respectively to create the Bragg angle to be used, and the pitch and roll are adjusted respectively through the rotation axis and tilt stage of the goniometer, and the parallelism between the two multilayers is maintained. The Goniometer Stage that controls the 1st multilayer is fixed to the entire frame and rotates to adjust the Bragg angle, and the Goniometer Stage that controls the 2nd multilayer can move in

the horizontal direction.

The factors that have a significant impact on the performance of DMM are as follows:

- (1) Cooling device for reducing multilayer temperature deviation
- (2) Vibration due to cooling device or structural characteristics
- (3) High-angle resolution goniometer for increasing energy resolution
- (4) Precision driving device for precise alignment of multilayer and stable operation
- (5) Vacuum chamber for maintaining ultra-high vacuum for a long time
- (6) Stable support structure for efficient alignment of DMM

4.3.5 Mirror

The mirror system has various shapes and sizes of mirror reflection surfaces depending on the experimental purpose of the beamline. Accordingly, the types of drive axes for the mirror adjustment device and the overall configuration of the device are manufactured in various forms. In order to design and manufacture a mirror device, technical calculations such as thermal analysis, mechanical (structural) analysis, and vibration analysis are required, as well as specialized knowledge and technology in various fields such as design technology for precision mechanical devices, assembly technology, control technology, and testing and measurement technology for precision assembled devices. The types of mirror devices installed in the 4GSR beamline by function are as follows:

- Collimation mirror device that reduces the divergence angle of the photon beam emitted from the storage ring's bending magnet and insertion devices such as the undulator or wiggler to make it enter the spectrometer and increase the energy resolution
- HHL (High Heat Load) mirror device installed in front of the spectrometer to reduce beam instability due to high heat load when white light is directly irradiated to the spectrometer crystal
- Vertical (VFM), horizontal (HFM), vertical + horizontal (KB) mirror devices to focus the monochromatic beam emitted from the spectrometer onto the sample
- Mirror devices to change the path of the beam

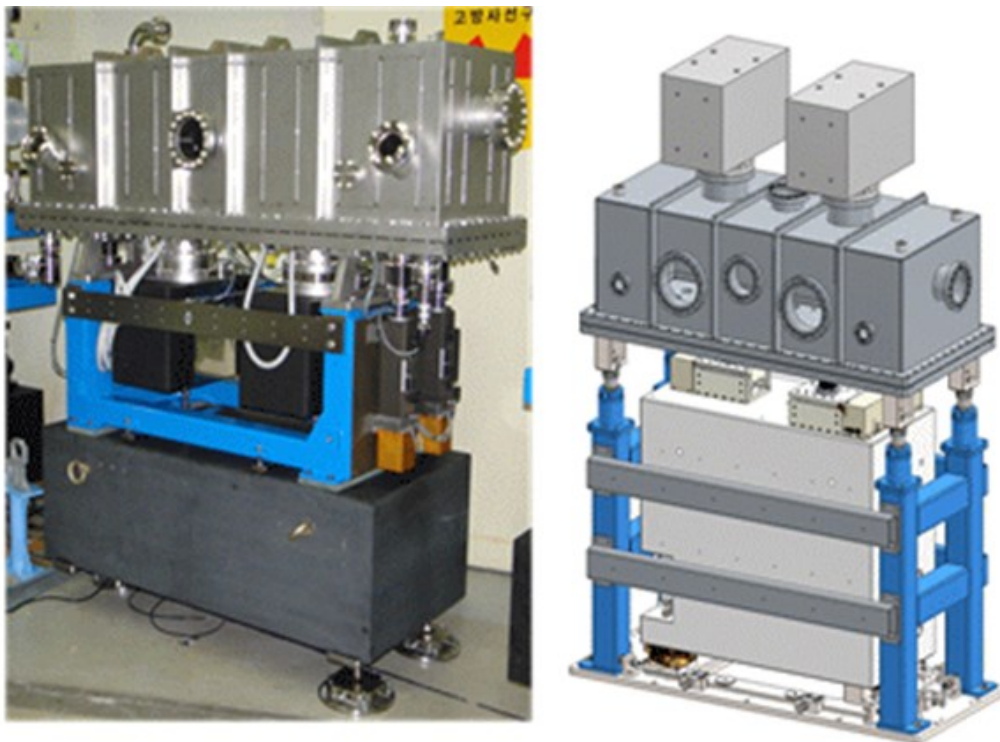
Custom design and manufacturing are required depending on the request for the beamline experiment method or surrounding environment.

A. First mirror system (M1)

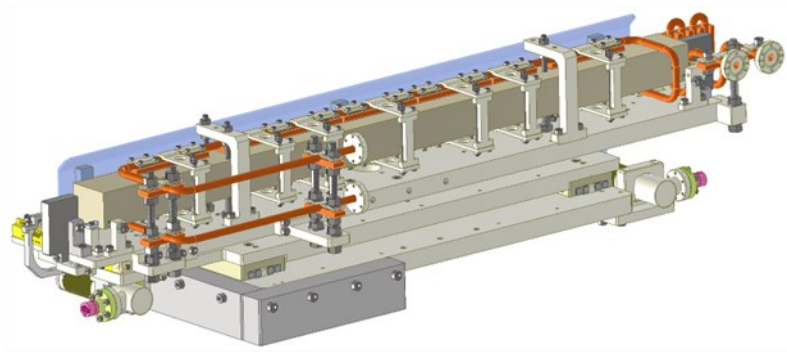
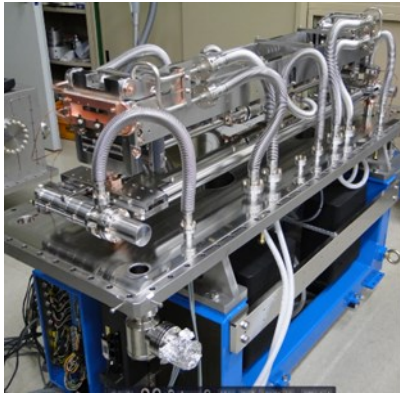
The M1 mirror, which is installed first in front of the spectrometer in the beamline, is installed for the sole or common purpose of reducing high heat load, removing high order harmonics, and focusing. In order to minimize the thermal deformation of the mirror due to the high thermal load of the mirror installed in front of the spectrometer, a cooling system is absolutely necessary. The 4GSR beam has the characteristics of low emittance and high power,

so the mirror surface is subjected to a high thermal load, and if efficient cooling is not achieved, the beam stability is greatly reduced. The design of the M1 mirror device requires technical calculations of thermal analysis, structural analysis, and vibration analysis as described above, and must also be accompanied by a design of mechanical and electrical safety devices to ensure that the beam is irradiated only to the mirror when adjusting the mirror position. The M1 mirror is generally adjustable in the five axes of Pitch, Roll, Yaw, x, and y, and can be installed by manufacturing the mirror surface with a fixed radius according to the experimental purpose of the beamline. Also, in order to adjust the mirror radius, the mirror reflection surface is manufactured as a flat surface and a mirror bending device can be installed to adjust the radius according to the experiment.

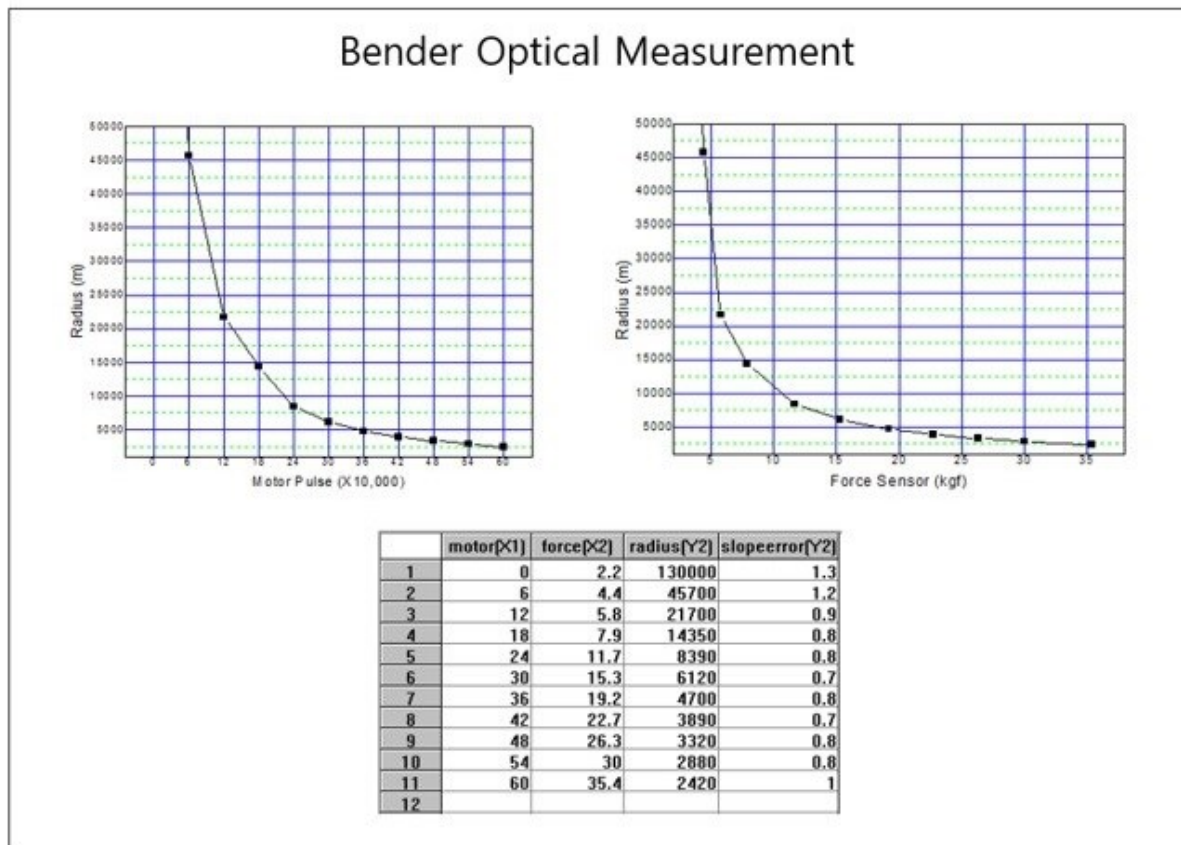
The UHV encoder, limit switch, precision angle sensor and motor temperature sensor are applied to improve the mechanical position precision and reproducibility of the device. The drive system for controlling the device consists of actuators controlled by stepper motors that can be used in UHV environments (5×10^{-10} torr), and all signal lines are led out of the vacuum chamber through feed-through. <Figure 4.3.5.1> and <Figure 4.3.5.2> show the external and internal appearances of the collimating mirror of PLS-II and 4GSR. Also, <Table 4.3.5.1> shows the detailed manufacturing specifications of the M1 Mirror Manipulator.



<Figure 4.3.5.1> Vacuum chamber & girder of M1 mirror manipulator in PLS-II and 4GSR.



<Figure 4.3.5.2> M1 mirror manipulator of PLS-II and 4GSR.



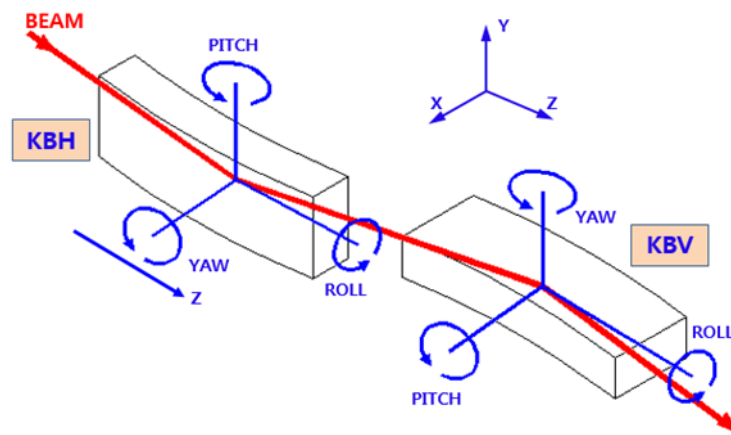
<Figure 4.3.5.3> Radius & slope error of M1 bendable mirror.

<Table 4.3.5.1> Specifications of M1 mirror manipulator

Motion	Parameters	Specification
Horizontal Axis (x-axis)	Driver	Horizontal actuator (UHV)
	Range	±15 mm
	Resolution	0.02 μm (motor) / 0.10 μm (encoder)
	Precision	0.2 μm (linear encoder)
	Drive type	5P Harmonic Step Motor
Vertical Axis (z-axis)	Driver	Vertical actuator
	Range	±15 mm
	Resolution	0.05 μm (motor) / 0.10 μm (encoder)
	Precision	0.2 μm (linear encoder)
	Drive type	5P Harmonic Step Motor
Roll	Driver	Vertical actuator
	Range	±2.60° (±45.45 mrad)
Axis distance = 220 mm	Resolution	0.094 arcsec (0.455 μrad) (encoder)
	Precision	0.375 arcsec (1.818 μrad) (encoder)
	Drive type	5P Harmonic Step Motor
Pitch (separate installation of PZT)	Driver	Vertical actuator
	Range	±2.68° (±46.73 mrad)
Axis distance = 1070 mm	Resolution	0.019 arcsec (0.093 μrad) (encoder)
	Precision	0.077 arcsec (0.374 μrad) (encoder)
	Drive type	5P Harmonic Step Motor
Yaw	Driver	Horizontal actuator
	Range	±2.14° (±37.38 mrad)
Axis distance = 1070 mm	Resolution	0.008 arcsec (0.037 μrad) (encoder)
	Precision	0.077 arcsec (0.374 μrad) (encoder)
	Drive type	5P Harmonic Step Motor
Mirror Bender Actuator (if installed)	Driver	Bender actuator
	Range	±12 mm (100 kgf)
	Resolution	0.02 μm
	Precision	0.1 kgf (by force sensor)
	Drive type	5P Harmonic Step Motor
Base Alignment System	Driver	Manual adjustment
	Range	Z direction, ±25 mm (with roll, pitch)
		X, Y, Z direction, ±15 mm
UHV Angle Sensor X & Y axis	Range	X & Y: ±1 deg
	Resolution	0.0001 deg

B. KB mirror manipulator

The KB mirror is installed in a vacuum chamber with two mirrors combined to focus the beam horizontally and vertically, and is mainly installed close to the sample to focus the photon beam directly on the sample with a size of several microns or less in width and height. The KB mirror device can be divided into two types: Kinematic structure and Pivot structure, depending on the structure of the stage for mirror positioning and alignment and the design method of the joint and pivot structure for mirror angular movement. Recently, with the development of mirror machining technology, it is possible to process both tangential and sagittal radii on a single mirror surface. Therefore, it is possible to manufacture an ellipsoidal mirror capable of focusing horizontally and vertically at a single location while shortening the focusing distance, so that the KB function can be replaced with a single mirror. <Figure 4.3.5.4> shows the KB Mirror Manipulator coordinate system.

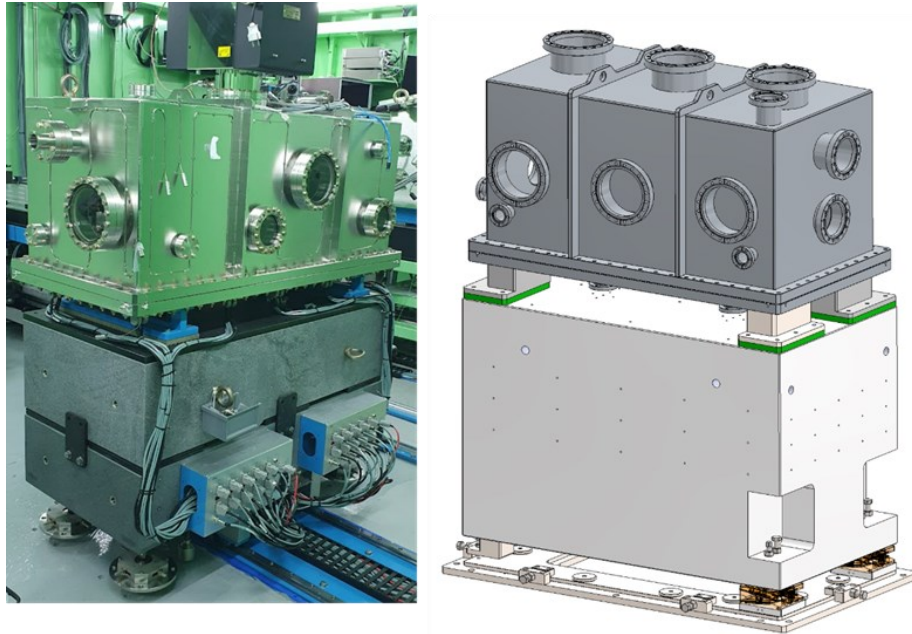


<Figure 4.3.5.4> Coordinate system of KB mirror manipulator.

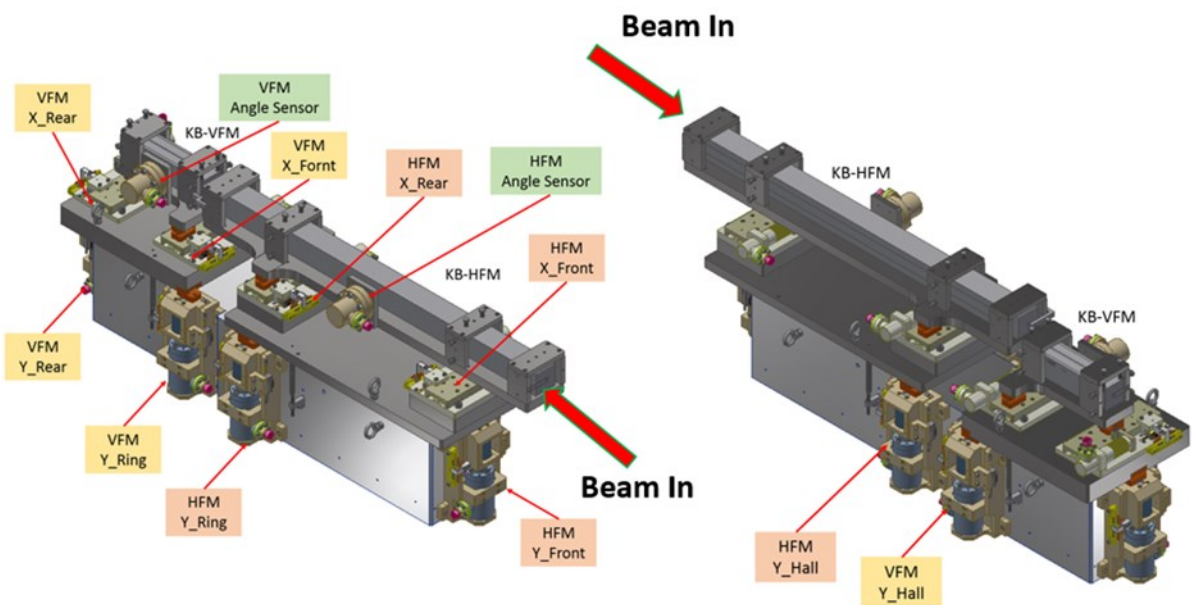
(1) Kinematic KB Mirror Manipulator

The Kinematic KB mirror consists of a three-point support structure consisting of a combination of Cone, Vee, and Flat, as shown in <Figure 4.3.5.7>, and S-DLC coated steel balls are assembled between each Mount for precise displacement, enabling angular movements in the three axes of Pitch, Roll, and Yaw. The KB mirror of the kinematic structure has a stable 3-point support for the stage for linear and angular motion, and is also structurally strong against external vibrations due to the laminated assembly, and is also strong against vibrations that may occur inside the device due to the cooling device. The problem with the KB mirror is that the Pitch, Roll, and Yaw axes are not independent structures, so when one axis moves, unintended coupling occurs in the other axis, and also, since the center of rotation

of the angular motion of the mirror is not at the center of the mirror, translational displacement occurs in the other axis when one axis moves for mirror alignment, so unnecessary compensation motions for the axes must be performed. <Figure 4.3.5.5> shows the external appearance of the Kinematic KB mirror, and <Figure 4.3.5.6> shows the internal structure of the device. <Table 4.3.5.2> and <Table 4.3.5.3> show the detailed specifications of the Kinematic Horizontal KB Mirror Manipulator and the Kinematic Vertical KB Mirror Manipulator. The 4GSR beamline will be equipped with KB mirror devices of both Kinematic and Pivot Bearing types depending on the beamline characteristics.



<Figure 4.3.5.5> Kinematic KB mirror manipulator (External shape).



<Figure 4.3.5.6> Kinematic KB mirror manipulator (Internal shape).

<Table 4.3.5.2> Specifications of Kinematic KBH systems

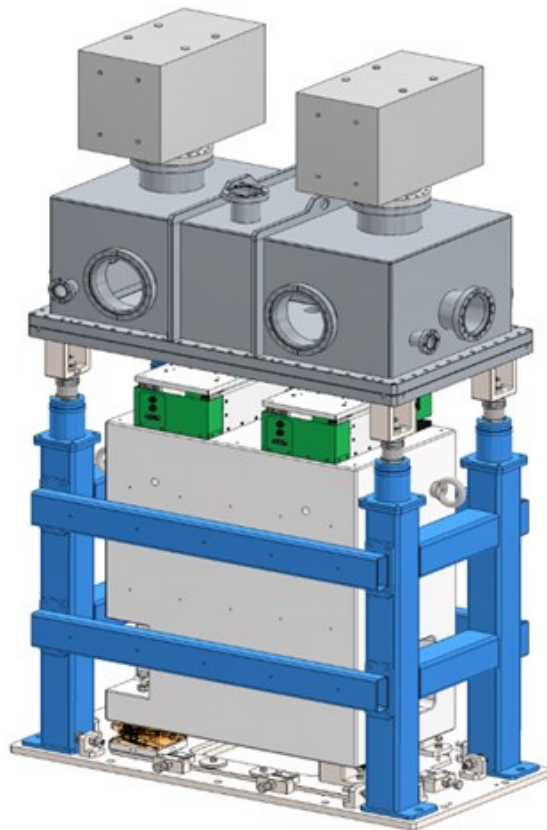
Axis(7) / spec.	Motor resolution	Encoder resolution	Precision	Range
Pitch axis (separate installation of PZT)	≤ 0.05 (0.25 μrad)	≤ 0.1 (0.485 μrad)	≤ 0.2 (0.97 μrad)	$\geq \pm 1.5$ deg.
Roll axis	≤ 0.1 (0.485 μrad)	≤ 0.2 (0.97 μrad)	≤ 0.5 (2.42 μrad)	$\geq \pm 1.5$ deg.
Yaw axis	≤ 0.1 (0.485 μrad)	≤ 0.1 (0.97 μrad)	≤ 0.5 (2.424 μrad)	$\geq \pm 1.5$ deg.
X axis	≤ 0.05 μm	≤ 0.1 μm	≤ 0.2 μm	$\geq \pm 10.0$ mm
Y axis	≤ 0.05 μm	≤ 0.1 μm	≤ 0.2 μm	$\geq \pm 10.0$ mm
Z axis	≤ 0.05 μm	≤ 0.1 μm	≤ 0.2 μm	$\geq \pm 10.0$ mm

<Table 4.3.5.3> Specifications of Kinematic KBV systems

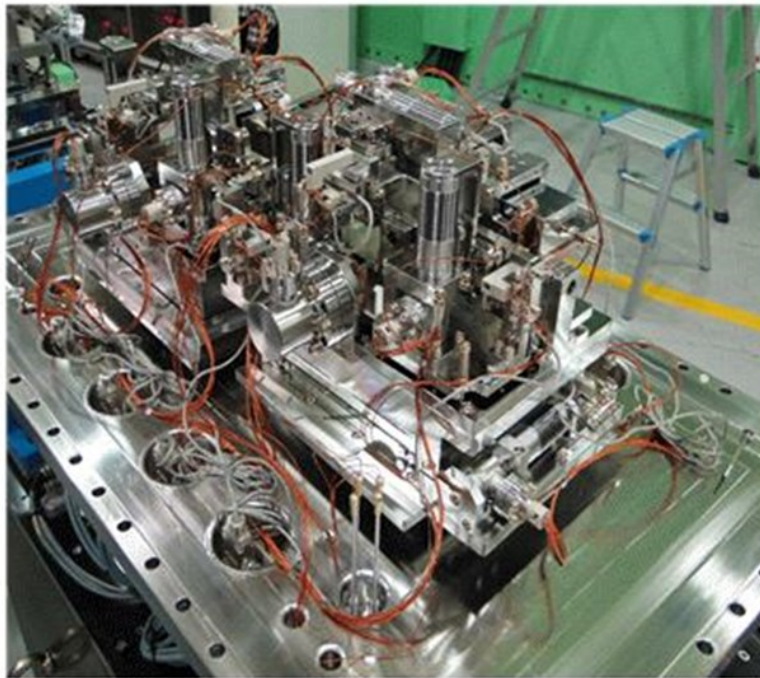
Axis(7) / spec.	Motor resolution	Encoder resolution	Precision	Range
Pitch axis (separate installation of PZT)	≤ 0.05 (0.25 μrad)	≤ 0.1 (0.485 μrad)	≤ 0.2 (0.97 μrad)	$\geq \pm 1.5$ deg.
Roll axis	≤ 0.1 (0.485 μrad)	≤ 0.2 (0.97 μrad)	≤ 0.5 (2.42 μrad)	$\geq \pm 1.5$ deg.
Yaw axis	≤ 0.1 (0.485 μrad)	≤ 0.1 (0.97 μrad)	≤ 0.5 (2.424 μrad)	$\geq \pm 1.5$ deg.
X axis	≤ 0.05 μm	≤ 0.1 μm	≤ 0.2 μm	$\geq \pm 10.0$ mm
Y axis	≤ 0.05 μm	≤ 0.1 μm	≤ 0.2 μm	$\geq \pm 10.0$ mm
Z axis	≤ 0.05 μm	≤ 0.1 μm	≤ 0.2 μm	$\geq \pm 10.0$ mm

(2) Pivot Bearing KB Mirror

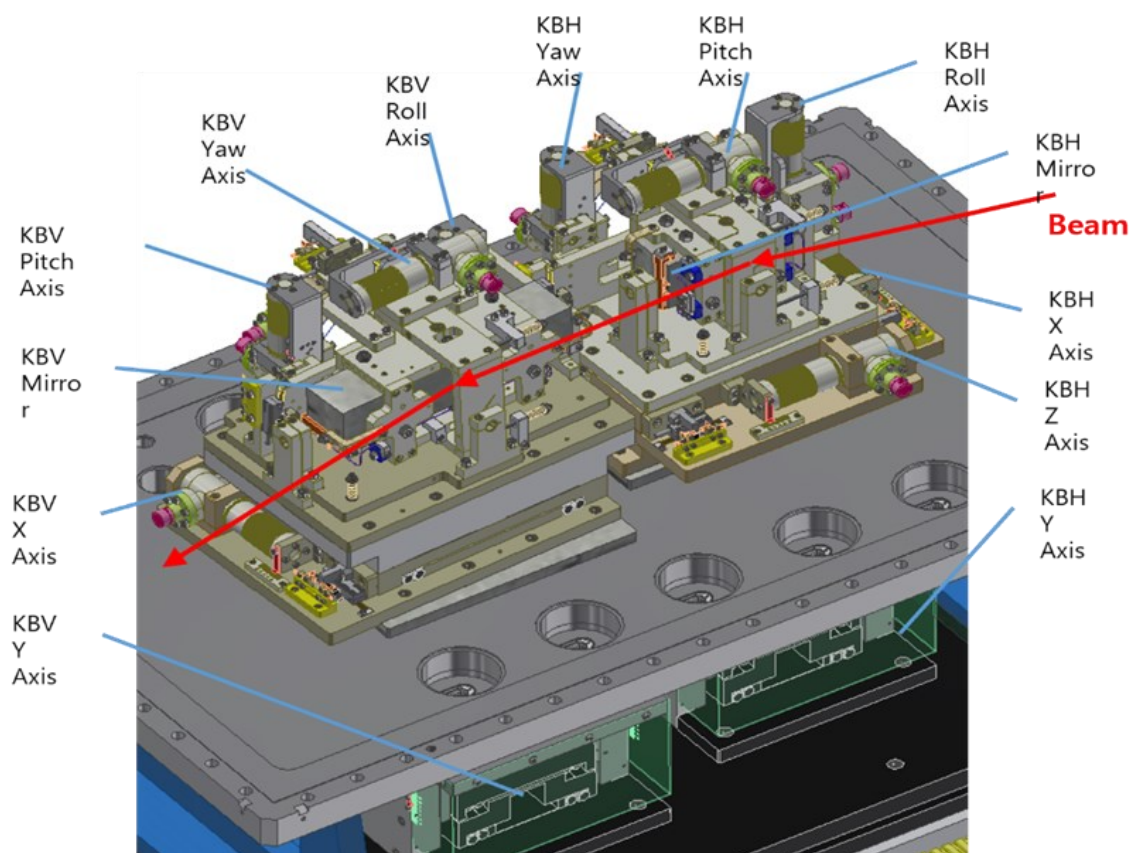
The Pivot Bearing KB mirror device structure is shown in <Figure 4.3.5.8> and <Figure 4.3.5.9>, and the parts for the rotation of the three axes of Pitch, Roll, and Yaw are applied with a Pivot Bearing that can rotate without physical friction and backlash. When aligning the mirror, the rotation center of the three-axis angular displacement coincides with the center of the mirror reflection surface, so the required displacement angle value and the input angle value correspond one-to-one when changing the angle for mirror alignment. Also, since all angular displacement axes operate independently, there is less coupling, making mirror alignment easier than the Kinematic KB mirror device. The actuator for the axis movement is connected to the sine-bar structure, and the sine bar length can be increased to increase the resolution. The structural problem of the Pivot Bearing KB is that it requires multiple links to convert the linear motion of the Pivot Bearing and the actuator, which are installed for mirror rotational motion, into rotational motion by connecting them with a sine bar. Therefore, it is a structure vulnerable to vibration in the direction of the actuator motion. Installation can be considered in beamline with solid ground and no concerns about vibration, and it is scheduled to be installed in beamline where frequent beam alignment is required due to the nature of the experiments.



\<Figure 4.3.5.7> Pivot KB mirror manipulator (External shape).



<Figure 4.3.5.8> Pivot KB mirror manipulator (Internal shape)



<Figure 4.3.5.9> Pivot KB mirror manipulator (Internal modeling)

<Table 4.3.5.4> Specifications of Pivot KBH systems

Axis(6) / spec.	Motor resolution	Encoder resolution	Precision	Range
Pitch axis (separate installation of PZT)	≤ 0.05 (0.25 μrad)	≤ 0.1 (0.485 μrad)	0.2 (0.97 μrad)	$\geq \pm 1.5$ deg.
Roll axis	≤ 0.1 (0.485 μrad)	≤ 0.2 (0.97 μrad)	0.5 (2.42 μrad)	$\geq \pm 1.5$ deg.
Yaw axis	≤ 0.1 (0.485 μrad)	≤ 0.1 (0.97 μrad)	0.5 (2.424 μrad)	$\geq \pm 1.5$ deg.
X axis	$\leq 0.05 \mu\text{m}$	$\leq 0.1 \mu\text{m}$	0.2 μm	$\geq \pm 10.0$ mm
Y axis	$\leq 0.05 \mu\text{m}$	$\leq 0.1 \mu\text{m}$	0.2 μm	$\geq \pm 10.0$ mm
Z axis	$\leq 0.05 \mu\text{m}$	$\leq 0.1 \mu\text{m}$	0.2 μm	$\geq \pm 10.0$ mm

<Table 4.3.5.5> Specification of Pivot KBV systems

Axis(5) / spec.	Motor resolution	Encoder resolution	Precision	Range
Pitch axis (separate installation of PZT)	≤ 0.05 (0.25 μrad)	≤ 0.1 (0.485 μrad)	0.2 (0.97 μrad)	$\geq \pm 1.5$ deg.
Roll axis	≤ 0.1 (0.485 μrad)	≤ 0.2 (0.97 μrad)	0.5 (2.42 μrad)	$\geq \pm 1.5$ deg.
Yaw axis	≤ 0.1 (0.485 μrad)	≤ 0.1 (0.97 μrad)	0.5 (2.424 μrad)	$\geq \pm 1.5$ deg.
X axis	$\leq 0.05 \mu\text{m}$	$\leq 0.1 \mu\text{m}$	0.5 μm	$\geq \pm 10.0$ mm
Y axis	$\leq 0.05 \mu\text{m}$	$\leq 0.1 \mu\text{m}$	0.5 μm	$\geq \pm 10.0$ mm